



LUND UNIVERSITY

SARs for the Antiparasitic Plant metabolite Pulchrol

Terrazas Villarroel, Paola

2021

[Link to publication](#)

Citation for published version (APA):

Terrazas Villarroel, P. (2021). *SARs for the Antiparasitic Plant metabolite Pulchrol*. Lund University.

Total number of authors:

1

Creative Commons License:

Unspecified

General rights

Unless other specific re-use rights are stated the following general rights apply:

Copyright and moral rights for the publications made accessible in the public portal are retained by the authors and/or other copyright owners and it is a condition of accessing publications that users recognise and abide by the legal requirements associated with these rights.

- Users may download and print one copy of any publication from the public portal for the purpose of private study or research.
- You may not further distribute the material or use it for any profit-making activity or commercial gain
- You may freely distribute the URL identifying the publication in the public portal

Read more about Creative commons licenses: <https://creativecommons.org/licenses/>

Take down policy

If you believe that this document breaches copyright please contact us providing details, and we will remove access to the work immediately and investigate your claim.

LUND UNIVERSITY

PO Box 117
221 00 Lund
+46 46-222 00 00

SARs for the Antiparasitic Plant Metabolite Pulchrol

SARs for the Antiparasitic Plant Metabolite Pulchrol

Paola Terrazas



LUND
UNIVERSITY

DOCTORAL DISSERTATION

by due permission of the Faculty of Science, Lund University, Sweden.
To be defended in lecture hall C, Kemicentrum, on Thursday 17th of June
2021 at 14:00

Faculty opponent

Professor Patricia Mollinedo

Chemistry Research Institute, San Andres University, Bolivia

Organization LUND UNIVERSITY Centre of Analysis and Synthesis Department of Chemistry Author(s) Paola Terrazas	Document name Doctoral Thesis	
	Date of issue	
	Sponsoring organization Swedish International Development Cooperation Agency (SIDA)	
Title and subtitle Sars for the antiparasitic plant metabolite pulchrol.		
Abstract <p>Pulchrol, a natural compound isolated from the roots of the vegetal specie <i>Bouyeria pulchra</i> has been shown to possess potential antiparasitic activity toward Trypanosomatids, particularly against <i>Trypanozoma cruzi</i>, which causes the Chagas disease; and moderately against <i>Leishmania</i> species, responsible for Leishmaniasis. In this investigation, several pulchrol analogues were prepared and assayed toward <i>T. cruzi</i> epimastigotes, and <i>L. braziliensis</i> and <i>L. amazonensis</i> promastigotes, to develop structure activity relationship studies (SARs).</p> <p>Analogues with transformations in the three rings of the pulchrol's scaffold were prepared. Initially, compounds with transformations at the benzylic position in the A-ring were assayed to evaluate the role of the benzylic alcohol in pulchrol. The results showed that an hydrogen bond acceptor group is important for the antitypanosomatid activity and that ester groups with bulky alkyl substituents increase the potency toward all parasites. Analogues with transformations in the B- and C-rings, were focused on the variation of lipophilicity. In the B-ring, the methyl substituents placed at position 6 in pulchrol were replaced for two hydrogen atoms, just one methyl substituent, or two longer alkyl substituents. The biological activity results showed that longer chains with less than four carbon atoms are beneficial for the activity. A methoxy substituent is placed at position 2 in pulchrol's C-ring, in this study, analogues with the methoxy substituent placed in different positions or replaced with alkyl substituents were prepared, the results showed that compounds with hydrophobic groups in the C-ring increased the potency.</p> <p>Several analogues with more than one modification in different rings were also prepared. The combination of carbonyl groups in the A-ring with bulky alkyl groups in the C-ring was the most beneficial for the activity. In contrast, esters substituted with a hydrophobic group in the A-ring and bulky alkyl groups in the C-ring hampered the activity. A hydrogen bond acceptor at the benzylic position in the A-ring, as well as an additional hydroxyl group at position 1 in the C-ring (as in cannabinal) appeared to be important for the activity. The combination of different functionalities also seemed to have an effect in the orientation of the molecule inside the target protein.</p> <p>Our results showed that differences between the active sites for the different parasites may exist, however, preliminary pharmacophore hypotheses based on our biological results showed that the main pharmacophoric features are two hydrogen bond acceptor groups (one at the benzylic position and one on the B-ring's oxygen) and three hydrophobic features (two in the B-ring at position 6, and one in the C-ring at position 2 or 3).</p> <p>A qualitative evaluation of ADMET-descriptors calculated <i>in silico</i>, showed that most of the molecules have potential as orally administered substances, however, further studies focused on the development of compounds with more potency and focused on the optimization of the ADME characteristics are recommended.</p>		
Key words pulchrol, pulchral, SARs, antiparasitic, <i>Leishmania braziliensis</i> , <i>L. amazonensis</i> , <i>Trypanozoma cruzi</i> , <i>Bouyeria pulchra</i> , leishmaniasis, Chagas disease, synthesis, pharmacophore ADMET.		
Classification system and/or index terms (if any)		
Supplementary bibliographical information		Language English
ISSN and key title		ISBN 978-91-7422-816-8 978-91-7422-817-5
Recipient's notes	Number of pages	Price
	Security classification	

I, the undersigned, being the copyright owner of the abstract of the above-mentioned dissertation, hereby grant to all reference sources permission to publish and disseminate the abstract of the above-mentioned dissertation.

Signature

Date 2019-xx-xx

SARs for the Antiparasitic Plant Metabolite Pulchrol

Paola Terrazas



LUND
UNIVERSITY

Coverphoto by Paola Terrazas

Copyright pp 1-87 (Paola Terrazas)

Paper 1 © 2020 by the Authors (Licensee MDPI)

Paper 2 © 2020 by the Authors (Licensee MDPI)

Paper 3 © by the Authors (Manuscript unpublished)

Paper 4 © by the Authors (Manuscript unpublished)

Faculty of Science
Department of Chemistry
Centre for Analysis and Synthesis


ISBN 978-91-7422-816-8 (printed version)

978-91-7422-817-5 (digital version)

Printed in Sweden by Media-Tryck, Lund University
Lund 2021



Media-Tryck is a Nordic Swan Ecolabel
certified provider of printed material.
Read more about our environmental
work at www.mediatryck.lu.se

MADE IN SWEDEN 

To my Mom, my Dad, my Sister and my beloved David

Table of Contents

Popular summary	10
List of papers.....	11
Abbreviations.....	12
1 Introduction	14
1.1 Natural products and their uses.....	14
1.2 Synthetic natural products	15
1.3 Natural products as a source of new drugs	17
1.4 Drug discovery approaches.....	18
1.5 Neglected tropical diseases.....	19
1.6 Trypanosomatid diseases	20
1.6.1 The Chagas disease.....	20
1.6.2 Leishmaniasis	23
1.7 Secondary metabolites from <i>Bourreria pulchra</i>	27
1.8 Aim of the thesis	28
2 Modifications in the A-Ring	29
2.1 Background.....	29
2.1.1 Benzochromenes.....	29
2.1.2 Bioactive benzochromenes	30
2.1.3 Synthesis of benzo[<i>c</i>]chromenes	32
2.2 Pulchrol synthesis	32
2.3 Transformations of the benzyl alcohol functionality	34
2.4 Antiparasitic activity.....	38
2.4.1 Antiparasitic activity toward <i>T. cruzi</i>	38
2.4.2 Antiparasitic activity toward <i>L. braziliensis</i>	39
2.4.3 Antiparasitic activity toward <i>L. amazonensis</i>	40
2.5 Conclusions.....	41
3 Modifications in the B- and C-ring.....	43
3.1 Modification in the B-ring	43
3.2 Modifications in the C-ring.....	45

3.3	Antiparasitic Activity.....	46
3.3.1	Antiparasitic activity toward <i>T. cruzi</i>	49
3.3.2	Antiparasitic activity toward <i>L. braziliensis</i>	50
3.3.3	Antiparasitic activity toward <i>L. amazonensis</i>	50
3.4	Conclusions.....	51
4	Combined modifications.....	53
4.1	Modification on the A-, B- and C- rings.....	54
4.2	Antiparasitic activity and selected functionalities	57
4.2.1	Antiparasitic activity toward <i>T. cruzi</i>	57
4.2.2	Antiparasitic activity toward <i>L. braziliensis</i>	59
4.2.3	Antiparasitic activity toward <i>L. amazonensis</i>	59
4.3	Conclusions.....	60
5	Pharmacophore design and qualitative evaluation of predicted ADME- descriptors.....	62
5.1	Development of pharmacophore hypotheses.....	64
5.1.1	Pharmacophore hypothesis for <i>T. cruzi</i>	65
5.2	Qualitative analysis of ADMET-descriptors	70
5.3	Conclusions.....	73
6	General Conclusions	74
7	Acknowledgments	77
8	References	79

Popular summary

Leishmaniasis and Chagas are neglected diseases caused by trypanosomatid parasites from the genus *Leishmania* and *Trypanosoma*, respectively. These diseases occur primarily in tropical and subtropical regions, affecting mainly people from underdeveloped countries that live in distant rural places with insufficient access to medical care. The development of appropriate treatments has been overlooked by the big pharmaceutical companies, and current treatments mostly come from repurpose drug studies, presenting several disadvantages such as unwanted side effects, and the need for parenteral administration that may require hospitalization in some cases.

The complex life cycles of the *Leishmania* and *Trypanosoma* parasites makes it difficult to understand their infection mechanisms, making the development of new drugs challenging. However, empirical knowledge obtained from traditional medicine, may contribute to the isolation and identification of new natural products with potential antiparasitic activity. Such is the case of natural product pulchrol, isolated from the roots of the vegetal specie *Bourreria pulchra*, traditionally used to treat cutaneous diseases, infections and fevers in Yucatan, Mexico. After its isolation, pulchrol has been shown to possess interesting activity toward *T. cruzi*, and several *Leishmania* species.

In this investigation, several pulchrol analogues systematically modified were prepared to be used in structure-activity relationship studies. The effects that transformations of pulchrol's substituents produced in the antiparasitic activity were evaluated. A hydrogen bond acceptor at the benzylic position in pulchrol's A-ring, ethyl substituents in the B-ring, and isopropyl substituents in the C-ring were found to be important for the activity. A pharmacophore hypothesis developed for *T. cruzi* agreed with the observations made during the SAR studies.

The absorption, distribution, metabolism, excretion and toxicity (ADMET) potential of pulchrol's derivatives was evaluated qualitatively. Most of them were able to be absorbed orally, and therefore had potential as orally administered drugs.

List of papers

This thesis summarizes and supplements the following papers.

Paper 1

Terrazas, P.; Salamanca, E.; Dávila, M.; Manner, S.; Giménez, A.; Sterner, O. SAR:s for the Antiparasitic Plant Metabolite Pulchrol. 1. The benzyl alcohol functionality. *Molecules*. **2020**, *25*, 3058.

Contribution: Performed all the synthetic work, contributed to the formulation of the research problem, the interpretation of the data, and to writing the manuscript.

Paper 2

Terrazas, P.; Salamanca, E.; Dávila, M.; Manner, S.; Giménez, A.; Sterner, O. SAR:s for the Antiparasitic Plant Metabolite Pulchrol. 2. B- and C-ring substituents. *Molecules*. **2020**, *25*, 4510.

Contribution: Performed all the synthetic work, contributed to the formulation of the research problem, the interpretation of the data, and to writing the manuscript.

Paper 3

Terrazas, P.; Salamanca, E.; Dávila, M.; Manner, S.; Giménez, A.; Sterner, O. SAR:s for the Antiparasitic Plant Metabolite Pulchrol. 3. New substituents in A/B-rings and A/C-rings. *In manuscript*.

Contribution: Performed all the synthetic work, contributed to the formulation of the research problem, the interpretation of the data, and to writing the manuscript.

Paper 4

Terrazas, P.; Dávila, M.; Manner, S.; Sterner, O. SAR:s for the Antiparasitic Plant Metabolite Pulchrol. 4. Pharmacophore design hypothesis and qualitative assessment of predicted pharmacokinetic properties. *In manuscript*.

Contribution: Performed all the computational work, contributed to the formulation of the research problem, the interpretation of the data, and to writing the manuscript.

Abbreviations

A375	Human malignant melanoma cells
A546	Human lung carcinoma cells
ADMET	Absorption, distribution, metabolism, excretion and toxicity
BEDROC	Boltzmann-Enhanced Discrimination of Receiver Operating Characteristics
Caco-2	Human colorectal adenocarcinoma cells
CB1	Cannabinoid receptor type 1
CB2	Cannabinoid receptor type 2
CNS	Central nervous system
DIBALH	Diisobutylaluminum hydride
DME	1,2-Dimethoxyethane
DMF	Dimethylformamide
ER β	Estrogen receptor beta
HCT116	Human colon carcinoma cells
HBA	Hydrogen bond acceptor
HBD	Hydrogen bond donor
HegG-2	Human hepatoma cells
HERG	Human ether-à-go-go related gene
IC ₅₀	Half maximal inhibitory concentration
<i>P</i>	Partition coefficient
MCF7	Human Caucasian breast adenocarcinoma
MeCN	Acetonitrile
MeLi	Methyl lithium

MeMgBr	Methyl magnesium bromide
MW	Molecular weight
NaSEt	Ethanethiolate
NCE	New chemical entity
NTD	Neglected tropical diseases
PSA	Polar surface area
QPlogBB	Predicted brain/blood partition coefficient
QPlogHERG	Predicted IC ₅₀ value for blockage of HERG K ⁺ channels
QPlogKhsa	Prediction of binding to human serum albumin
QPlogPo/w	Predicted octanol/water partition coefficient
QPlogS	Predicted aqueous solubility
QPPCaco	Predicted apparent Caco-2 cell permeability
QPpolarz	Predicted polarizability
RAW	Mouse monocyte macrophage
RMSD	root-mean-square deviation
SARs	Structure activity Relationship studies
SASA	Total solvent accessible surface area
SI	Selectivity index
SW1116	Human colorectal adenocarcinoma cells
THC	Δ^9 -Tetrahydrocannabinol
TBAF	Tetrabutylammonium fluoride
TBDPSCI	<i>Tert</i> -Butyldiphenylsilane
THF	Tetrahydrofuran

1 Introduction

1.1 Natural products and their uses

Natural products are compounds generated by living organisms. The secondary metabolism transforms primary metabolites to produce secondary metabolites, also known as natural products [1].

Primary metabolites are compounds essential for life, and most of them and their biosynthetic pathways are common for all organisms. Secondary metabolites, on the other hand, are specific for different groups of organisms, their purposes are in general not understood but they appear to interact with the external environment, for example attracting other species or repelling predators as a defence mechanism [1-3]. These metabolites are produced as a result of millions of years of evolution in which organisms have adapted to various abiotic and biotic stresses [2-5].

Humans have found practical uses for many secondary metabolites, traditionally from plants, but recently also from microorganisms. We have used natural products as pesticides, flavouring agents, fragrances, and especially as drugs to treat different illnesses [2]. Knowledge on the traditional therapeutic use of plants was obtained on an empirical basis from rather early in history, reports found in Mesopotamia approximately 2400 BC, a compendium of traditional medicine (Ebers Papyrus) written around 1500 BC in Egypt [4, 6], and all the documents from the traditional Chinese medicine that have been recorded for thousands of years [6, 7] evidence the existence of this knowledge.

So far, traditional medicine has served as a starting point for rational drug discovery. One example is opium and its traditional use as analgesic, which afterward led to the isolation of morphine [8, 9]. Likewise, various compounds such as taxol isolated from the pacific yew (*Taxus brevifolia*) [10]; camptotecin isolated from the Chinese plant *Camptotheca acuminata* [11]; and the vinca alkaloids obtained from the Madagascar periwinkle (*Cantharanthus roseus*) [12], are used to treat various forms of cancer [13, 14]. In addition, we can mention examples of anti-parasitic drugs found in nature, like quinine, isolated from the bark of the Cinchona trees (e.g., *Cinchona officinalis*), which were traditionally used to counteract shivering caused by low temperatures or fever in South America [15]. Similarly, the natural product artemisinin isolated from the sweet wormwood (*Artemisia annua*), was used in Chinese traditional medicine to treat fever, inflammation and malaria

(see Figure 1) [16, 17]. Both the abovementioned compounds have been important for treating patients with malaria.

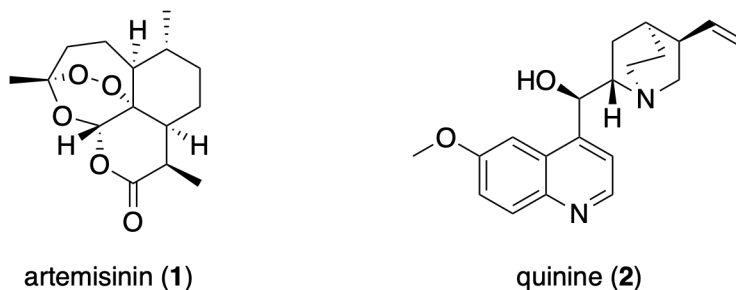


Figure 1
Antimalarial natural products artemisinin and quinine

Ethnopharmacology based on the world's almost inapprehensible biodiversity provides an extremely valuable tool for drug discovery; nevertheless, ethnic traditional knowledge and natural habitats are endangered, and may decline or disappear, with all of their valuable information, due to the growth of urban and farm areas [6, 18]. Besides the environmental factors, there are also other challenges for natural product discovery: the composition, altitude, process, and storage conditions; are factors that need to be controlled during the harvesting process [4, 6]. The isolation and purification processes are also expensive, time consuming and often impractical to scale up; on top of that, the amounts of secondary metabolites obtained are in general small and may be insufficient for the testing of a wider range of biological activities [4-6].

Due to the challenges described above, the interest in natural product-based drug discovery has declined, leaving natural product research to a major extent to universities and start-up companies [6].

1.2 Synthetic natural products

Synthetic chemists have solved the problem of insufficient amounts of metabolites isolated from natural sources by designing synthetic routes to prepare them in the laboratory. This solution made possible to test natural products more extensively in various biological assays. Once a biologically active compound would have been found, it was possible to prepare derivatives and analogues based on its structure, looking for improvements in the activity or therapeutic properties that may lead to a potential drug [5, 19].

Natural product synthesis also enriched the chemical variety of prior purely synthetic compounds, providing privileged scaffolds belonging to biologically active pharmacophores [4, 5, 19, 20]. The first natural product synthesized as a drug was salicylic acid, a natural oxidation product of the glucoside salicin that was isolated from the bark of the white willow (*Salix alba*). Salicylic acid was developed to the less irritating prodrug Aspirin by acetylation. Later other drugs such as Chloroquine and Mefloquine were produced inspired by quinine, to be used to combat malaria (for the structures see Figure 2) [6].

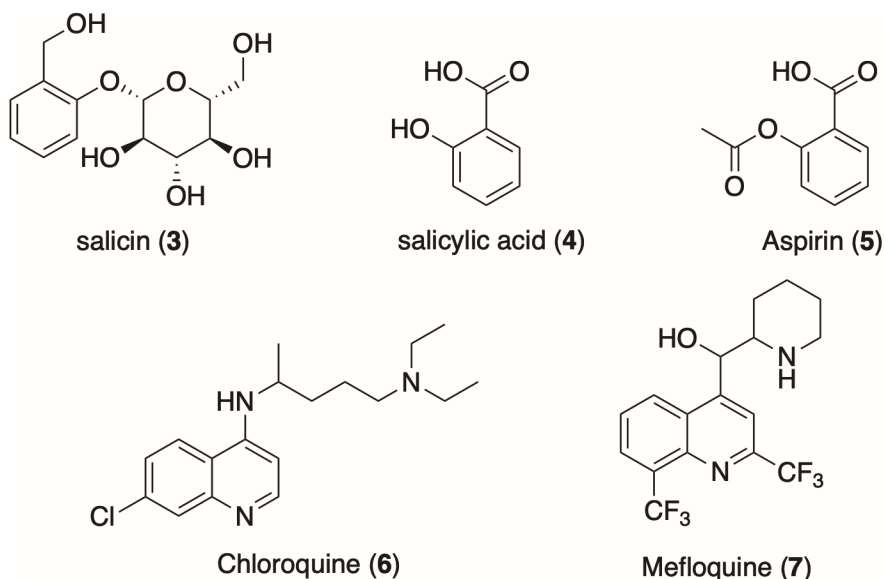


Figure 2

Above, natural products salicin, salicylic acid and its synthetic derivative Aspirin. Below, synthetic derivatives Chloroquine and Mefloquine

Ultimately, natural product's synthetic derivatives have prevailed over natural products as a result of the advantages of the synthetic process. Before 1940, unmodified natural products and their derivatives represented 43% and 14%, respectively, of all new chemical entities (NCEs) approved as drugs. Since then, until 2000, unmodified natural products and their derivatives represented 5.3% and 28% respectively [21].

Nevertheless, true natural products continue to be an important source of new molecular scaffolds, which could lead to the development of novel drug candidates after conducting structure-activity relationship studies based on synthetic analogues [5]. Nowadays, the definition for therapeutic natural products has broadened to include chemically modified natural compounds and purely synthetic medicinal compounds inspired by them [21].

1.3 Natural products as a source of new drugs

Apart from its chemical diversity, natural products may possess potential selectivity, since they are in contact with natural macromolecules during the complete development of their biosynthetic pathways. As many of those biochemical building blocks are common to all living organisms, natural compounds could possess an inherent selectivity for binding macromolecules in the human body [4, 6].

Another advantage is the vast biodiversity that can produce bioactive compounds with different chemical scaffolds. Only approximately 6% of the existing plant species have been investigated pharmacologically, and just about 15% phytochemically, so there remains a huge number of new plant metabolites that can be found in the approximately 310 000 plant species described so far [6].

Despite the advantages, the pharmaceutical industry is not investing as much in natural products as in synthetic molecules, mainly because of the high costs for the isolation and characterization of substances [21]. However, among the drugs approved between 1981 and 2019, it can be noted that natural products and natural inspired products still play an important role in drug discovery (Figure 3). From the 1603 drugs approved during this period, 588 were synthetic drugs, 286 natural derivatives, 254 natural inspired synthetic drugs, and 69 natural products [22].

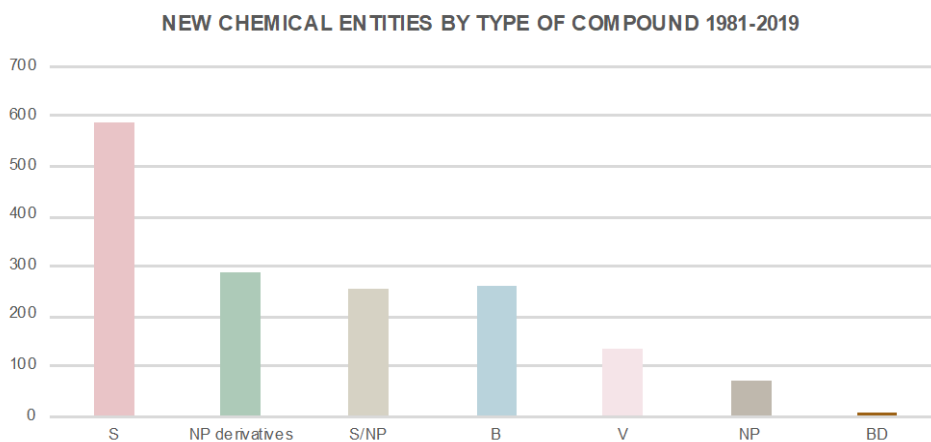


Figure 3

New chemical entities approved between 1981-2019. S (Synthetic compounds), NP (Natural products), S/NP (Synthetic compounds with natural product pharmacophore), B (Biological macromolecule), V (Vaccine), BD (Botanical drug) [22]

As can be seen, natural products still play a highly significant role in drug discovery as sources of bioactive chemical leads, and traditional medicine is still an important pool for the identification of new pharmacophores [5, 19, 20, 22].

1.4 Drug discovery approaches

The advantages of the structural singularity shown by natural bioactive products also carry some difficulties, when knowledge about the mode of action or the molecular target involved in their biological activity is lacking [23, 24]. Still, drug discovery research can be performed on cells or whole organisms without detailed knowledge of the target [23, 25, 26].

Phenotypic studies can be applied for diseases in which the mechanism or the drug target is unknown, which is the case in many understudied illnesses such as the neglected parasitic diseases [25, 27, 28]. In contrast, target-based studies may be more favourable for chemical lead optimization, but a mistaken selection of the target may result in undesirable outcomes [25, 26]. In order to perform target-based studies on parasitic diseases like Leishmaniasis, essential targets for its survival should be known and those must differ from human targets. Nonetheless, not many parasitic targets have been validated, therefore, phenotypic screening might work better for parasitic diseases in the first stages of research [29].

Another advantage for the phenotypic studies, regarding cell permeability is that the biological assays are usually performed over complex biological systems, as cells or living organisms, making the results more physiologically relevant [23, 25, 27]. Contrarily, in target-based studies the assays are performed directly in the target, and it may be uncertain if the molecule will work in more complex systems [6, 23, 25].

When a lead compound is found, a structure-activity relationship (SAR) study can be conducted and for this purpose analogues are synthesized and tested on a determined biological system, the correlations obtained between the biological activity and the structural variations can then be analysed [23, 30]. SAR studies are usually developed under the hypothesis that just one target is involved, albeit, this assumption may be false and multi-target binding can occur. After SAR studies, it is still desirable to identify the target that the lead compound is interacting with, especially for the subsequent stages on drug development [30].

In this context, the phenotypic approach has as the main purpose to discover new biologically active compounds [23]. Over the years, phenotypic studies have been shown to be more effective for the identification of first-in-class drugs, while target-based studies are more efficient to produce follower drugs [26]. During the last years, investment in drug discovery has increased, although an attrition rate on the identification of first-in-class drugs has been observed, difficulties during the selection of the target and decrease on phenotypic research are considered some of the factors [24]. However, both approaches may provide better results working together, as this may reduce attrition rates on first-in-class drug identification and improve subsequent drug optimization, which may also be beneficial in the discovery of new treatments for understudied diseases [23, 31].

1.5 Neglected tropical diseases

Neglected tropical diseases (NTDs) are a group of 17 infectious diseases, native from tropical and subtropical regions that affect around 1 billion people belonging to underprivileged populations in 149 countries [32]. NTDs may lead to death, disabilities and deformities that may produce psychological, social and economic damage [28, 33, 34], yet they have not received enough attention and their nonexistence in developed countries has made them invisible for industry and research [33, 35, 36]. Currently, some pharmaceutical industries have opened their compound libraries to find new repurpose drugs, nevertheless, investments in research for the identification of new lead compounds are still necessary [37, 38, 27].

Drug discovery for NTDs has been shown to be more successful using a phenotypic approach [24], mainly because there are few validated targets to perform target-based studies, and a little understanding of the complex life cycle of these pathogens [28].

Within the 1556 new drugs developed between 1975 and 2004, only 21 (representing approximately 1%) were aimed for NTDs [38]. From 1981 to 2019, 402 anti-infective drugs were approved, between them: 162 were antibacterial compounds, 186 antiviral compounds, 34 antifungal compounds and just 20 antiparasitic compounds. Among those, 2 were natural products, 7 natural product derivatives, 6 synthetic compounds, 3 synthetic compounds with natural product pharmacophore and 2 were vaccines (See Figure 4) [27, 22].

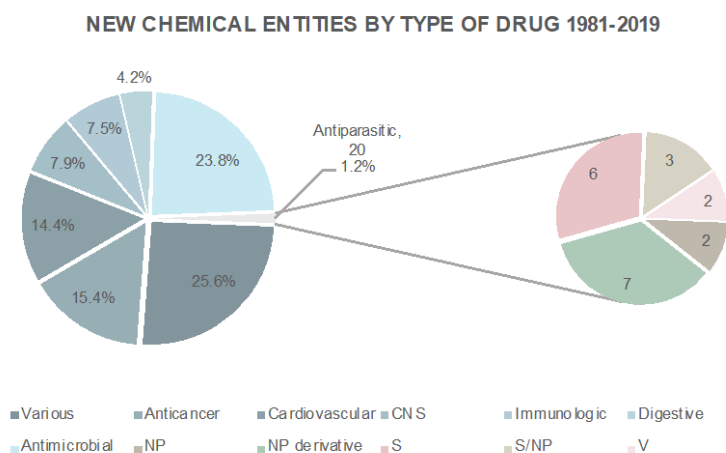


Figure 4

New chemical entities approved between 1981-2014 by type of drug and type of compounds approved as antiparasitic agents. S (Synthetic compounds), NP (Natural products), S/NP (Synthetic compounds with natural product pharmacophore), B (Biological macromolecule), V (Vaccine), BD (Botanical drug) [22]

1.6 Trypanosomatid diseases

Protozoan parasites from the genera *Trypanosoma* and *Leishmania* are members of the Trypanosomatidae family and the order Kinetoplastida. Some species belonging to those two genera are responsible for several neglected diseases, among them, *Trypanosoma cruzi*, which causes the Chagas disease, and several *Leishmania* species responsible for Leishmaniasis (See Figure 5) [39, 40].

Trypanosomatids from the genera *Trypanosoma* and *Leishmania* are dixenous parasites transmitted by hematophagous insects. During their life cycle, they are subjected to changes in morphology, cell biology and biochemistry, which make the understanding of their infectious processes challenging [37, 39, 40]. Nevertheless, some similarities observed in the molecular mechanisms and metabolic pathways of species from the genera *Trypanosoma* and *Leishmania* have made trypanosomatid-specific active sites a reasonable alternative to use in targets-based studies [39].

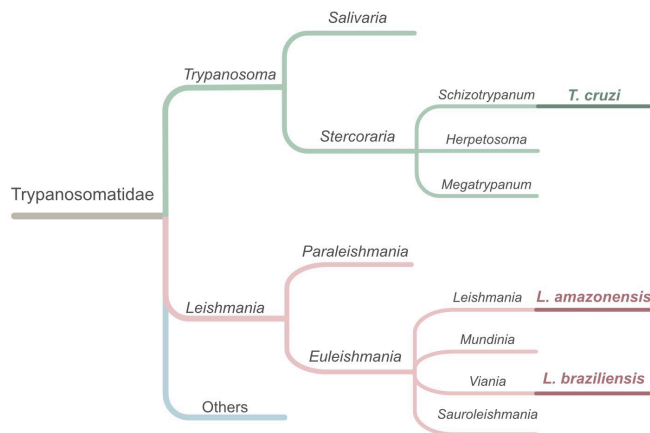


Figure 5

Taxonomic classification of the species under study *T. cruzi*, *L. braziliensis* and *L. amazonensis*

1.6.1 The Chagas disease

The Chagas disease, also known as American Trypanosomiasis, was discovered by Doctor Carlos Justiniano Chagas in Brazil at the beginning of the 20th Century. The protozoan parasite *Trypanosoma cruzi* causes the Chagas disease, which is transmitted by Triatomine bugs [41], these bugs live in the cracks of walls and bite their victims on exposed skin during the night. After the bite, they excrete *T. cruzi* trypomastigotes near the biting site making the victim to scratch the contaminated area, as a consequence, the disease is contracted [40, 41].

Chagas disease is endemic in 21 Latin American countries but nowadays it can be found in other continents (See Figure 6); most of the cases have been observed in Argentina, Brazil and Mexico [41]. This disease mostly affects people belonging to the lowest socioeconomic classes who may not have access to a proper social healthcare system nor have the resources to afford treatment privately [42, 43].

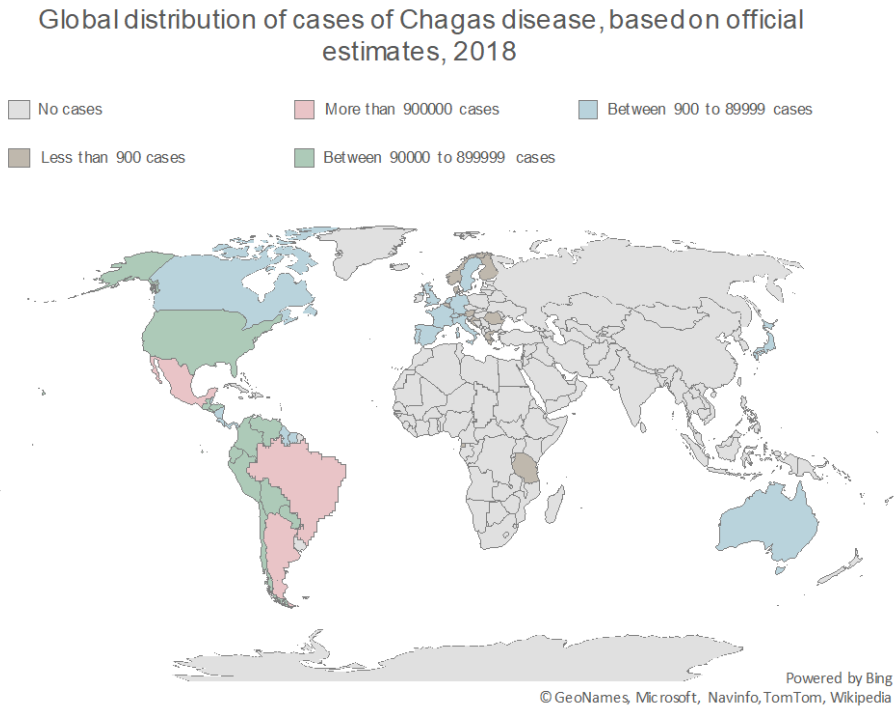


Figure 6
Chagas disease global distribution map based on official estimates for 2018 [44]

Currently around 6 to 7 million people are infected, 75 million people are at risk, and up to 30% of the chronically infected develop cardiac alterations [41].

The Chagas disease is developed in 2 phases: The acute phase and the chronic phase. During the acute phase, *T. cruzi* metacyclic trypomastigotes infect various cell types around the Triatomine bug bite, once inside the cell, they transform into amastigotes and multiply by binary fission. This process takes approximately 1 week, then the host cell ruptures and the amastigotes differentiate into motile trypomastigotes, which are released into the bloodstream and distributed throughout the body [45].

The acute phase continues until the immune system control the replication process, which takes around 2 months [45, 46]. Before that, another Triatomine bug

can ingest metacyclic trypomastigotes in a blood meal, to subsequently transform them into epimastigotes, which replicate in their midgut. Afterward, the epimastigotes move to the hindgut, where they differentiate into metacyclic trypomastigotes, closing the life cycle of the parasite (See Figure 7) [40].

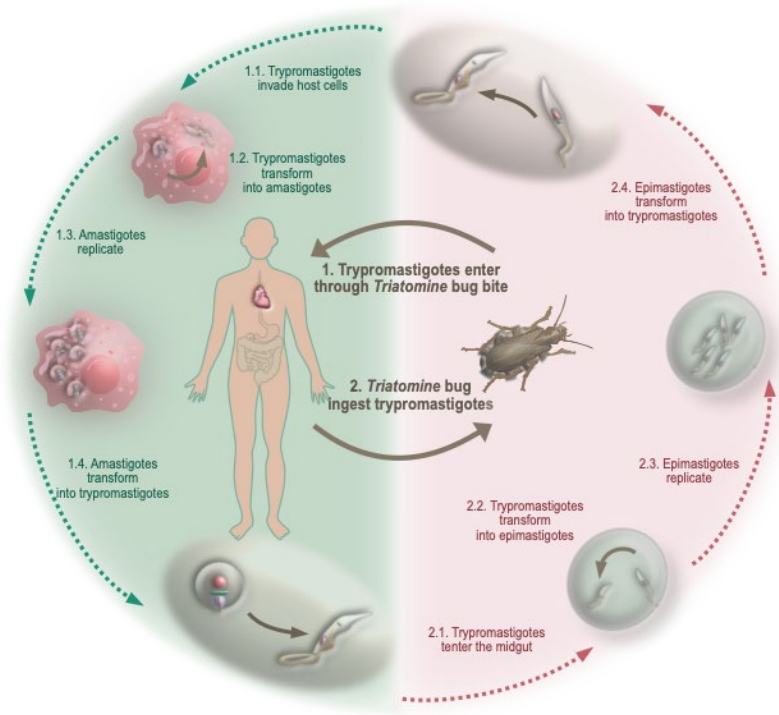


Figure 7
Life cycle of *T. cruzi*

During the acute phase, more than 50% of the infected does not show any symptoms, the rest may show a skin lesion around the bite site, eye swelling, fever, headache, enlarged lymph glands, pallor, muscle pain, difficulty in breathing, and abdominal pain as a result of the activation of the immune system [41, 46].

During the chronic phase, parasites may be hidden in different tissues for decades, producing eventually a chronic inflammatory response, which can predominantly lead to cardiomyopathy induced by the damage produced in the heart tissue [41, 46]. It is thought that *T. cruzi* is also present in the adipose tissue, where the parasite can hide for a long time, as a result of nutrient availability and longevity (approximately 10 years) of adipose cells [47].

Approximately 30% of the infected develop cardiac problems and 10% gastrointestinal problems [41], an early diagnosis is essential for the treatment [41,

42], which may take between 30 to 60 days and involves the nitro-heterocyclic drugs, benznidazole or nifurtimox, which nevertheless, have produced adverse effects in 40% of the patients [43, 48, 49].

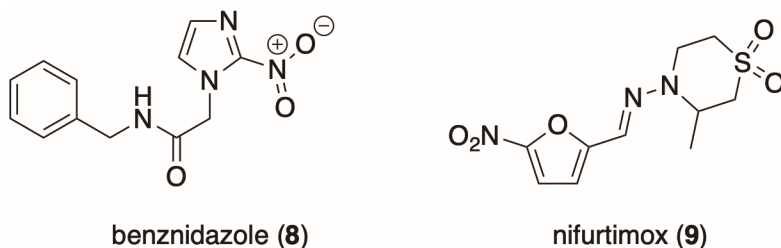


Figure 8
Benznidazole y nifurtimox

Benznidazole is the least effective during the chronic face and high-dose treatment has been observed to produce, occasionally, hypersensitivity, digestive intolerance, anorexia, asthenia, headache and sleeping disorders [46, 49].

1.6.2 Leishmaniasis

Leishmaniasis, also caused by trypanosomatid parasites, is transmitted by the bite of an infected female *Phlebotomine* sandfly [50]. Leishmaniasis can be found in three forms: cutaneous, mucocutaneous and visceral, and several *Leishmania* species can produce them (See Figure 9).

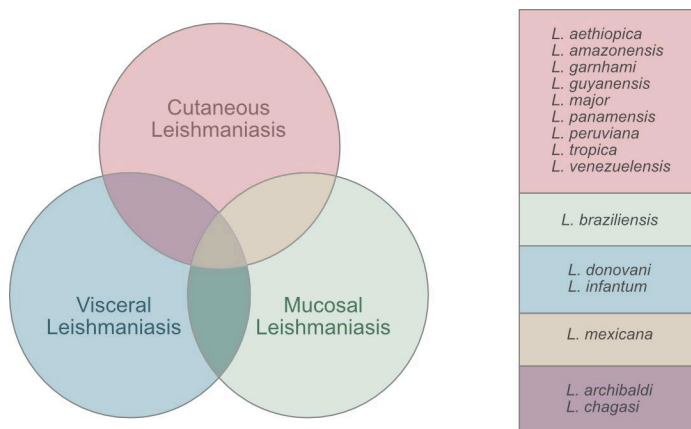


Figure 9
The three main types of Leishmaniasis and the species that produce them [50]

The development of localized lesions in the skin that heal spontaneously, is the characteristic of cutaneous leishmaniasis, nevertheless some cases require treatment to heal the wounds: When *L. amazonensis* causes the infection, ulcers spread via lymphatics (diffuse form); and when *L. tropica* causes it, lesions around the edges of healed ulcers develop (recidivans form) [51, 52].

Mucosal leishmaniasis, which is mainly produced by *L. braziliensis* causes the destructive inflammation of mucous membranes, generating non-self-healing wounds in the nose, mouth, pharynx and larynx [50-52].

Visceral leishmaniasis caused by *L. donovani* and *L. infantum* is the only fatal form of the disease, producing fever, weight loss and enlargement of the spleen and liver [50, 52, 53].

All Leishmaniasis forms may remain asymptomatic for long periods, and around 700 000 to 1 million new cases are registered mainly in the poorest regions of Africa, Latin America and East Asia. The infected also face socio-economic stigmas in different regions, which have damaging effects on their mental health [50, 54].

Global distribution of cases of all leishmaniasis types, based on reported cases, 2005-2018

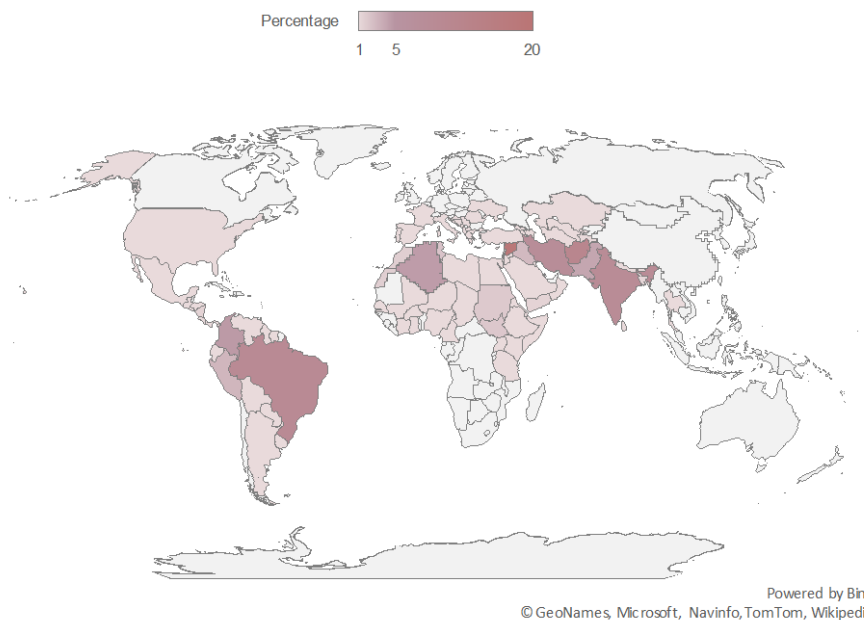


Figure 10
Leishmaniasis global distribution map based on reported cases during 2005 to 2018 [55]

Leishmania parasites life cycle begins with the bite of an infected female *Phlebotomine* sandfly, through which *Leishmania* promastigotes are transferred to the human host. The host's macrophages phagocytize the promastigotes, which differentiate into amastigotes that replicate until the cell breaks. The amastigotes are then spread throughout the body, now, another sandfly can ingest them during a blood meal. Inside the sandfly, the amastigotes travel to its gut, where they are transformed into promastigotes, and replicate to later migrate to the hypostome in order to infect another vertebrate host [51].

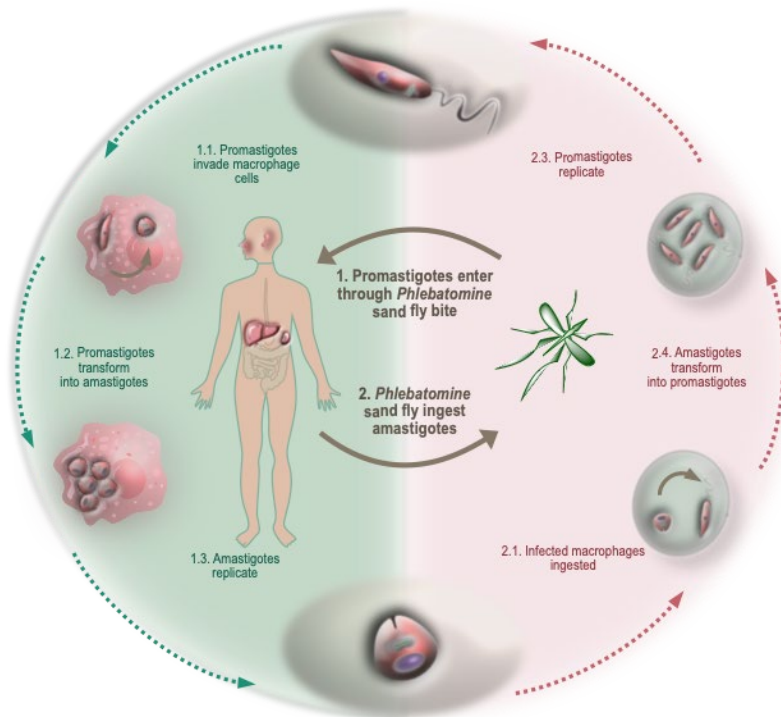
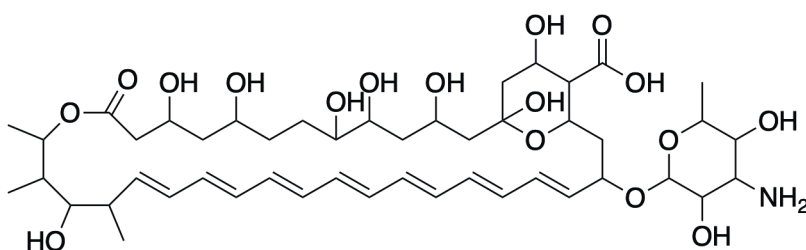


Figure 11
Life cycle of *Leishmania* spp.

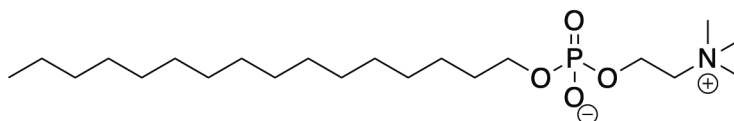
Leishmania promastigotes get into the host without alarming the immune system, by naturally dying inside the sandfly generating apoptotic-like promastigotes, which are injected mixed with the living parasites, producing a non-aggressive activation of the immune system [56, 57]. It is still unknown how the parasites survive inside the macrophage, how they are distributed in the body, and how the immune response is modulated. However, proteins related to the immune system appear to be important [53, 57]. Different proteins are expressed by different *Leishmania* parasites, as well as in their different morphological forms (promastigote and

amastigote), which produce difficulties in the identification of potentially useful molecular target [53].

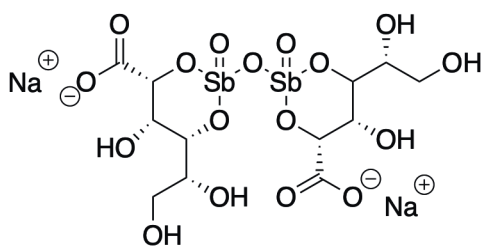
As Leishmaniasis infective process is not well understood, there are no specific treatment yet. Some of the currently used drugs have been discovered in repurpose studies, and not all information about their mode of action is known [52]. Pentavalent antimonials, for example, act through reduced Sb^{III} , however the mechanism is not understood [51, 58, 59]. Amphotericin B has been used before as antifungal and seems to act on the parasites by inhibiting ergosterol biosynthesis, however; the adverse effects observed and the need of hospitalization are inconvenient factors [59]. Miltefosine is the only drug that can be taken orally, but serious side effects have been reported; in addition, *L. braziliensis* have not shown sensitivity to this drug [59].



Amphotericin (10)



Miltefosine (11)



Sodium stibogluconate (12)

Figure 12
Amphotericin B, Miltefosine and sodium stibogluconate

Currently new compounds which possess immunomodulatory and antileishmanial activity are being studied. Leishmaniasis is known to compromise the immune response, therefore it might be convenient to also identify such immunomodulatory substances as potential drug candidates [60].

1.7 Secondary metabolites from *Bouerreria pulchra*

Pulchrol and pulchral are natural benzo[*c*]chromenes isolated from the heptane fraction of *Bouerreria pulchra*'s roots [61]. This plant, also known as "Bakalche" is native from the Yucatan province in Mexico, where is traditionally used to treat cutaneous diseases, injuries, viral infections and fevers [62, 63]. Antiparasitic studies on *B. pulchra* have also been developed, and showed that the ethanolic extract obtained from its leaves possess potent activity against *T. cruzi* [64].

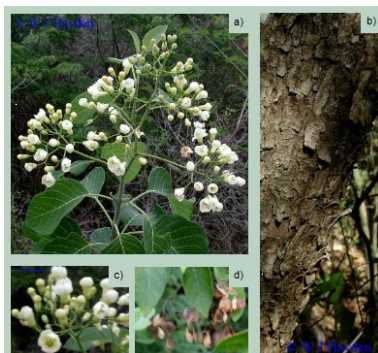


Figure 13
a) *Bouerreria Pulchra*, b) Bark, c) Flowers, d) Fruits [65]

Further antiparasitic studies on the compounds isolated from *B. pulchra* (pulchrol and its analogue pulchral, Figure 14) have reported potential toxicity against several *Leishmania* species (*L. braziliensis*, *L. amazonensis*, *L. mexicana*) and particularly against *T. cruzi* [61]. Pulchrol's possible potential as antiparasitic compound, and the low yields in which it was obtained during the isolation process, have led to the development of a synthetic route which was reported earlier [66, 67].

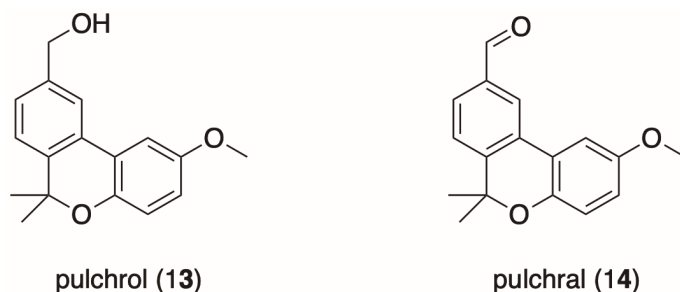


Figure 14
Structures of pulchrol and pulchral

1.8 Aim of the thesis

The objective of this thesis is to find the structure-activity relationships (SARs) for pulchrol and its synthetic analogues relative to their bioactivity measured toward various trypanosomatids. From this analysis, we expect to grasp on the possible role that different functionalities play in the antiparasitic activity presented here, additionally we will depict a preliminary view of the space surrounding pulchrol in a possible active site by presenting a pharmacophore hypothesis. As a consequence of our findings, we hope to contribute to the knowledge on antiparasitic compounds with potential to treat NTDs, particularly Leishmaniasis and the Chagas disease, we also expect our results will be of good use, for developing further studies on the pulchrol scaffold.

For this investigation, several synthetic pulchrol analogues were prepared with systematic modifications in different positions of the benzo[*c*]chromene scaffold. Each one of the prepared analogues was assayed *in vitro* against *T. cruzi* epimastigotes, *L. braziliensis* promastigotes and *L. amazonensis* promastigotes. Additionally, their cytotoxicity was measured in murine macrophage cell lines (RAW) to calculate their selectivity indexes as the ratio between the cytotoxicity and the antiparasitic activity.

Initially, some improvements in the previously published pulchrol synthetic route that are implemented here are presented in Chapter 2, in addition SARs for the analogues with transformations on the benzyl alcohol in the A-ring are discussed. In Chapter 3 the synthesis of analogues with modifications on the B- and C-rings are described and their SARs discussed. In Chapter 4 analogues with more than one modification are presented, among those the natural compounds didehydroconicol and cannabinol, their SARs are discussed in Chapter 4. Finally, Chapter 5 summarizes the antiparasitic activity in a pharmacophore hypothesis, and a qualitative analysis of the ADMET properties for the compounds is presented.

2 Modifications in the A-Ring

2.1 Background

2.1.1 Benzochromenes

Compounds belonging to the benzochromene type of molecule are often found in nature, and many of them have been isolated from endophytic fungi, lichens, vegetal and marine species [61, 68-74], benzochromenes with different substitution patterns have also been prepared synthetically [75-81]. Many natural and synthetic benzochromenes possess a wide range of bioactivities and they might be promising molecules for developing lead compounds with therapeutic applications [82].

Benzochromenes are polycyclic aromatic compounds characterized for the presence of a chromene moiety as part of their structure. The chromene structural form, features an oxygen heterocycle and appears to be an important component in several biologically active compounds. This molecular scaffold is formed by the fusion of a benzene ring with a pyran ring system. In turn, the fusion of a second benzene ring with the chromene moiety generate the benzochromene scaffold, which can be classified into four categories according to the position where the benzene ring is placed: benzo[*c*]chromenes, benzo[*f*]chromenes, benzo[*g*]chromenes and benzo[*h*]chromenes [82], their basic structural forms can be observed in Figure 15.

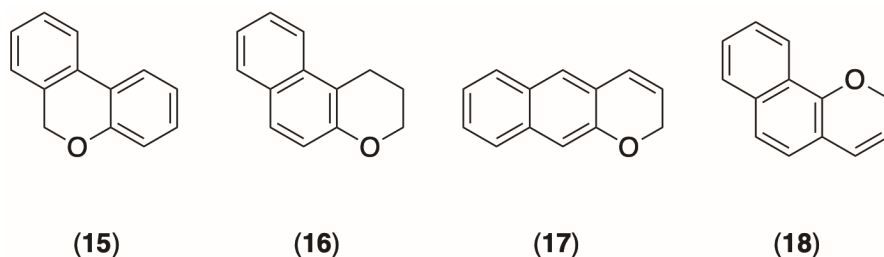


Figure 15

Different types of benzochromenes : (15) benzo[*c*]chromene, (16) Benzo[*f*]chromene, (17) Benzo[*g*]chromene, (18) Benzo[*h*]chromene [82]

2.1.2 Bioactive benzochromenes

Compounds bearing an angular benzochromene scaffold have been isolated from natural sources or prepared in the laboratory synthetically and they have been shown to possess activity toward diverse biological systems. For instance, the natural benzo[*f*]chromene **19** was isolated from the roots of *Pentas bussei*, a plant known also as Mdohe in Kenya, where is traditionally used to treat gonorrhoea, syphilis and dysentery [73]. Natural benzo[*c*]chromene, didehydroconicol (**20**), was also isolated from the marine ascidian *Aplidium aff. Densum* and showed to possess an effect as bacteriostatic [74]. Another natural benzo[*c*]chromene, cannabiol (**21**), is one of the constituents of the leaves of *Cannabis sativa* [83], and it possesses binding affinity with the endocannabinoid receptor CB2 [84, 85] and with biological targets related to the immune system [86, 87]. Additionally, benzo[*c*]chromene-6-ones, known as graphislactones (structural type **22**), have been isolated from lichens belonging to the *Graphis* genus and different endophytic fungus species [68-72]. Some of those natural compounds are active toward the colorectal adenocarcinoma cell line SW1116 [71]. Further studies on graphislactones have also led to the development of a synthetic route to obtain them in the laboratory [75].

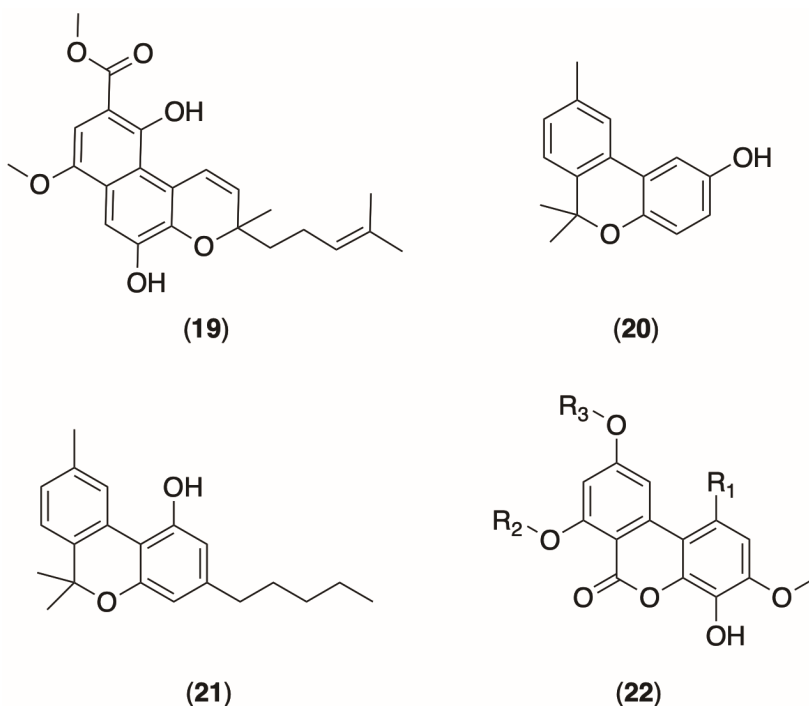


Figure 16
Natural bioactive benzo[*c*]chromenes

Benzo[*f*]chromene derivatives with structural forms **23** and **24**, have been prepared synthetically and have been found to possess antibacterial and antifungal activity respectively [76, 78]. Derivatives bearing the benzo[*f*]chromen-3-one skeleton (**25**) have been shown to be active toward cancer cell lines A546 (lung carcinoma), MCF7 (breast cancer) and A375 (melanoma), when they are substituted with alkyl groups [77]. Similarly, synthetic benzo[*h*]chromenes with alkyl substituents (generic structure **26**), have been found to possess anticancer activity toward cell lines MCF7, HCT116 (colon carcinoma) and HepG-2 (hepatocyte carcinoma) [79]. Besides, synthetic hydroxylated derivatives of natural benzo[*c*]chromen-6-one, urolithin (**27**), have been shown to possess potential as treatment of Alzheimer disease, since they have been shown to inhibit acetyl- and butyryl-cholinesterase enzymes [80]. Moreover, benzo[*c*]chromenes and benzo[*c*]chromen-6-ones, **28** and **29**, have been found to be selective ligands for the estrogen receptor ER β [81].

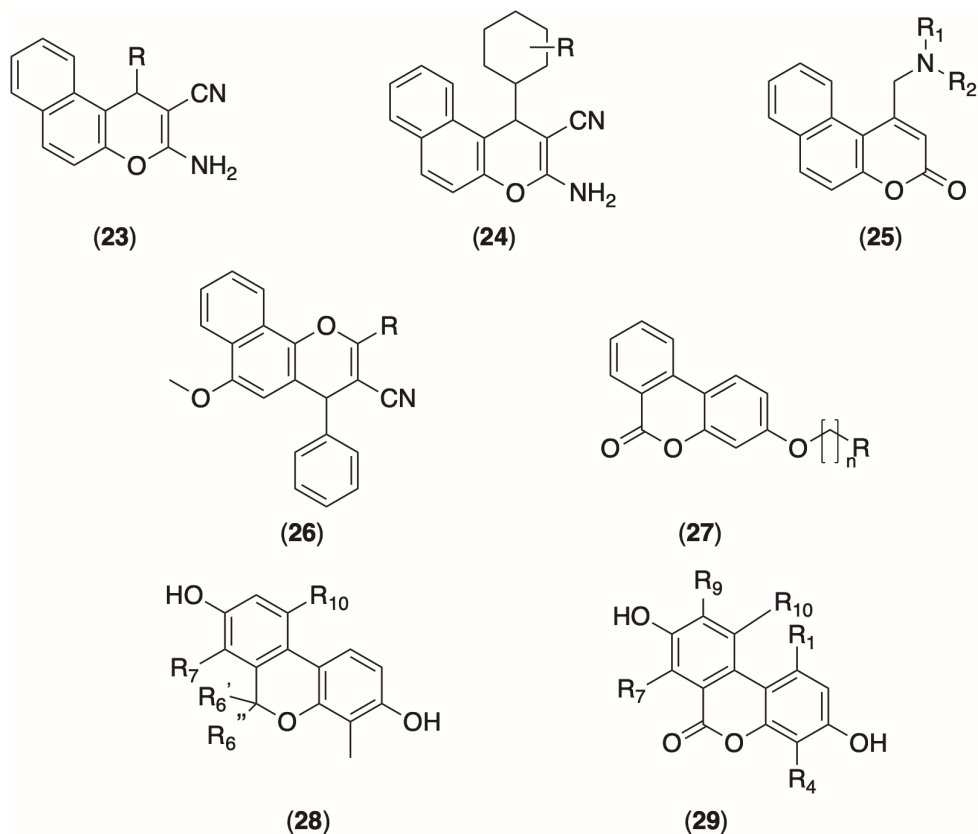


Figure 17
Synthetic bioactive benzochromenes

2.1.3 Synthesis of benzo[*c*]chromenes

There are primarily two synthetic strategies used to prepare benzo[*c*]chromenes: One way is by intramolecular biaryl formation from phenylbenzyl ethers through functionalization of C-H aromatic bonds (path A, Figure 18) and subsequent cyclization. This strategy can be developed either by transition-metal catalysed reactions using palladium [88, 89] or in the absence of transition-metals using potassium *tert*-butoxide to promote the biaryl formation via a single electron transfer [90-92]. Another important synthetic strategy to prepare the biaryl intermediate is by metal catalysed Suzuki-Miyaura cross-coupling reaction between an *o*-halo-benzoic acid and a 2-methoxyphenylboronic acid, followed by cyclization (path B, Figure 18) [93, 94].

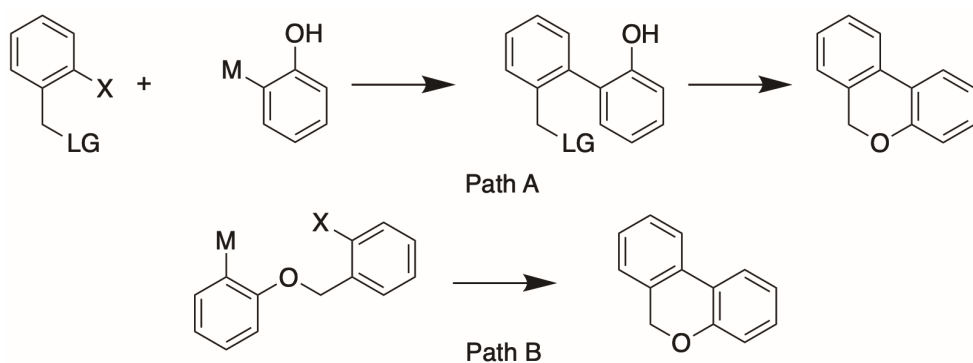


Figure 18
Main strategies for the synthesis of benzo[*c*]chromenes

Other synthetic routes to obtain the biaryl intermediate are by dicarbonyl cycloaddition to chromenes [95] or through Diels-Alder cyclo-addition reaction under high pressure [96, 97].

2.2 Pulchrol synthesis

The synthesis of the natural benzo[*c*]chromene pulchrol (**13**) was previously developed in our group and was first reported in 2014. In order to prepare the biaryl intermediate **33**, which is crucial in the synthesis of pulchrol (**13**), a Suzuki-Miyaura coupling reaction was performed between a 2-methoxyphenylboronic acid and a halogenated ester. Subsequently, the biaryl intermediate **33** was cyclised by acid catalysis, after being subjected to double alkyl addition to the ester group to form a tertiary alcohol (**34**) [66].

In this investigation we prepared pulchrol based on this synthetic route, however, in order to increase the yield and improve the reaction conditions, some modifications were introduced (see Figure 19).

In a similar way as in the synthetic route reported in 2014 [66], we have used the commercially available 3-iodo-4-(methoxycarbonyl)benzoic acid (**30**) as the starting material. In accordance with the previously published procedure, the starting material was reduced to the corresponding benzyl alcohol (methyl 4-(hydroxymethyl)-2-iodobenzoate (**31**), using a borane-tetrahydrofuran complex in THF as solvent, at 0 °C (step a). Afterward, the benzylic hydroxyl group was protected with *tert*-butyldiphenylchlorosilane (TBDPSCI) using pyridine as solvent (step b) to obtain intermediate **32**.

To obtain the biaryl intermediate (**33**), a Suzuki-Miyaura coupling reaction between 2,5-dimethoxyphenylboronic acid and the intermediate **32** was conducted using palladium-tetrakis(triphenylphosphine) (Pd(PPh₃)₄) as catalyst and K₂CO₃ as base in dimethoxyethane (DME)/H₂O 4:1 as solvent (step c). In the investigation published in 2014, this reaction was reported to work successfully at 120 °C yielding 83% of the biaryl intermediate **33**, yet 14 h were required for the reaction to be completed [66]. Here, we performed this reaction by microwave-assisted Suzuki-Miyaura coupling, which has been reported to reduce the reaction times and increase the yields [98]. As a result, we obtained 85%-90% yield of the biaryl intermediate (**33**) in 30 min, executing the reaction at 100 °C in a microwave reactor.

For the synthesis of the intermediate **34**, the ester group in **33** was transformed into a tertiary alcohol by a double alkyl addition using two equivalents of methyllithium (MeLi) in THF at 0 °C (step d) instead of MeMgBr in THF at 40 °C [66]. As a result, the reaction time decreased from 18 h [66] to 8 h. Furthermore, due to the milder conditions in which the reaction was conducted, a cleaner product that was considerably easier to purify was obtained and the yield of the product (**34**) was comparable to that reported before [66].

Finally, during the cyclization step (step e) a larger excess of hydroiodic acid (HI) (10 equiv) was used to obtain pulchrol (**13**), this made possible to avoid the formation of cannabidiol-type biaryl by-products and to obtain the deprotected product directly, in Figure 17 the scheme for the synthetic route used to prepare pulchrol is shown.

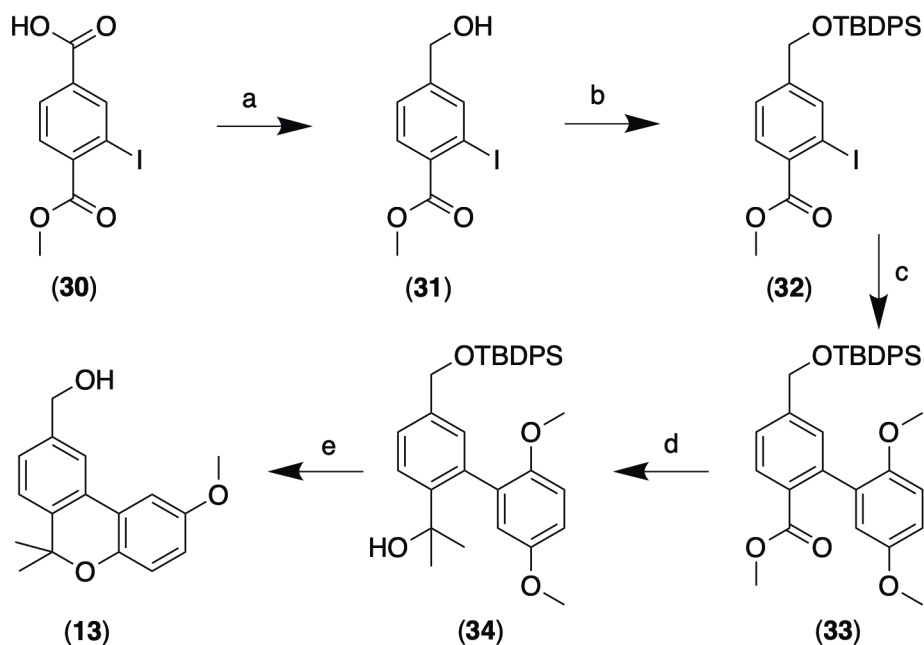


Figure 19

Synthetic route to prepare pulchrol. Reagents and conditions: (i) Borane-THF complex, dry THF, 0 °C (ii) TBDPSCI, pyridine (iii) Microwave reaction: 2,5-dimethoxyphenylboronic acid, K₂CO₃, tetrakis(triphenylphosphine)palladium(0) in DME/Water 4:1, 30 min, 100 °C (iv) MeLi, dry THF, 0 °C (v) HI 55% wt, MeCN.

2.3 Transformations of the benzyl alcohol functionality

The focus in this part of our investigation is to understand the importance of the benzyl alcohol functionality for the antiparasitic activity. With that in mind, we have prepared several analogues with systematic variations in the benzyl alcohol region (the A-ring), using pulchrol as starting material (See Figure 20 for the structural types). A reduced pulchrol analogue was used to evaluate the importance of the hydroxyl group for the bioactivity, and various transformations on the benzyl alcohol were performed to determine its role, either as hydrogen bond donor or hydrogen bond acceptor. We have also prepared analogues with substituents of different bulk and size to explore the space availability, and to evaluate possible Van der Waals interactions around the benzyl alcohol region (See the experimental part in Paper 1 for details).

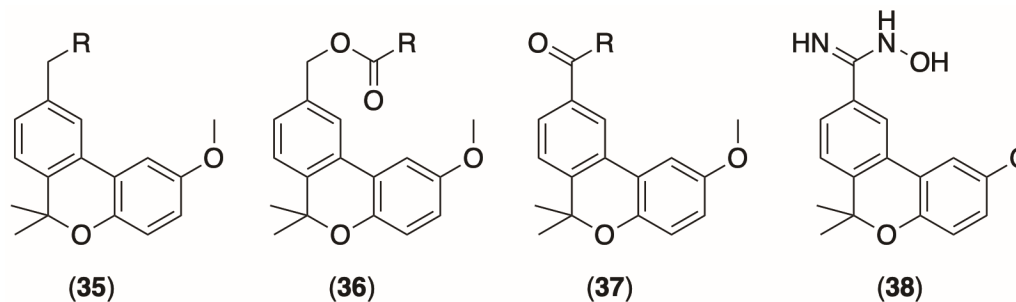


Figure 20

Pulchrol's analogues structural. **35a** R = H; **35b** R = Cl; **35c** R = methoxy; **35d** R = isopropoxy; **35e** R = 4-methylpentyloxy; **35f** R = isopropylamino; **35g** R = isobutylamino; **35h** R = isopentylamino; **36a** R = Me; **36b** R = isopropyl; **36c** R = *tert*-butyl; **36d** R = propyl; **36e** R = isobutyl; **36f** R = neopentyl; **36g** R = pentyl; **36h** R = 2-cyclopentylethyl; **36i** R = vinyl; **36j** R = 2-furanyl; **36k** R = phenyl; **36l** R = cyclohexyl; **37a** R = H; **37b** R = Me; **37c** R = OH; **37d** R = methoxy; **38** R = NH₂. See Experimental part for synthetic details.

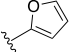
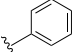
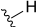
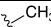
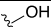
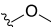
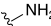
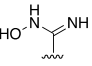
Table 1 contains the bioactivity results obtained from the *in vitro* assays toward *T. cruzi*, *L. braziliensis* and *L. amazonensis*. Additionally, the cytotoxicity measured on the murine macrophage cell line (RAW) is presented alongside the selectivity index, which was calculated as the ratio between the cytotoxicity and the antiparasitic activity for each one of the analogues.

Table 1

Antileishmanial, antitrypanosomal and cytotoxic activity of the pulchrol analogues, compared to the positive controls Benznidazole and Miltefosine. See Paper 1 for the experimental details.

Mol.	R	<i>T. cruzi</i>		<i>L. braziliensis</i>		<i>L. amazonensis</i>		Cytotoxicity ^a
		IC ₅₀ (μM)	SI ^b	IC ₅₀ (μM)	SI ^b	IC ₅₀ (μM)	SI ^b	IC ₅₀ (μM)
13		18.5 ± 9.6	1.7	59.2 ± 11.8	0.5	77.7 ± 5.6	0.4	30.7 ± 1.1
35a		51.1 ± 17.7	2.0	69.6 ± 5.9	1.4	85.3 ± 5.9	1.2	99.5 ± 22.0

35b		38.1 ± 0.4	1.6	17.1 ± 0.1	3.5	35.0 ± 2.8	1.7	59.2 ± 14.5
35c		24.6 ± 3.5	1.3	49.2 ± 15.8	0.7	56.3 ± 12.0	0.6	33.1 ± 2.1
35d		12.9 ± 0.3	2.5	35.2 ± 3.2	0.9	35.2 ± 3.8	0.9	32.0 ± 0.3
35e		9.0 ± 0.6	3.5	127.2 ± 11.3	0.3	28.2 ± 8.5	1.1	31.6 ± 5.6
35f		70.6 ± 9.6	0.4	83.5 ± 32.1	0.4	67.8 ± 13.8	0.4	29.5 ± 9.6
35g		15.4 ± 4.0	0.8	25.8 ± 6.2	0.5	15.4 ± 3.1	0.8	12.3 ± 1.2
35h		5.9 ± 1.2	1.3	15.9 ± 0.9	0.5	17.7 ± 7.4	0.4	7.4 ± 2.4
36a		14.4 ± 1.6	2.3	28.8 ± 0.3	1.1	26.9 ± 0.6	1.2	32.7 ± 22.4
36b		8.8 ± 0.9	3.0	17.6 ± 0.9	1.5	26.7 ± 2.4	1.0	26.4 ± 5.9
36c		6.4 ± 0.1	3.0	17.4 ± 1.7	1.1	20.5 ± 0.6	1.0	19.8 ± 0.9
36d		16.2 ± 3.2	6.4	57.8 ± 2.4	1.8	79.3 ± 9.4	1.3	102.8 ± 35.3
36e		4.2 ± 1.1	6.7	13.1 ± 0.4	2.2	14.5 ± 0.1	1.9	28.2 ± 9.0
36f		5.7 ± 0.3	3.3	20.0 ± 4.2	1.0	19.5 ± 0.8	1.0	19.0 ± 3.0
36g		22.8 ± 5.7	2.3	27.7 ± 0.3	1.9	42.3 ± 8.7	1.2	52.1 ± 8.1
36h		8.4 ± 3.3	6.1	122.4 ± 27.9	0.4	30.9 ± 3.0	1.6	50.7 ± 17.7
36i		13.1 ± 0.5	3.9	24.3 ± 0.8	2.1	40.5 ± 8.7	1.3	51.3 ± 8.2
36j		7.4 ± 0.9	5.4	5.7 ± 0.5	7.0	6.9 ± 1.7	5.8	40.1 ± 12.6

36k		3.8 ± 0.3	7.9	12.8 ± 0.1	2.4	12.8 ± 1.8	2.4	30.5 ± 3.6
36l		5.9 ± 0.5	4.7	21.0 ± 4.3	1.3	21.9 ± 7.7	1.3	27.8 ± 10.7
37a		24.2 ± 4.1	1.6	24.2 ± 7.5	1.6	29.8 ± 11.2	1.3	38.8 ± 3.7
37b		21.2 ± 9.2	1.5	28.3 ± 7.1	1.1	43.2 ± 8.2	0.7	31.9 ± 7.1
37c		56.3	4.4	65.1 ± 16.5	3.8	198.7	1.2	246.2 ± 24.6
37d		31.8 ± 2.4	1.2	18.4 ± 5.7	2.1	59.0 ± 1.3	0.7	38.2 ± 2.7
37e		134.5 ± 38.8	0.4	144.7 ± 43.1	0.3	120.7 ± 21.2	0.4	49.8 ± 17.7
38		33.4 ± 14.9	0.8	52.0 ± 18.6	0.5	52.0 ± 16.7	0.5	26.4 ± 1.5
Benznidazole		19.2 ± 7.7	3.9					74.7 ± 9.1
Miltefosine				13.0 ± 1.2	5.9	10.8 ± 1.5	7.1	76.6 ± 3.2

^a Toxicity was measured on RAW cells, see Experimental for details, ^b SI, selectivity index (cytotoxicity/anti-protozoal activity).

2.4 Antiparasitic activity

Previous investigations have reported that natural product pulchrol (**13**) is toxic toward some trypanosomatid parasites [61]. In this investigation, the antiparasitic activity of pulchrol (**13**) is measured toward *T. cruzi*, *L. braziliensis* and *L. amazonensis* (See Table 1). Pulchrol was found to have potent antiparasitic activity toward *T. cruzi* epimastigotes ($IC_{50} = 18.5 \mu\text{M}$), which is comparable to the bioactivity measured for the positive control, benznidazole ($IC_{50} = 19.2 \mu\text{M}$), currently used to treat the Chagas disease. In addition, biological assays showed that pulchrol is moderately toxic toward *L. braziliensis* and *L. amazonensis* (IC_{50} values: $59.2 \mu\text{M}$ and $77.7 \mu\text{M}$ respectively). Other *Leishmania* species, like *L. mexicana* (not included here) have also been found to be more sensitive to pulchrol ($IC_{50} = 17 \mu\text{M}$) in previously reported studies [61].

Since pulchrol structure (**13**) does not contain functionalities that are associated with reactivity or unspecific biological activity, we were motivated to synthesize and assay analogues of **13**. For this study, the natural products pulchrol and pulchral (**13** and **35a**), together with 25 analogues were prepared and assayed against the abovementioned parasites. Their cytotoxicity was measured in a mammalian murine macrophage RAW cell line in order to get an impression of the compound's selectivity. The biological results are presented in Table 1.

2.4.1 Antiparasitic activity toward *T. cruzi*

Our initial aim was to evaluate the importance of the hydroxyl group for pulchrol's activity, to achieve this objective, pulchrol (**13**) was reduced to the 9-methyl analogue **35a**. This analogue showed to be considerably less active ($IC_{50} = 51.1 \mu\text{M}$) compared to **13**, consequently evidencing the relevance of the benzyl alcohol.

To mimic possible Van der Waals interactions around the benzylic carbon, the hydroxyl group in pulchrol (**13**) was replaced with a chlorine atom (**35b**). However, the bioactivity measured for **35b** ($IC_{50} = 38.1 \mu\text{M}$) was found to be inferior compared to that shown by **13**, suggesting that the biological activity is favoured by interactions involving the oxygen atom in the benzylic position.

The benzyl alcohol possible participation in binding interactions within the active site drove us to evaluate its role as either hydrogen bond donor or hydrogen bond acceptor. To determine its hydrogen bond donor capacity, methyl ether **35c** was prepared and assayed. Analogue **35c** showed to be slightly less active ($IC_{50} = 24.6 \mu\text{M}$) than **13**, indicating that the hydroxyl group acts more as a hydrogen bond acceptor. Bulkier ethers **35d** and **35e** were also prepared, however, contrary to the

bioactivity results reported for the methyl ether **35c**, they were more potent than **13** ($IC_{50} = 12.9$ and $9.0 \mu\text{M}$, respectively), suggesting that lipophilic interactions occur in a hydrophobic pocket placed near the benzyl alcohol oxygen in the target protein. The bulkier ethers also showed better selectivity compared to pulchrol and the methyl ether analogue (**13** and **35c**, respectively). Substituted amines bearing bulky alkyl groups were also prepared (**35f**, **35g**, and **35h**), somewhat surprisingly, the isopropylamino analogue **35f** was found to be considerably less potent and selective than the isopropyl ether **35d**. On the other hand, the larger isobutyl and isopentyl amine analogues **35g** and **35h** ($IC_{50} = 15.4$ and $5.9 \mu\text{M}$, respectively) were as potent as **35e** (the pulchrol ether with the largest substituent).

Pulchrol esters **36a** to **36l** were also prepared and assayed. The results of the antitrypanosomal assays showed that most of the esters were more potent and selective compared to pulchrol (**13**). Amongst them, saturated esters **36a** to **36i**, showed good antitrypanosomal activity, particularly those prepared from acids with branched alkyl groups. Notably, the 3-methylbutanoic acid ester **36e** showed the highest potency and selectivity within this group ($IC_{50} = 4.2 \mu\text{M}$ and $SI = 6.7$). Similarly, all unsaturated esters (**36j-36l**) showed potent antitrypanosomal activity and high selectivity, indicating that π - π interactions with the binding pocket are favourable. The most potent and selective analogue between the unsaturated esters was found to be the furan-2-carboxylic acid ester **36k** ($IC_{50} = 3.8 \mu\text{M}$, $SI = 7.9$), which also showed the best results within all the analogues prepared in this part of the investigation. Furthermore, **36k** showed to be considerably more potent and even two times more selective than the positive control Benznidazole.

The benzyl alcohol in pulchrol (**13**) was also partially and totally oxidized to obtain the 1'-carbonyl analogues (**37a - 37e**) included in this study. The aldehyde **37a** and the methyl ketone **37b** were found to be equipotent compared to **13**, and similar selectivity indexes to pulchrol's were calculated for both analogues. In contrast, the carboxylic acid **37c** and the ester **37d** were less potent and less selective than pulchrol (**13**). However, it was the amide **37e**, which showed the lower toxicity toward *T. cruzi* and the highest cytotoxicity among all analogues in this study.

Finally, analogue *N*-hydroxy-9-carboximidamide **38**, which was obtained as a by-product was also assayed toward *T. cruzi*. It was found to possess considerably low potency, although, it was still more potent than the 9-carboxamide **37e**. The low antitrypanosomal activity measured for analogue **38** evidence the importance of lipophilic substituents around the benzylic position for the biological activity.

2.4.2 Antiparasitic activity toward *L. braziliensis*

To begin evaluating the importance of the benzyl alcohol in the antiparasitic activity toward *L. braziliensis*, the hydroxyl group was reduced to a methyl group (**35a**). Similar to the results obtained with *T. cruzi*, analogue **35a** was found to be slightly less potent than **13**, evidencing the importance of the benzyl alcohol. However, the benzyl chloride (**35b**) showed an interesting potency ($IC_{50} = 17.1 \mu\text{M}$) and selectivity ($SI = 3.5$) toward *L. braziliensis*, in contrast to *T. cruzi*. Therefore, the presence of an oxygen atom in the benzylic position may not be as important for *L. braziliensis* as it is for *T. cruzi*. These differences in the antiparasitic effects showed by **35b** indicate that the molecular targets in the two species are different.

Ethers **35c** to **35e** were also prepared and assayed. Two of them, one substituted with a methyl group (**35a**) and the other with an isopropyl group (**35b**) were slightly more potent than **13**, while the 4-methylpentyl ether **35e** showed to be considerably less potent, meaning that ethers with bulky substituents are not as favourable for the activity against *L. braziliensis* as they are for *T. cruzi*. Alternatively, the secondary amines **35f** to **35h** showed an identical trend in relation to *T. cruzi*, and the isopentylamino analogue **35h** ($IC_{50} = 15.9 \mu\text{M}$) was one of the most potent analogues against *L. braziliensis*.

Most of the esters (**36a-36l**) showed to be more potent than pulchrol (**13**) toward *L. braziliensis*, except the 3-cyclopentylpropanoate acid ester **36h**. As for *T. cruzi*, the saturated esters showed that bulky substituents are better for the bioactivity than straight alkyl chains. Similarly, all unsaturated esters (**36k-36l**) were more potent than pulchrol (**13**). However, unlike the results observed with *T. cruzi*, the selectivity showed by analogue **36k** was not as favourable, and its bioactivity was just as good as that of the positive control. Instead, the vinyl ester **36j** was the analogue that showed the highest potency and selectivity toward *L. braziliensis* ($IC_{50} = 5.7 \mu\text{M}$ and $SI = 7.0$), which were also better than those of the positive control.

Within the 1'-carbonyl analogues, it was observed that the aldehyde **37a**, the methyl ketone **37b** and especially the methyl ester **37d** were more potent, while the carboxylic acid **37c** and the *N*-hydroxy-9-carboximidamide (**38**) were just as good as **13**. Finally, the carboxamide **37e** was the least potent of all analogues.

2.4.3 Antiparasitic activity toward *L. amazonensis*

In the same way as before, the benzyl alcohol in pulchrol (**13**) was replaced for a methyl group to obtain analogue **35a**. Similar to the other parasites, no improvements in the antiparasitic activity were observed against *L. amazonensis*. The bioactivity observed for the chlorinated analogue (**35b**) was two times more potent compared to pulchrol's, following the same trend observed with *L. braziliensis*. All the ethers (**35c-35e**) prepared in this investigation were more potent than pulchrol (**13**). The bioactivity observed for the methyl and isopropyl ethers (**35c** and **35d**) was not as significant as the potency showed by the 4-methylpentyl

ether **35e**, although **35e** was found to possess a low activity toward *L. braziliensis*. For the secondary amines the observed bioactivity followed the same trend observed with *T. cruzi* and *L. braziliensis*. the isopropylamino analogues **35f** showed lower potency than the isobutyl- and isopentylamino analogues **35g** and **35h**. For the esters **36a** to **36l**, the results obtained were closely related to those observed with *L. braziliensis*, except for the 3-cyclopentylpropanoic acid ester **36h**, which was potent against *L. amazonensis*. As with *L. braziliensis*, the vinyl ester **36j** was the most potent among all compounds assayed in this part of the investigation, and its SI value (5.8) makes it the most selective compound.

Finally, the 9-carbonyl analogues were prepared and assayed toward *L. amazonensis*. The aldehyde and the methyl ketone (**37a-37b**) were more potent than **13**, while the increase in activity showed by the methyl ester **37d** and the *N*-hydroxy-9-carboximidamide **38** were minor. Following the results discussed for the other parasites, the carboxylic acid **37c** and the carboxamide **37e** were considerably less potent against *L. amazonensis* compared to **13**.

2.5 Conclusions

In this part of our investigation, we developed a more efficient synthetic protocol to prepare the natural products pulchrol and pulchral (**13** and **35a**), which were used as starting material for the preparation of 25 analogues with modifications on the benzylic alcohol functionality. The antiparasitic activity of all analogues, as well as the natural compounds **13** and **35a** was tested towards *T. cruzi* epimastigotes, as well as *L. braziliensis* and *L. amazonensis* promastigotes. However, the modifications were focused in just one part of the molecule, which prevented us from getting a full perspective of the structure activity relationships for pulchrol. For that reason, we present just general suggestions on the bioactivity trends in this part of the investigation.

Some other factors to consider are the complex biology of the trypanosomatid parasites under study, the lack of knowledge about the molecular targets in which pulchrol (**13**) and its analogues bind, and the differences that may exist in the binding sites between the parasites. Besides, variations in properties related to the structural diversity of the analogues could be responsible for the differences measured in the bioactivity and selectivity, for instance, the solubility may be responsible for the inability of a ligand to cross the cell membrane, and then, reach the target, producing a loss in the activity.

Having said that, we can understand from our biological results that the benzylic oxygen in pulchrol is important for the anti-parasitic activity against all parasites studied. However, the hydroxyl functionality was found to act more as a hydrogen bond acceptor than a hydrogen bond donor.

Most of the ethers and esters were more potent than pulchrol (**13**), particularly those substituted with branched alkyl groups. This indicates that a lipophilic pocket exists in the binding site; nevertheless, the shape and size of this pocket may differ between the parasites. The lipophilic pocket in *L. braziliensis* appears to have a limit on the space for approximately five carbons in the region in which the ester substituent is placed. On the other hand, *T. cruzi* and *L. amazonensis* targets seems to feature flat hydrophobic regions, in which the aromatic and planar substituents interact, increasing the activity as a result.

The analogue that showed the best potential as antiparasitic was the vinyl ester **36j**, which was more potent than pulchrol, most of the other analogues, and our positive controls (benznidazole and nifurtimox). Besides, its selectivity indexes were above 5 for all three organisms. Acrylic esters like **36j** react as Michael acceptors with highly reactive nucleophiles present in the active site. Thus, the enhanced potency and selectivity shown by **36j** may be due to a role as Michael acceptor, if this would be true, analogues from **36j** could be used to fish out molecular targets for trypanosomatid parasites.

3 Modifications in the B- and C-ring

In the last chapter, the importance of the benzyl alcohol for the antiparasitic activity of our lead compound pulchrol was determined, and how transformations of this functionality affect the biological activity was discussed [99]. In this part of the work, we wanted to study how substituents and combinations of substituents in the B- and C-rings affect the antiparasitic activity of pulchrol. To prepare the synthetic analogues for this part of the study, some modifications to the synthetic strategy used to prepare the compounds described in Chapter 2 were added. Some intermediates obtained previously were used as precursors for the synthesis of the compounds studied here.

From pulchrol's structure, we can see that there is only one position available for modification in the B-ring (position 6). To evaluate the effect that different substituents may have on the biological activity, the methyl substituents were replaced with longer alkyl groups, with one alkyl group and a hydrogen atom, and with two hydrogen atoms. Additionally, we intended to investigate the effect that transformations in the C-ring may produce, thus we have prepared analogues with different substitution patterns in three of the four available positions of the C-ring. Analogues with a methoxy group in positions different from C-2 (as in pulchrol), and compounds in which the methoxy group was replaced for alkyl substituents, were prepared. Finally, an analogue with no substituents in the C-ring was prepared, to evaluate the importance of the 2-methoxy substituent in pulchrol. Altogether we prepared 16 new analogues (**8a-8g**, **10a-10h**) with differences in the substituents and substitution pattern in the B- and C-rings. All of them were tested toward *T. cruzi* epimastigotes, as well as *L. amazonensis*, and *L. braziliensis* promastigotes. Their cytotoxicity was measured in murine macrophage cells (RAW), and a selectivity index was calculated for each compound as the ratio between the cytotoxicity and the antiparasitic activity.

3.1 Modification in the B-ring

To prepare the analogues with modifications in the B-ring, a synthetic approach partially based on the previously published synthetic route to obtain pulchrol [66] was used, and the common intermediate **33** was the starting point for the preparation of the B-ring derivatives (see Figure 21).

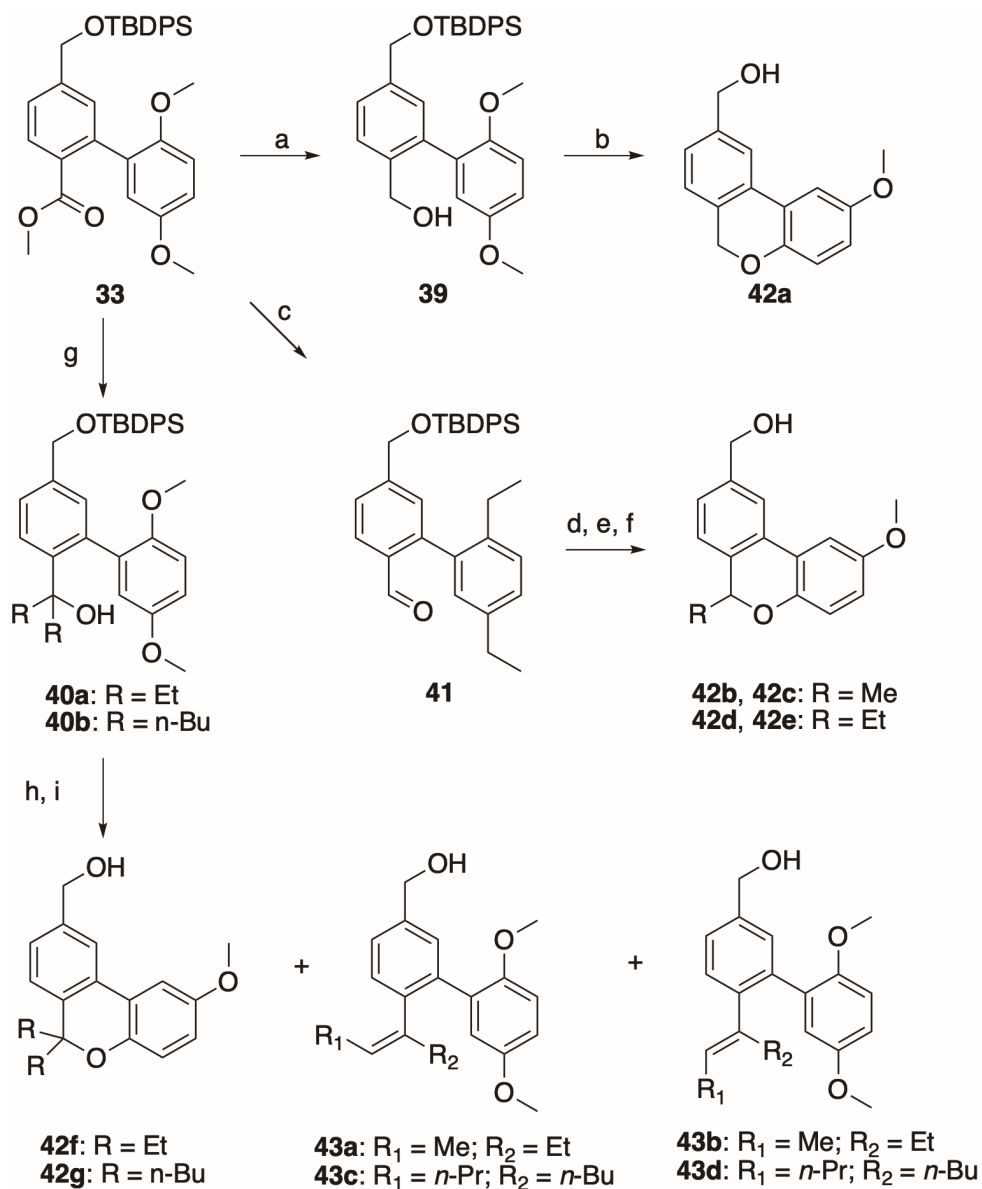


Figure 21

Synthetic route to prepare the B-ring analogues. Reagents and conditions: a) **33** (1 equiv), DIBALH (2.4 equiv), dry toluene, -78 °C; b) **39** (1 equiv), NaSEt (4 equiv), dry DMF, 110 °C; c) **33** (1 equiv), morpholine (2 equiv), DIBALH (1 equiv), dry THF, 0 °C; d) **41** (1 equiv), corresponding organolithic reagent (2 equiv), dry THF, 0 °C or -78 °C depending on the organolithic reagent; e) PBr₃ (0.34 equiv), Lil (3 equiv), dry CH₂Cl₂, rt; f) TBAF (2 equiv), THF, rt; g) **33** (1 equiv), organolithic reagent (4 equiv), dry THF, 0 °C or -78 °C depending on the organolithic reagent; h) **40** (1 equiv), HI (10 equiv), MeCN, rt; i) TBAF (1.1 equiv), THF, rt.

Initially compound **42a** substituted with two hydrogen atoms at position 6 was prepared to evaluate the importance of the alkyl substituents in the B-ring. To prepare **42a**, intermediate **33** was expected to react with NaSEt in dry DMF at 110 °C to yield the *ortho*-demethylated phenol **39** as intermediate, but instead we obtained the cyclized and deprotected 6,6-didemethylated compound (**42a**). It was the main product, but was obtained in low yields (7%). We also prepared the monosubstituted analogues **42b** – **42e** to evaluate the effect that just one alkyl substituent at C-6 may have in the antiparasitic activity. Compounds **42b** to **42e** were prepared by partially reducing the ester intermediate **33** to aldehyde **41**, which after organometallic alkyl addition was cyclized using PBr₃ in the presence of LiI [100]. The product of the reaction was a racemic mixture from which the enantiomers were separated by high-pressure liquid chromatography (HPLC) using a normal phase semipreparative chiral column. The pure enantiomers **42b** - **42e** were obtained in low yields (below 10%). Their absolute configuration was not determined, since all the enantiomers showed to possess equipotent antiparasitic activity (see Section 3.3).

To get some understanding of the space availability around the B-ring, longer alkyl groups were inserted at position 6. Intermediate **33** was used as the starting material to obtain intermediates **40a** and **40b** after double alkyl addition to the ester group using ethyllithium and butyllithium, respectively. Subsequently, intermediates **40a** and **40b** were cyclized following the procedure used to obtain pulchrol [99], the resulting products were the 6,6-diethyl and 6,6-dibutyl analogues **42f** and **42g**. However, the excess in hydroiodic acid used to avoid the formation of the cannabidiol byproducts during pulchrol synthesis [99], was not favourable during the preparation of **42f** and **42g**, and the cannabidiol-like compounds **43a** and **43b** were obtained together with **42f**, while **43c** and **43d** were formed together with **42g**. The mixtures were separated by semipreparative HPLC and the desired products were obtained in moderate yields (**42f**, 30%; **42g**, 56%).

3.2 Modifications in the C-ring

For the analogues with modification in the C-ring, the same procedure used for pulchrol was applied [99]. However, during the Suzuki-Miyaura coupling, different 2-methoxyphenylboronic acids were used, and the reaction time was increased from 30 to 60 min, resulting in the obtention of intermediates **44a-44h** in good yields (75%-92%). The procedure was then followed by the approach used for the synthesis of pulchrol, and after cyclization it was noted that most of the analogues substituted with alkyl groups in the C-ring were obtained in higher yields (72%-85%) than those substituted with methoxy groups.

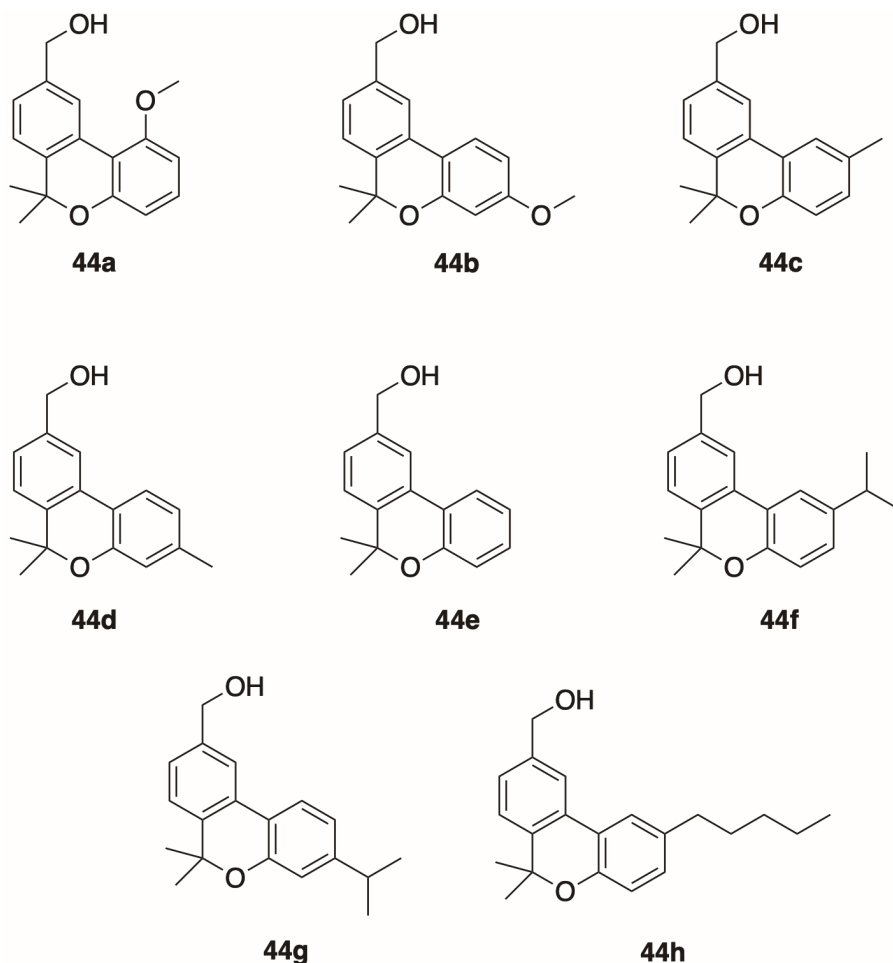


Figure 22
Analogues with modifications in the C-ring

3.3 Antiparasitic Activity

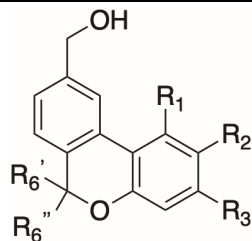
As was indicated in previous chapters, pulchrol has shown to possess activity toward trypanosomatid parasites. The most interesting activity was noted toward *T. cruzi* epimastigotes (IC_{50} 18.5 μ M), whereas moderate activity was observed against *L. braziliensis* and *L. amazonensis* promastigotes (59.2 μ M and 77.7 μ M, respectively).

In Chapter 2, we have discussed the effects that modifications on pulchrol's benzylic alcohol have in the antiparasitic activity. From the results we concluded

that the lipophilic and unsaturated ester analogues of pulchrol significantly increased the potency toward the parasites studied. In Chapter 3, we conducted an evaluation of the effect that modifications in the B- and C-rings have in the biological activity measured toward *T. cruzi* epimastigotes, and *L. braziliensis* and *L. amazonensis* promastigotes. The cytotoxicity was measured on mammalian murine macrophage cell lines (RAW), and the selectivity index was calculated as the ratio between cytotoxicity and the antiparasitic activity (see Table 2).

Table 2

Antileishmanial, antitrypanosomal and cytotoxic activity of the pulchrol analogues, compared to the positive controls Benznidazole and Miltefosine. See Paper 2 for the experimental details.



Mol	R ₆ '	R ₆ ''	R ₁	R ₂	R ₃	<i>T. cruzi</i>		<i>L. braziliensis</i>		<i>L. amazonensis</i>		Cytotoxicity ^a
						IC ₅₀ (μM)	SI ^b	IC ₅₀ (μM)	SI ^b	IC ₅₀ (μM)	SI ^b	
13	Me	Me	H	OMe	H	18.5 ± 9.6	1.7	59.2 ± 11.8	0.5	77.7 ± 5.5	0.4	30.7 ± 1.1
42a	H	H	H	OMe	H	66.0 ± 18.2	1.3	248.1 ± 54.1	0.3	132.1 ± 29.3	0.6	82.6 ± 9.5
42b	Me	H	H	OMe	H	35.9 ± 11.7	1.0	156.1 ± 23.4	0.2	156.1 ± 58.5	0.2	37.1 ± 3.9
42c	H	Me	H	OMe	H	67.1 ± 31.2	0.8	128.8 ± 24.6	0.4	71.8 ± 12.5	0.7	52.7 ± 9.0
42d	Et	H	H	OMe	H	51.8 ± 9.2	0.6	45.9 ± 20.3	0.7	71.4 ± 1.1	0.4	30.0 ± 3.7
42e	H	Et	H	OMe	H	37.0 ± 0.7	1.2	45.1 ± 19.2	1.0	70.3 ± 3.7	0.6	44.4 ± 11.5
42f	Et	Et	H	OMe	H	10.4 ± 0.3	4.2	46.9 ± 5.0	0.9	36.9 ± 3.4	1.2	43.6 ± 15.1
42g	Bu	Bu	H	OMe	H	22.8 ± 8.5	1.5	29.3 ± 1.4	1.2	25.4 ± 1.1	1.4	35.3 ± 17.5
44a	Me	Me	OMe	H	H	92.5 ± 14.8	0.5	48.1 ± 18.5	1.0	179.8	0.3	48.1 ± 18.5
44b	Me	Me	H	H	OMe	88.4	0.7	37.4 ± 1.1	1.6	66.6 ± 7.4	0.9	59.2 ± 25.9
44c	Me	Me	H	Me	H	31.5 ± 7.9	1.3	39.3 ± 2.4	1.0	64.9 ± 12.6	0.6	39.3 ± 1.6
44d	Me	Me	H	H	Me	33.0 ± 3.9	1.1	40.1 ± 8.3	0.9	51.9 ± 13.8	0.7	35.4 ± 7.9
44e	Me	Me	H	H	H	50.8 ± 6.2	1.2	74.9 ± 16.6	0.8	91.6 ± 5.4	0.7	62.4 ± 6.2
44f	Me	Me	H	<i>i</i> -Pr	H	12.4 ± 3.5	0.7	18.1 ± 0.7	0.5	15.6 ± 2.8	0.6	8.9 ± 3.5
44g	Me	Me	H	H	<i>i</i> -Pr	14.2 ± 4.2	1.6	19.1 ± 1.1	1.1	21.2 ± 7.1	1.0	22.0 ± 7.2
44h	Me	Me	H	<i>n</i> -Pen	H	6.4 ± 0.3	2.0	16.4 ± 0.3	0.8	16.8 ± 1.9	0.8	12.9 ± 3.2
Benznidazole						19.2 ± 7.7	3.9					74.7 ± 9.1
Miltefosine								13.0 ± 1.2	5.9	10.8 ± 1.5	7.1	76.6 ± 3.2

^a Toxicity was measured on RAW cells, see Experimental for details, ^b SI, selectivity index (cytotoxicity/anti-protozoal activity).

3.3.1 Antiparasitic activity toward *T. cruzi*

Initially, the 6,6-didemethyl analogue **42a** was prepared, to see how the lack of alkyl substituents in pulchrol's B-ring would affect its antiparasitic activity. After being assayed against *T. cruzi*, compound **42a** showed to be considerably less active than pulchrol, suggesting that the methyl groups at C-6 are important for the activity, however analogue **42a** was also less cytotoxic compared to pulchrol.

Analogues with just one alkyl substituent were prepared to determine whether the antiparasitic activity would increase or decrease with respect to pulchrol. The results from the biological assays showed the 6-methyl monosubstituted enantiomers **42b** and **42c** to possess less potency than pulchrol toward *T. cruzi*, and similar results were obtained for the 6-ethyl enantiomers **42d** and **42e**. Therefore, the two alkyl substituents in the B-ring appear to be important for the antitrypanosomal activity.

To continue exploring the space availability around C-6, the methyl substituents in the B-ring were replaced with longer alkyl groups. Compound **42f** was substituted with two ethyl groups at position 6, which increased the selectivity and activity (SI 4.2, $IC_{50} = 10.4 \mu\text{M}$) compared to pulchrol. Analogue **42f** is one of the most potent compounds toward *T. cruzi* in this study. On the other hand, analogue **42g** substituted at C-6 with two butyl groups, was not as active ($IC_{50} = 22.8 \mu\text{M}$) as **42f**, indicating that around this position may exist a lipophilic pocket with limited size.

To evaluate the effects that transformations in the C-ring may produce, compounds with the methoxy group in different positions in the C-ring were prepared. Compound **44a** with the methoxy substituent at C-1 and compound **44b** with the methoxy substituent at C-3, were found to be less potent and selective than pulchrol toward *T. cruzi*. Similarly, compounds with methyl substituents at C-2 (**44c**) and C-3 (**44d**) were equipotent to each other and less potent than pulchrol (with the methoxy group at C-2), yet more potent than analogues **44a** and **44b**. In contrast, analogue **44e** (with no substituents in the C-ring) showed to be slightly less potent than **44c** and **44d**. We observed that a methyl group in position 3 (**44d**) was preferred over a methoxy group in the same position. However, the opposite was true when the methoxy group was placed in position 2 (as in pulchrol), possibly due to hydrogen bond acceptor interactions with the protein target around this position.

We also prepared analogues with bulkier and longer alkyl substituents to explore the space surrounding positions 2 and 3 in the C-ring. Compounds **44f** and **44g**, substituted with isopropyl groups at positions 2 and 3, respectively, and analogue **44h** substituted with a n-pentyl group at C-3 were prepared and assayed toward *T. cruzi*. The results obtained from the biological assays showed that compounds **44f** and **44g** were more potent than pulchrol and equipotent to analogue **42f** (the most active compound among those with transformations in the B-ring), while compound **44h** (with a n-pentyl substituent at C-2) was found to be the most active compound

in this part of our investigation ($IC_{50} = 6.4 \mu\text{M}$), showing three times higher potency than pulchrol and the positive control benznidazole. The results observed for compounds **44f**, **44g**, and **44h**, suggest that lipophilic interactions at C-2 are more important than any possible hydrogen bond interactions in which the methoxy group of pulchrol may be involved.

3.3.2 Antiparasitic activity toward *L. braziliensis*

Similar to the results obtained for *T. cruzi*, the analogue with no alkyl substituents in the B-ring (**42a**) was less potent than pulchrol towards *L. braziliensis*, and also the monomethyl enantiomers **42b** and **42c** were less active compared to pulchrol. However, the monoethyl enantiomers (**42d** and **42e**), and the 6,6-diethyl analogue (**42f**) were equipotent with pulchrol. The only compound with modifications in the B-ring that showed to be more potent than pulchrol was analogue **42g** substituted with two *n*-butyl groups at position 6 ($IC_{50} = 29.3 \mu\text{M}$).

Within the antiparasitic activity results obtained for the analogues with transformations in the C-ring, we observed that changing the position of the methoxy group (placed at position 2 in pulchrol) to C-1 and C-3 (**44a** and **44b**) produced similar results to those observed for analogues **44c** and **44d**, substituted with methyl groups at C-2 and C-3, respectively. All of the previously mentioned analogues (**44a** – **44d**) were slightly more potent than pulchrol. The analogue with no methoxy or alkyl substituents on the C-ring (compound **44e**) showed lower activity toward *L. braziliensis* compared to pulchrol. However, compounds with bulkier and longer alkyl substituents (**44f** to **44h**) were found to possess considerably higher activity than analogues substituted with methoxy groups. Analogues **44f** and **44g** substituted with isopropyl groups at C-2 and C-3, respectively and compound **44h** substituted with a *n*-pentyl group at C-2 were all more potent than pulchrol. Compounds **44g** and **44h** were the most interesting (IC_{50} values of $19.1 \mu\text{M}$ and $16.4 \mu\text{M}$ respectively), showing comparable bioactivity with respect to our positive control Miltefosine, albeit the selectivity indexes calculated for **44g** and **44h** were lower than that of Miltefosine.

3.3.3 Antiparasitic activity toward *L. amazonensis*

The bioactivity results toward *L. amazonensis* showed that analogues substituted with two alkyl groups at position 6 in the B-ring are more potent than compounds substituted either with just one alkyl group or two hydrogen atoms at the same position (**42a**). Analogues with longer alkyl substituents such as the 6,6-diethyl analogue **42f** and the 6,6-dibutyl analogue **42g** were more potent than pulchrol toward *L. amazonensis*.

Different from the results obtained for *T. cruzi*, we observed that the analogue with a methoxy substituent at C-3 in the C-ring (**44a**) was slightly more potent than pulchrol (**13**). In contrast, analogue **44b**, in which the methoxy substituent was placed at C-1, showed to possess considerably less potency. Analogues with methyl substituents at positions 2 and 3 (**44c** and **44d**) showed no significant differences in the antiparasitic activity compared to the analogues with methoxy substituents in those same positions. Compound **44e**, with neither alkyl nor methoxy substituents in the C-ring was also less active than pulchrol. Similar to the results obtained for *T. cruzi* and *L. braziliensis*, the analogues substituted at positions 2 and 3 with bulkier and longer alkyl groups (**44f**, **44g** and **44h**) were more active than pulchrol.

3.4 Conclusions

In this chapter, analogues with variations in the B- and C-ring were prepared and assayed. In the B-ring there is just one position available for transformations, C-6, which has two methyl substituents in the natural product pulchrol. In this part of the investigation, we intended to evaluate the role that alkyl substituents at position 6 have on the antiparasitic activity. Therefore, we prepared analogues with no alkyl substituents at C-6 (**42a**), with just one alkyl substituent (**42b** to **42e**), and with two alkyl substituents (**42f** and **42g**).

The biological activities measured, show that the unsubstituted analogue **42a** is less potent, and the presence of alkyl substituents in the B-ring is obviously important for the antiparasitic activity. The 6-alkyl monosubstituted analogues affect parasites in different ways, the 6-methyl enantiomers **42b** and **42c** were less potent than pulchrol toward *T. cruzi* and *L. braziliensis*, while the analogue **42c** was found to be equipotent to pulchrol against *L. amazonensis*. Apparently, the methyl substituents in pulchrol's B-ring are not only important for lipophilic interactions, but they may also improve the orientation of the molecule inside the active site. The 6-ethyl enantiomers (**42d** and **42e**) were more potent than pulchrol toward the *Leishmania* parasites but still less potent toward *T. cruzi*. In contrast, the 6,6-disubstituted analogues **42f** and **42g**, with longer alkyl substituents at C-6 were more potent toward all parasites, the increase in the antileishmanial activity seems to be improved with the length of the alkyl substituents. However, for *T. cruzi* it was found that the 6,6-diethyl (**42f**) analogue is more interesting than the 6,6-dibutyl analogue (**42g**). Notably, analogue **42f** was found to be more potent and selective than the positive control Benznidazole.

To study the effect that transformations in the C-ring has on the antiparasitic activity, we have prepared and assayed an analogue with no substituents in the C-ring with the intention to evaluate the role of the 2-methoxy group in pulchrol's activity. We have also prepared analogues with the methoxy group placed in different

positions in the C-ring, and finally analogues with alkyl substituents instead of methoxy substituents.

The low bioactivity showed by compound **44e** indicate the importance that substituents in the C-ring have for the potency. Particularly, the 2-methoxy group in pulchrol seems to have an important role possibly participating in hydrogen bond acceptor interactions with the binding site. A methoxy substituent at positions 2 or 3 was better for the antiparasitic activity than at position 1. Methyl groups instead of methoxy groups in the C-ring showed no significant differences in the biological results. On the other hand, bulkier and longer alkyl groups at positions 2 and 3 (**44f**, **44g** and **44h**) improved the antiparasitic activity considerably. Compound **44h** substituted with an n-pentyl group in C-2, was the most active compound toward *T. cruzi*. For the *Leishmania* parasites compounds **44h**, **44f** and **44g**, all showed interesting bioactivities.

Most of the changes in this part of the study were related to the lipophilicity of the compounds and their ability to participate in van der Waals interactions with the active site. Our results showed that alkyl groups are beneficial for the antiparasitic activity possibly participating in hydrophobic interactions with the active site, but also perhaps by improving the orientation of the molecules in the target protein. Anyhow, there is still very little knowledge about pulchrol's molecular targets in the trypanosomatid parasites we have studied. Further studies developed systematically would increase our understanding and provide more information about the binding sites.

4 Combined modifications

In previous chapters the antiparasitic activity of analogues of pulchrol (**13**) with variations in the A-ring, concretely transformations of the benzyl alcohol functionality of pulchrol [99]; the activity of analogues with different substituents at positions 1, 2, and 3 in the C-ring; and the activity of analogues substituted with different alkyl groups in the B-ring was discussed [101]. In this chapter, the effects that two functionalities placed in different rings may have on the antiparasitic activity will be investigated (see Figure 23). Additionally, cannabinol (**21**) and its 3-methyl analogue **48c** (see Figure 23), were prepared and assayed. Our main objective in this part is to get more information about the chemical surroundings of any active site to which pulchrol possibly binds.

Compounds with the benzo[*c*]chromene scaffold possess different kinds of biological activities [80, 81, 86, 102, 103, 104], and the effects of the natural tricyclic cannabinoids are probably the most studied. Cannabinoids with the benzochromene scaffold are found together with Δ^9 -tetrahydrocannabinol (THC, **6**, see Figure 1) in the leaves of *C. sativa*. THC is the compound responsible for the psychotropic effect experienced by *C. sativa* consumers, this effect is triggered when THC binds to the cannabinoid receptor CB1 which is mainly expressed in the brain cells. In contrast to THC, the natural benzo[*c*]chromene cannabinol (**21**), which possesses the same skeleton as pulchrol, has higher affinity for CB2, another cannabinoid receptor, which has been reported not to produce psychotropic effects [85, 87, 102, 104, 105, 106].

Structure-activity relationship studies have revealed that hydroxyl groups at C1 and C1', with bulky alkyl substituents at C-3 are important for the CB1 affinity [106, 107], whereas bulky substituents at C-2 and a lactone in the B-ring are beneficial for the affinity to CB2 receptors [104, 107].

Cannabinoids with the benzo[*c*]chromene scaffold have also been shown to possess immunomodulatory properties [87, 108, 109] and to inhibit keratinocyte proliferation, which makes them interesting for treating psoriasis [110]. They were also found to possess some antinociceptive properties [108], antineoplastic activity on Lewis lung tumours [103], and antibacterial activity [102].

4.1 Modification on the A-, B- and C- rings

Analogues of pulchrol with a combination of two modifications in the A-, B, and C-rings (See Figure 23) were prepared. In order to do this, the synthetic approach previously reported in this investigation [66, 99] was utilized.

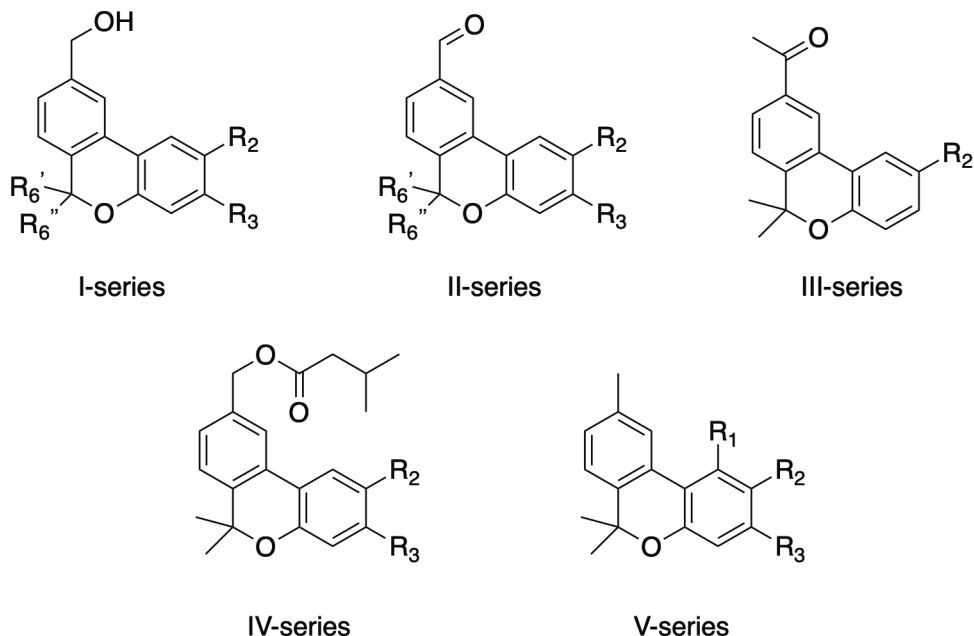


Figure 23

Series of the analogues with modification in the A-, B- and C-rings. *I-series*: **13**, $R_2 = \text{OMe}$, $R_3 = \text{H}$, $R_6' = \text{Me}$, $R_6'' = \text{Me}$; **44f**, $R_2 = i\text{-Pr}$, $R_3 = \text{H}$, $R_6' = \text{Me}$, $R_6'' = \text{Me}$; **44g**, $R_2 = \text{H}$, $R_3 = i\text{-Pr}$, $R_6' = \text{Me}$, $R_6'' = \text{Me}$; **42c**, $R_2 = \text{OMe}$, $R_3 = \text{H}$, $R_6' = \text{Me}$, $R_6'' = \text{H}$; **42b**, $R_2 = \text{OMe}$, $R_3 = \text{H}$, $R_6' = \text{H}$, $R_6'' = \text{Me}$. *II-series*: **37a**, $R_2 = \text{OMe}$, $R_3 = \text{H}$, $R_6' = \text{Me}$, $R_6'' = \text{Me}$; **45a**, $R_2 = i\text{-Pr}$, $R_3 = \text{H}$, $R_6' = \text{Me}$, $R_6'' = \text{Me}$; **45b**, $R_2 = \text{H}$, $R_3 = i\text{-Pr}$, $R_6' = \text{Me}$, $R_6'' = \text{Me}$; **45c**, $R_2 = \text{OMe}$, $R_3 = \text{H}$, $R_6' = \text{Me}$, $R_6'' = \text{H}$; **45d**, $R_2 = \text{OMe}$, $R_3 = \text{H}$, $R_6' = \text{H}$, $R_6'' = \text{Me}$. *III-series*: **37b**, $R_2 = \text{OMe}$; **46a**, $R_2 = i\text{-Pr}$. *IV-series*: **36e**, $R_2 = \text{OMe}$, $R_3 = \text{H}$; **47a**, $R_2 = i\text{-Pr}$, $R_3 = \text{H}$; **47b**, $R_2 = \text{H}$, $R_3 = i\text{-Pr}$. *V-series*: **35a**, $R_1 = \text{H}$, $R_2 = \text{OMe}$, $R_3 = \text{H}$; **20**, $R_1 = \text{H}$, $R_2 = \text{OH}$, $R_3 = \text{H}$; **48a**, $R_1 = \text{H}$, $R_2 = i\text{-Pr}$, $R_3 = \text{H}$; **48b**, $R_1 = \text{H}$, $R_2 = \text{H}$, $R_3 = i\text{-Pr}$; **48c**, $R_1 = \text{OH}$, $R_2 = \text{H}$, $R_3 = \text{Me}$; **21**, $R_1 = \text{OH}$, $R_2 = \text{H}$, $R_3 = n\text{-Pentyl}$.

The compounds belonging to the **I-series** were previously discussed, and here were used as precursors to prepare the analogues of the **II-**, **III-**, **IV-** and **V-series**. These series contain analogues with transformations in the B- or C-rings combined with different functionalities in the A-ring, such as 1'-aldehyde (**II-series**), 1'-methyl ketone (**III-series**), 3-methylbutanoic acid ester (**IV-series**) and 9-methyl (**V-series**) (See Figure 23). Additionally, cannabiol (**21**) and its analogue **48c** were obtained through iodine-mediated deconstructive annulation in a one-pot synthesis, using citral and resorcinol analogues as starting material [111]. All the molecules prepared in this part of the study were assayed in vitro toward *T. cruzi* epimastigotes, as well as *L. braziliensis* and *L. amazonensis* promastigotes (See Table 3). The

biological activity data obtained were compared with the bioactivity reported earlier for the compounds used as precursors here (**I**-series). Comparisons with the previously reported compounds **37a** (pulchral), **37b**, **36e**, and **35a** [99], which are related to the analogues prepared for this chapter, are discussed as well. As before, the cytotoxicity of the analogues in murine macrophage cells (RAW) was also determined, and the selectivity index (SI) as the ratio between the cytotoxicity and the antiparasitic activity was calculated.

Table 3

Antileishmanial, antitrypanosomal and cytotoxic activity of the pulchrol analogues, compared to the positive controls Benznidazole and Miltefosine. See Paper 3 for the experimental details.

Serie	Structure	Mol.	R1	R2	R3	R6'	R6''	<i>T. cruzi</i>		<i>L. braziliensis</i>		<i>L. amazonensis</i>		Cytotoxicity
								IC ₅₀ (μM)	SI ^b	IC ₅₀ (μM)	SI ^b	IC ₅₀ (μM)	SI ^b	IC ₅₀ (μM)
I		13	H	OMe	H	Me	Me	18.5 ± 9.6	1.7	59.2 ± 11.8	0.5	77.7 ± 5.5	0.4	30.7 ± 1.1
		44f	H	<i>i</i> -Pr	H	Me	Me	12.4 ± 3.5	0.7	18.1 ± 0.7	0.5	15.6 ± 2.8	0.6	8.9 ± 3.5
		44g	H	H	<i>i</i> -Pr	Me	Me	14.2 ± 4.2	1.6	19.1 ± 1.1	1.1	21.2 ± 7.1	1.0	22.0 ± 7.2
		42b	H	OMe	H	Me	H	35.9 ± 11.7	1.0	156.1 ± 23.4	0.2	156.1 ± 58.5	0.2	37.1 ± 3.9
		42c	H	OMe	H	H	Me	67.1 ± 31.2	0.8	128.8 ± 24.6	0.4	71.8 ± 12.5	0.7	52.7 ± 9.0
II		37a	H	OMe	H	Me	Me	24.2 ± 4.1	1.6	24.2 ± 7.5	1.6	29.8 ± 11.2	1.3	38.8 ± 3.7
		45a	H	<i>i</i> -Pr	H	Me	Me	10.7 ± 4.3	2.0	12.1 ± 4.6	1.8	11.4 ± 3.6	1.9	21.4 ± 5.4
		45b	H	H	<i>i</i> -Pr	Me	Me	7.1 ± 1.4	3.5	17.8 ± 1.8	1.4	17.8 ± 0.7	1.4	25.0 ± 7.1
		45c	H	OMe	H	Me	H	125.8 ± 7.9	0.2	70.8 ± 19.7	0.3	44.0 ± 1.6	0.5	20.4 ± 5.5
		45d	H	OMe	H	H	Me	170.3 ± 7.9	0.2	118.0 ± 0.8	0.3	80.6 ± 4.7	0.4	35.4 ± 2.8
III		37b	H	OMe	H	Me	Me	21.2 ± 9.2	1.5	28.3 ± 7.1	1.1	43.2 ± 8.2	0.7	31.9 ± 7.1
		46	H	<i>i</i> -Pr	H	Me	Me	3.4 ± 0.2	2.2	8.8 ± 1.0	0.8	9.5 ± 4.1	0.8	7.5 ± 2.0
IV		36e	H	OMe	H	Me	Me	4.2 ± 1.1	6.7	13.1 ± 0.4	2.2	14.5 ± 0.1	1.9	28.2 ± 9.0
		47a	H	<i>i</i> -Pr	H	Me	Me	10.9 ± 3.8	1.6	272.9 ± 0.0	0.1	25.9 ± 5.5	0.7	17.2 ± 5.5
		47b	H	H	<i>i</i> -Pr	Me	Me	13.6 ± 5.7	3.1	63.3 ± 4.4	0.7	43.7 ± 8.2	1.0	42.0 ± 2.7
V		35a	H	OMe	H	Me	Me	51.1 ± 17.7	2.0	69.6 ± 5.9	1.4	85.3 ± 5.9	1.2	99.5 ± 22.0
		20	H	OH	H	Me	Me	54.9 ± 0.2	0.5	30.4 ± 2.9	0.8	33.3 ± 5.4	0.8	25.0 ± 8.3
		48a	H	<i>i</i> -Pr	H	Me	Me	23.7 ± 8.6	1.8	49.2 ± 15.0	0.9	49.6 ± 4.5	0.9	42.8 ± 18.8
		48b	H	H	<i>i</i> -Pr	Me	Me	50.3 ± 11.3	2.1	311.6 ± 50.3	0.3	236.5 ± 48.8	0.4	105.1 ± 26.1
		48c	OH	H	Me	Me	Me	5.9 ± 2.0	4.1	15.7 ± 5.1	1.6	21.2 ± 2.4	1.1	24.4 ± 4.7
		21	OH	H	<i>n</i> -Pen	Me	Me	7.4 ± 0.6	2.2	10.3 ± 0.6	1.6	14.2 ± 1.3	1.1	16.1 ± 1.0
Benznidazole								19.2 ± 7.7	3.9			74.7 ± 9.1		
Miltefosine										13.0 ± 1.2	5.9	10.8 ± 1.5	7.1	76.6 ± 3.2

^a Toxicity was measured on RAW cells, see Experimental for details, ^b SI, selectivity index (cytotoxicity/anti-protozoal activity).

4.2 Antiparasitic activity and selected functionalities

As mentioned earlier, the natural products pulchrol (**13**) and pulchral (**37a**) have been studied in the past and both were active against *Trypanosoma* and *Leishmania* parasites. In previous chapters we have discussed the effect that individual transformations in the A-, B-, and C-rings have in the antiparasitic activity [99, 101]. We concluded that the benzyl alcohol functionality was important for pulchrol's activity possibly acting as a hydrogen bond acceptor, and that 1'-carbonyl analogues were active toward *Leishmania* species but not so much toward *T. cruzi*. The 9-methyl analogues were considerably less active than pulchrol, while the ester analogues showed higher potency than pulchrol, particularly when substituted with long and branched alkyl groups [99]. The modifications in the B- and C- rings were focused on variations in the lipophilicity and their effect on the antiparasitic activity. A preference for 6,6-dialkyl analogues was established, while longer and branched alkyl substituents in the C-ring increased the antiparasitic activity [101].

The analogues presented in this part of our investigation have in most cases transformations in the A- and C- rings, while a pair have transformations in the A- and B-rings. The functionalities evaluated in the A-ring are the 1'-aldehyde, the 3-methyl butanoic acid ester and the 9-methyl substituent. They were combined with isopropyl substituents at positions 2 and 3 in the C-ring (**45a** and **45b**; **47a** and **47b**; and **48a** and **48b** respectively), to investigate the effect on the antiparasitic activity. The effects of 1'-carbonyl analogues substituted with an isopropyl group at C-2, were further evaluated using the 1'-methyl ketone analogue **46**. The effects of the 9-methyl group with the more polar hydroxy functionality (analogue **20**, also found in nature) were evaluated. We also added to our study the natural compound cannabinal (**21**) and its analogue **48c** substituted with a 9-methyl group in the A-ring, a hydroxyl group at C-1 and an alkyl group at C-3 in the C-ring. Cannabinal (**21**) is substituted with a *n*-pentyl group at C-3 while analogue **48c** has a methyl group in this position. Finally, the effect of combining a 1'-aldehyde functionality with a 6-monomethyl substituent in the B-ring was also analysed by the testing of enantiomers **45c** and **45d** [101].

4.2.1 Antiparasitic activity toward *T. cruzi*

Previously (Paper 1 and 2), we observed that modifying the benzyl alcohol in pulchrol to a 1'-carbonyl functionality resulted only in a small effect on the antitrypanosomal activity (**13**, IC₅₀ = 18.5 μM; **37a**, IC₅₀ = 24.2 μM; and **37b**, IC₅₀ = 21.2 μM), and that replacing the methoxy group in pulchrol's C-ring for an isopropyl group either at position 2 or 3 was beneficial for the activity (**44f**, IC₅₀ = 12.4 μM and **44g**, IC₅₀ = 14.2 μM respectively) [99]. For this part of the study, we

prepared analogues with combinations between the 1'-carbonyl functionality in the A-ring and an isopropyl substituent at the C-ring's C-2 or C-3, these analogues were considerably more active and selective (**45a**, IC₅₀ = 10.7 μM, SI = 2.0; and **45b**, IC₅₀ = 7.1 μM, SI = 3.5) compared to their corresponding benzyl alcohols **44f** and **44g**, which biological activities were reported earlier [101] (see also Table 3). A change in the orientation inside the target may produce this improvement in the antitrypanosomal activity, resulting in stronger hydrophobic interactions for the isopropyl analogue. The analogue **46**, also with an isopropyl group at C-2 but with a methyl ketone functionality in the A-ring, was more active than the aldehyde **45a**, and it was the most potent compound toward *T. cruzi* in this investigation (IC₅₀ = 3.4 μM, SI = 2.2), being 6 times more active than the positive control (Benznidazole, IC₅₀ = 19.2 μM).

Contrary to the **II**- and **III**-series, compounds in the **IV**-series, substituted with a 3-methylbutanoic acid ester and an isopropyl group at either position 2 or 3, were less potent against *T. cruzi* (**47a**, IC₅₀ = 10.9 μM, SI = 1.6; **47b**, IC₅₀ = 13.6 μM, SI = 3.1) compared to the ester **36e** substituted with a methoxy group at C-2 (IC₅₀ = 4.2 μM, SI = 6.7) [99].

The compounds belonging to the **V**-series have a 9-methyl substituent in the A-ring and different substituents in the C-ring. In chapter 2 we mentioned that compound **35a** (substituted with a methoxy group at C-2 in the C-ring) was less potent than pulchrol (IC₅₀ = 51.1 μM) [99]. Here we replaced the methoxy substituent in **35a** by a hydroxyl group to obtain analogue **20** (also a natural product) which activity was comparable (IC₅₀ = 54.9 μM) to that of pulchrol. We understand that possibly both analogues (pulchrol and **20**) interact with the binding site in the same way but in rotated positions. The analogues **48a** and **48b** substituted with isopropyl groups in C-2 and C-3 were less active than pulchrol (IC₅₀ = 23.7 μM and IC₅₀ = 50.3 μM respectively), while cannabinal (**21**) and its analogue **48c**, substituted with alkyl groups at C-3 and an additional hydroxyl group at C-1 were the most potent and selective of the **V**-series (**21**, IC₅₀ = 7.4 μM, SI = 2.2; **48c**, IC₅₀ = 5.9 μM, SI = 4.1, respectively). Cannabinal's analogue **48c** (with a methyl group at C-3) was slightly more active than cannabinal, suggesting that the size of the C-3 substituent is less important for the activity than the hydroxyl group at C-1, which possibly participates in new hydrogen bond interactions.

Finally, the enantiomer analogues substituted with one alkyl group at C-6 and an aldehyde functionality at C-1' were considerably less active (**45c**, IC₅₀ = 125.8 μM; **45d**, IC₅₀ = 170.3 μM) compared to pulchrol (**13**, IC₅₀ = 18.5 μM) and their synthetic precursors (benzyl alcohols **42b** and **42c**) [101]. The aldehyde may produce a change in orientation, resulting in the weakening of hydrophobic interactions around position 6 in the B-ring.

4.2.2 Antiparasitic activity toward *L. braziliensis*

As mentioned earlier (Chapter 2), in contrast to the results obtained for *T. cruzi*, compounds **37a** and **37b** with a 1'-carbonyl functionality in the A-ring and a 2-methoxy group in the C-ring were considerably more potent (**37a**, $IC_{50} = 24.2 \mu\text{M}$; and **37b**, $IC_{50} = 28.3 \mu\text{M}$) than pulchrol (**13**, $IC_{50} = 59.2 \mu\text{M}$) [99]. In Chapter 3, we observed that analogues substituted with isopropyl groups at C-2 or C-3 increased the potency (**44f**, $IC_{50} = 18.1 \mu\text{M}$; and **44g**, $IC_{50} = 19.1 \mu\text{M}$) compared to pulchrol [101]. Here, we evaluated the combination of both functionalities. Analogues **45a** and **45b** with an isopropyl group at C-2 and C-3, respectively, were more potent (**45a**, $IC_{50} = 12.1 \mu\text{M}$; and **45b**, $IC_{50} = 17.8 \mu\text{M}$) than pulchrol (**13**) and their precursors **1b** and **1c**. Similar to the results obtained with *T. cruzi*, the 2-isopropyl ketone **46** was the most potent compound toward *L. braziliensis* ($IC_{50} = 8.8 \mu\text{M}$, $SI = 0.8$) in this investigation. Analogues **45a** and **46** are more potent than the positive control Miltefosine ($IC_{50} = 13.0 \mu\text{M}$, $SI = 5.9$), but their selectivity is lower.

As with *T. cruzi* the 3-methylbutanoic acid esters **47a** and **47b**, substituted with isopropyl groups at C-2 and C-3, were less potent (**47a**, $IC_{50} = 272.9 \mu\text{M}$; and **47b**, $IC_{50} = 63.3 \mu\text{M}$) than the ester analogue **36e** ($IC_{50} = 13.1 \mu\text{M}$) [99].

In chapter 2 we observed that analogue **35a** substituted with a 9-methyl group in the A-ring and a 2-methoxy substituent in the C-ring was less active ($IC_{50} = 69.6 \mu\text{M}$) than pulchrol (**13**, $IC_{50} = 59.2 \mu\text{M}$) [99]. Here, we transformed the **35a**'s methoxy substituent at C-2 into a hydroxyl substituent to obtain analogue **20**, in addition we prepared analogues **48a** and **48b** substituted with an isopropyl group at C-2 and C-3, respectively. Opposite to the results obtained with *T. cruzi*, analogues **48a** and **20** were more potent (**48a**, $IC_{50} = 49.2 \mu\text{M}$; and **20**, $IC_{50} = 30.4 \mu\text{M}$) than pulchrol (**13**) and **35a**. However, **48b** was inactive ($IC_{50} = 311.6 \mu\text{M}$) toward *L. braziliensis*, suggesting that a limit in the volume exist around position 3 in the C-ring. Cannabinol (**21**) and its analogue **48c** were more active and selective ($IC_{50} = 10.3 \mu\text{M}$, $SI = 1.6$ and $IC_{50} = 15.7 \mu\text{M}$, $SI = 1.6$, respectively) than **35a** and pulchrol (**13**). In contrast to the results observed for *T. cruzi* the longer chain in cannabinol (**21**) was more favourable for the activity toward *L. braziliensis* than the methyl group in **48c**.

Similar to *T. cruzi*, aldehyde enantiomers **45c** and **45d** were less potent and selective ($IC_{50} = 70.8 \mu\text{M}$, $SI = 0.3$ and $IC_{50} = 118.0 \mu\text{M}$, $SI = 0.3$, respectively) than pulchrol (**13**), but more potent than their benzyl alcohol precursors **42b** and **42c** ($IC_{50} = 156.1 \mu\text{M}$ and $IC_{50} = 128.8 \mu\text{M}$, respectively) [101].

4.2.3 Antiparasitic activity toward *L. amazonensis*

In Chapter 2 and 3, we observed that pulchral (**37a**) and the aldehydes with isopropyl substituents at C-2 and C-3 in the C-ring (**45a** and **45b**) were more potent

than pulchrol [99, 101]. Here, analogues **45a** and **45b** showed to benefit the activity. Similar to the results obtained for *L. braziliensis*, the aldehyde and methyl ketone analogues with an isopropyl group at C-2 showed the best activities (**45a**, $IC_{50} = 11.4 \mu\text{M}$; **46**, $IC_{50} = 9.5 \mu\text{M}$, respectively) of the compounds studied in this part of our investigation. They are both comparable with the positive control Miltefosine ($IC_{50} = 10.8 \mu\text{M}$). The ester analogues substituted with isopropyl groups at C-2 and C-3 (**47a** and **47b**) were less active and selective than **36e** (with a methoxy substituent on C-2, $IC_{50} = 14.5 \mu\text{M}$, $SI = 1.9$) as observed for *T. cruzi* and *L. braziliensis*. Similarly, most of the compounds from the VI-series were more potent than pulchrol (**13**, $IC_{50} = 77.7 \mu\text{M}$), the only inactive compound from this series was analogue **48b** (with an isopropyl substituent at C-3, $IC_{50} = 236.5 \mu\text{M}$). On the other hand, cannabinal was the most potent compound from the V-series (**21**, $IC_{50} = 14.2 \mu\text{M}$, $SI = 1.1$) followed by its analogue **48c** ($IC_{50} = 21.2 \mu\text{M}$, $SI = 1.1$). Similar to the other parasites, the 6-monomethyl aldehyde enantiomers **45c** ($IC_{50} = 44.0 \mu\text{M}$) and **45d** ($IC_{50} = 80.6 \mu\text{M}$) were less potent than the corresponding 6,6-dimethyl aldehyde **37a** (pulchral, $IC_{50} = 29.8 \mu\text{M}$) [99].

4.3 Conclusions

The combination of isopropyl substituents at positions 2 and 3 in the C-ring and the 1'-carbonyl functionality in the A-ring of the pulchrol scaffold was beneficial for the activity toward the three parasites studied in this investigation. However, the 3-isopropyl aldehyde analogue was more potent toward the *Leishmania* parasites than the 2-isopropyl aldehyde, while the opposite was observed for *T. cruzi*, therefore some differences may exist between the parasites binding sites. Despite that, the 2-isopropyl ketone showed the best activity toward all parasites in this chapter, suggesting that the methyl group in the ketone favours binding in the three species.

Analogues with a methylbutanoic acid ester in the A-ring combined with an isopropyl substituent at C-2 or C-3, were not as active as the ester analogues with a methoxy group at C-2. Moreover, the 2-isopropyl ester was inactive toward *L. braziliensis*, suggesting a limited space around C-2 in the binding site.

The combination of lipophilic substituents in the A- and C-rings (9-methyl and isopropyl substituents in the A- and C-rings, respectively) was unfavourable for the antiparasitic activity. The presence of substituents able to participate in hydrogen bond interactions appears to be an important factor for the activity.

Analogues with the methoxy or hydroxyl functionalities at C-2 combined with a 9-methyl functionality in the A-ring produced different effects for the different parasites. For *T. cruzi*, both analogues were equipotent, but less active than pulchrol. A rotation of the molecules may enable the methoxy and hydroxy groups at C-2 to

bind in the same position as the benzylic alcohol in pulchrol does, however the interaction is weaker. A similar situation may occur for the *Leishmania* species, but instead of weaker interactions stronger ones are produced, increasing the potency of the 2-methoxy and 2-hydroxyl analogues.

A different sort of combination, which includes the 9-methyl functionality in the A-ring, a hydroxy group at C-1 and an alkyl group at C-3 (like in cannabinol, **21**) is favourable for the antiparasitic activity and selectivity. A hydroxyl substituent at position 1 in the C-ring seems to help enhance the antiparasitic activity.

Finally, the combination of a 1'-aldehyde functionality with the 6-monomethyl substituted enantiomers seems to generate an unfavourable change in orientation in the binding site of the *T. cruzi* and *L. braziliensis* parasites. For *L. amazonensis*, the enantiomers showed different results. The bioactivity showed by one of them was comparable with its benzyl alcohol precursor and pulchrol, while the other enantiomer was slightly more potent.

5 Pharmacophore design and qualitative evaluation of predicted ADME-descriptors

Several computational tools used in drug design have contributed to the understanding of the bioactivity of different ligands, and have helped reducing the time and costs spent in the development of new drugs [112]. Among these tools, ligand-based pharmacophore modeling is important for assisting in drug discovery if no macromolecular target structure is available [112-114].

A pharmacophore model is an abstract 3D representation of common steric and electronic features shared by a set of active molecules that presumably interact with a specific biological target [112, 113, 115]. Pharmacophore models are defined by features capable of interaction with biological targets. Hydrogen bond donors, hydrogen bond acceptors, aromatic rings, hydrophobic centers and electrostatic groups are the most common features taken into account in pharmacophore development [112-114, 116]. The relationship of those features in the space is defined by the pharmacophore, which can also make use of exclusion volume constraints to further define the space around the ligands [114, 116].

The common pharmacophore features are identified by aligning low-energy conformers and establishing the better overlay of features [112-114]. Nonetheless, the conformation that the ligand adopts when is bound to the target is in reality unknown. Therefore, it is necessary to assume that the low-energy conformations used will resemble that of the bound ligand [113].

Several software applications can be used for developing pharmacophore models. Here, we used the PHASE module from the Schrödinger suit for the development of pharmacophore hypotheses.

PHASE uses an exhaustive partitioning algorithm to cluster conformers into multiple k-point pharmacophores grouped by feature similarity. The common pharmacophores are identified using a binary decision tree that groups pharmacophores with similar inter-site distances. The pharmacophores are further classified after alignment with each other to reveal poor superpositions. The quality of the alignment is measured by the root-mean-square deviation (RMSD) of the position of each feature and the average cosine of the angles formed by the

corresponding pairs of vector features. After this process, PHASE select one model as the pharmacophore hypothesis [117-119].

The study of structure-activity relationships and the analysis of the spatial distribution of pharmacophoric features are important for understanding possible binding interactions with a protein target. However, it is also important to assess the pharmacokinetic characteristics of the ligands to evaluate their potential as orally administered drugs.

The oral availability of a drug can be evaluated analysing pharmacologically-relevant descriptors predicted *in silico*. Here, we have used QikProp from the Schrödinger suit to predict several descriptors.

The absorption, distribution, metabolism, excretion and toxicity (ADMET) can be evaluated considering the Lipinski's "Rule of 5," The Jorgensen's "Rule of three," and other predicted properties related to the ability of ligands to cross membranes or interact with certain targets.

Lipinski's "Rule of 5" can be used as a guideline to predict which ligands may be orally active, if the ligand complies with at least three of the rules is considered a substance with potential for oral administration. As stated by Lipinski compounds with molecular weight lower than 500 Da, less than five hydrogen bonds donors ($HBD < 5$), less than 10 hydrogen bond acceptors ($HBA < 10$), and octanol/water partition coefficient values below 5 ($\log P < 5$) are probably orally absorbed [120].

Jorgensen's "rule of three" is also used to predict the oral availability of drugs, Jorgensen considers the predicted aqueous solubility ($Q\log S > -5.7$), the predicted apparent Caco-2 cell permeability ($QPPCaco > 22$ nm/s) and the number of likely metabolic reactions the drug may experience ($\#metabol < 7$) [121 -123].

An overall ADME-compliance descriptor ($\#star$), calculated by QikProp, can also be used to assess the pharmacokinetic profile of drugs. The $\#star$ descriptor considers the molecular weight, the dipole moment, the ionization potential, the electron affinity, the total solvent accessible area (and its components), the polar surface area, the total solvent accessible volume, the number of rotatable bonds, the number of hydrogen bond donors and hydrogen bond acceptors, the globularity, the polarizability, the hexadecane/gas partition coefficient, the octanol/gas partition coefficient, the octanol/water partition coefficient, the aqueous solubility, the predicted binding to human serum albumin, the brain/blood partition coefficient, and the number of likely metabolic reactions. The $\#star$ parameter is measured on a scale from 0 to 5, where 0 is the value for the most drug-like compound and 5 for the least drug-like compound [122-126].

QikProp also calculates the predicted central nervous activity (CNS), and the predicted IC_{50} value for the blockage of HERG k^+ channels.

In this part the study a pharmacophore hypothesis for *T. cruzi* generated in PHASE (Schrödinger, 2021-1) is presented, as well as the qualitative evaluation of ADMET-predicted values calculated by QikProp (Schrödinger, 2021-1).

5.1 Development of pharmacophore hypotheses

In previous chapters we discussed the effects that modifications on the pulchrol scaffold have on the antiparasitic activity towards *T. cruzi*, *L. braziliensis* and *L. amazonensis* [99, 101, 127].

In this part of the investigation a pharmacophore hypothesis is presented. The antiparasitic activity data obtained for 54 of the ligands prepared in this study were used for developing several pharmacophore models. The main pharmacophoric features recognized by the PHASE algorithm were two hydrogen bond acceptors and three hydrophobic sites. Features common to all analogues (A, B and C-ring centroids) were excluded from the calculations. The features recognized by PHASE were present in most of the active and some inactive ligands, therefore excluded volumes were generated to identify regions around the ligand where clashing with the binding site could explain low bioactivity.

Different scores were calculated to evaluate the pharmacophore models. The PhaseHypo score, which combines the BEDROC (Boltzmann-Enhanced Discrimination of Receiver Operating Characteristics) score and the survival score, was used to rank the pharmacophore models (see Eq. 2 in Paper 4). In turn, the survival score combines the vector score, site score, volume score, selectivity score, inactive score and the number of matches (see Eq. 3 in Paper 4).

The vector, site and volume scores measure how well the ligands are aligned to the model in terms of directionality, root-mean-deviation of inter-site distances, and volume overlap. The selectivity score estimates the uniqueness of the model toward active ligands, and the inactive score estimates how well inactive ligands match the model. The BEDROC score measures the extent to which the hypothesis extracts active ligands from a diverse set of 1000 drug-like decoys. Finally, the fitness score evaluates how well each ligand align to the model.

The scores were used to evaluate pharmacophore models generated for *T. cruzi*, *L. braziliensis* and *L. amazonensis*. Nine to ten models were obtained for each parasite, the top ranked models were selected for further analysis. The fitness scores showed that pharmacophore hypotheses developed for *L. braziliensis* and *L. amazonensis* did not explain the activity of the ligands accurately. However, the pharmacophore generated for *T. cruzi* showed fitness scores values in accordance with the activity of the ligands. Consequently, the pharmacophore hypothesis developed for *T. cruzi* is the only model showed in this chapter.

5.1.1 Pharmacophore hypothesis for *T. cruzi*

The score values calculated by PHASE for the five top ranked pharmacophore hypotheses developed for *T. cruzi* are shown in Table 4.

Table 4
Scoring results

Hypothesis	SuS ^a	SS ^b	VeS ^c	VS ^d	SeS ^e	NM ^f	IS ^g	BS ^h	PHS ⁱ
AAHHH_2	5.7257	0.8780	0.9766	0.7985	1.7109	23	2.3271	0.8823	1.226
AAHHH_1	5.7277	0.8832	0.9846	0.7873	1.7109	23	2.3219	0.8817	1.225
AAHHH_3	5.7010	0.8715	0.9643	0.8025	1.7010	23	2.3116	0.8829	1.225
AAHHH_6	5.6795	0.8774	0.9791	0.7657	1.6956	23	2.2873	0.8829	1.224
AAHHH_9	5.3596	0.6134	0.9642	0.7284	1.6919	23	2.2604	0.8772	1.199

^a Survival score, ^b Site score, ^c Vector score, ^d Volume score, ^e Selectivity score, ^f number of matches, ^g Inactive score, ^h BEDROC score, ⁱ PhaseHypo score.

The inter-site distances and angles for the highest ranked hypothesis (AAHHH_2) are shown in Paper 4 (See Table 2) and the shape of the pharmacophore is shown in Figure 24.

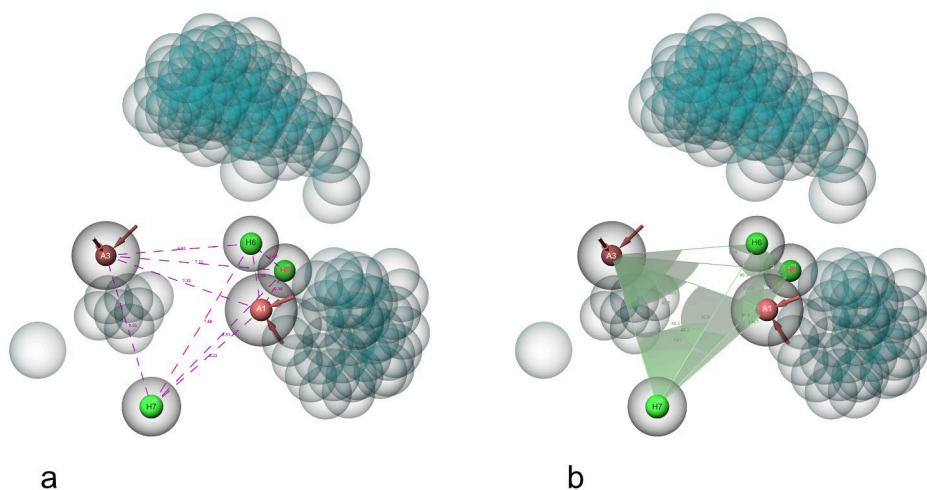


Figure 24
Pharmacophore hypothesis for *T. cruzi* (AAHHH_2). a) inter-site distances, b) inter-site angles

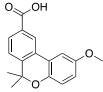
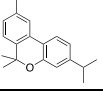
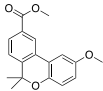
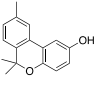
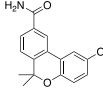
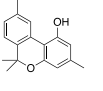
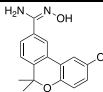
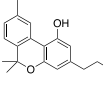
Related to pulchrol's activity, 27 ligands were considered active and 27 inactive, out of them 50 ligands aligned with AAHHH_2.

The excluded volumes were generated near C-6, and also close to the hydrogen bond acceptor sites (see Figure 24). The fitness scores for each ligand are shown in Table 5.

Table 5
Ligand scores for AAHHH_2

Mol	Structure	Activity ^a	Role	FS ^b	Mol	Structure	Activity ^a	Role	FS ^b
A-series					E-series				
13		18.50	active	2.6122	42a		66.04	inactive	2.0377
35a		51.11	inactive	2.3511	42b		35.90	inactive	2.2431
35b		38.09	inactive	2.3783	42c		67.11	inactive	2.3732
35c		24.62	inactive	2.8315	42d		36.99	inactive	2.2572
35d		12.80	active	2.9266	42e		51.79	inactive	2.1936
35e		9.08	active	2.8237	42f		10.39	active	2.4039
35f		70.64	inactive	2.3624	42g		22.85	inactive	2.0281
35g		15.36	None	*	45c		125.84	inactive	2.2288
35h		5.89	None	*	45d		170.28	inactive	2.2326
B-series					F-series				
36a		14.41	active	2.9512	44a		92.48	inactive	2.1944

36b		8.81	active	2.9518	44b		88.41	inactive	2.5229
36c		6.49	active	2.9481	44c		31.46	inactive	2.3457
36d		16.16	None	3.0000	44d		33.03	inactive	2.1414
36e		4.23	active	2.7896	44e		50.77	inactive	2.2084
36f		5.70	active	2.8770	44h		6.44	active	2.1978
36g		22.80	inactive	2.8537	G-series				
36h		8.36	active	2.5886	44f		12.39	active	2.5270
36i		13.14	active	2.6695	45a		10.70	active	2.5140
36j		7.40	active	2.9401	46		3.40	active	2.5006
36k		3.84	active	2.9057	47a		10.91	active	2.6385
36l		5.88	active	2.8945	48a		23.65	inactive	2.2265
C-series					H-series				
37a		24.23	inactive	2.5657	44g		14.17	active	2.3008
37b		21.25	inactive	2.5572	45b		7.13	active	2.0808
					47b		13.64	active	2.3253

37c		56.28	inactive	2.3696	48b		50.30	inactive	2.1138
I-series									
37d		31.84	inactive	2.5538	20		54.93	inactive	1.4595
37e		134.47	inactive	2.6114	48c		5.90	None	*
D-series									
38		33.42	inactive	2.5912	21		7.41	None	*

^a Activity measured in μM , ^b Fitness score, and * Ligands which did not align to the model

The ester **36d** was the reference ligand and had the highest fitness score (FS = 3). Ligand **48c** and natural product **21** (cannabinol) aligned poorly with the model despite their potency, while natural product **20** (didehydroconicol) with low activity toward *T. cruzi*, showed the lowest fitness score (FS = 1.4595).

Most of the inactive analogues showed low fitness scores. Analogues from the **E**-series, which had the absence of hydrophobic features H5 or H6 showed low fitness scores. Analogue **42g** with longer alkyl substituents on C-6 aligned with H5 and H6, however, the alkyl substituents appear to clash with the excluded volumes. The only compound from the **E**-series to show good alignment and no clashing was **42f**, substituted with two ethyl groups at C-6. The absence of substituents capable of aligning with feature H7 (C-ring) was also observed in the low scores calculated for **44e** and **44a**. Similarly, analogues without HBA in the A-ring showed low fitness scores. Figure 25 shows the alignment of inactive ligands **35a**, **42a**, **42c**, **45e**, and **44a**.

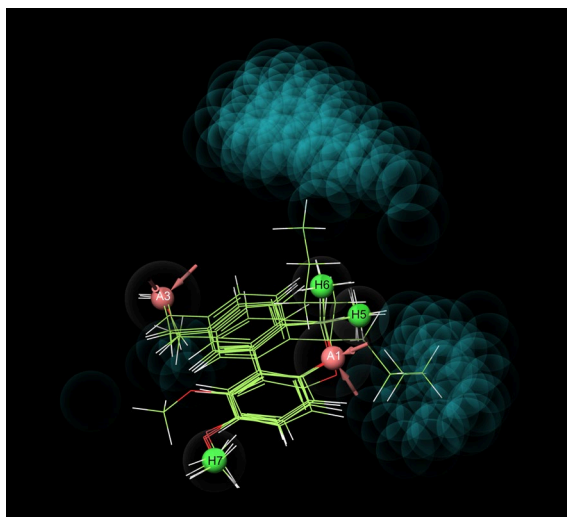


Figure 25
Inactive ligands **35a**, **42a**, **42c**, **45d**, and **44a** aligned to AAHHH_2

The esters from the **B**-series showed the best alignments along with ethers **35c**, **35d**, and **35e**, however, analogue **35c** was not active. Active ligands from the **G**-series had moderately good fitness scores and inactive analogue **48a** fit the model poorly. In contrast, amines **35g** and **35h** did not align well with the model in spite of their activity. Figure 26 shows the alignment of active ligands **13** (pulchrol), **36e**, **42f**, **44h**, and **46**.

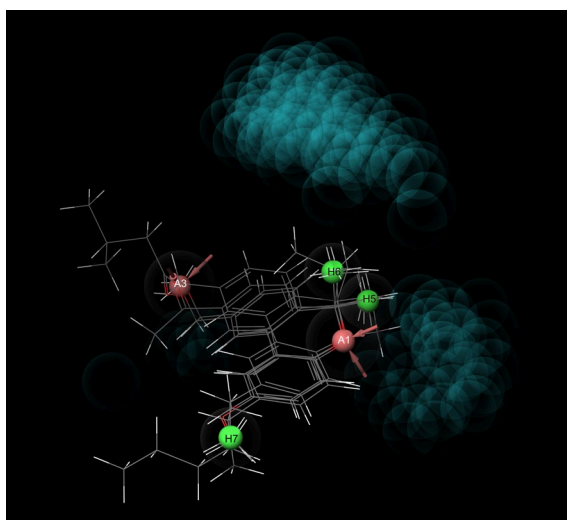


Figure 26
Active ligands **13**, **36e**, **42f**, **44h**, and **46** aligned to AAHHH_2

5.2 Qualitative analysis of ADMET-descriptors

The pharmacokinetic properties of all ligands in this investigation were evaluated using the 51 parameters predicted by QikProp (Schrödinger, 2021-1). The most relevant ADMET-descriptors are discussed below. A description of the parameters and their recommended range of values are presented in Table 6 [121-123].

Table 6
Description of the parameters predicted by QikProp used in this study

Descriptor	Description	Range ^a
#star ^b	Number of descriptor values that fall outside the 95% range of similar values for known drugs. A large number of stars suggest that a molecule is less drug-like than molecules with few stars.	0 - 5
SASA	Total solvent accessible surface area (Å ²) using a probe with 1.4 Å radius	300 - 1000
PSA	Van der Waals surface area (Å ²)	7 to 200
QPpolarz	Predicted polarizability (Å ³)	13 - 70
Lipinski's rule of 5	Number of violations of Lipinski's rule of five (Lipinski)	Maximum 4
MW	Molecular weight	130 - 725
DonorHB	Estimated number of hydrogen bonds that would be donated by the solute to water molecules in aqueous solutions.	0 - 6
AcceptorHB	Estimated number of hydrogen bonds that would be accepted by the solute to water molecules in aqueous solutions.	2 - 20
QPlogPo/w	Predicted octanol/water partition coefficient	-2 - 6.5
Rule of three	Number of violations of Jorgensen's rule of three.	Maximum 3
QPlogS	Predicted aqueous solubility	-6.5 - 0.5
QPPCaco	Predicted apparent Caco-2 cell permeability (nm/s) for non-active transport.	< 25 poor; > 500 great
#metabol	Number of likely metabolic reactions	1 - 8
#rotor	Number of non-trivial (not CX3), non-hindered (not alkene, amide, small ring) rotatable bonds.	0 - 15
Human Oral Absorption	Predicted qualitative human oral absorption. ^c	1 = low, 2 = medium, 3 = high
QPlogKh _{sa}	Prediction of binding to human serum albumin	-1.5 - 1.5
QPlogBB	for orally delivered drugs.	-3.0 - 1.2
CNS	Predicted central nervous activity on a -2 (inactive) to +2 (active) scale.	-2 - +2
QPlogHERG	Predicted IC ₅₀ value for blockage of HERG K ⁺ channels	Concern below -5

^a Recommended value for 95% of known drugs, ^b Descriptors included in #stars: Molecular weight, dipole moment, ionization potential, electron affinity, total solvent accessible area; hydrophobic, hydrophilic, π and weakly polar components of the SASA, polar surface area, total solvent accessible volume, number of rotatable bonds, hydrogen bond donors, hydrogen bond acceptors, globularity, polarizability, hexadecane/gas partition coefficient, octanol/gas partition coefficient, octanol/water partition coefficient, aqueous solubility, binding to human serum albumin, brain/blood partition coefficient, number of likely metabolic reactions.

The “#star” descriptor considers 29 other descriptors (see Table 6) and can be used to qualify the pharmacokinetic quality of the ligands. A distribution plot of the #star descriptor (see Figure 27a) shows that most of the compounds have #star values equal to 0 or 1. Few compounds may not be able to be orally absorbed according to de #star descriptor, among those, analogues with methyl substituents at position 9 in the A-ring (**35a**, **48a**, **48b**, **20**, and **48c**), chlorinated analogue **35b**, ester analogue **36h**, and the ether **35e**.

Parameters such as the total solvent accessible area (SASA), the total solvent-accessible volume, the globularity, the polar surface (PSA) and the predicted polarizability (QPpolrz) were inside the QikProp's recommended range of values for all ligands.

Most of the ligands complied with all Lipinski's rules [120]. All the molecular weight values were below 500 Da, none of the molecules had more than 5 HBD nor more 10 HBA, but 30% of the ligands had log *P* values above 5 (see Figure 27b). Log *P* values below 5 indicate a favourable hydrophilic/hydrophobic balance necessary in pharmacokinetics. Unfavourable effects such as an inability to cross cell membranes, binding to plasma protein and fast excretion may be observed in very hydrophilic compounds. Similarly, too hydrophobic ligands may be poorly absorbed if they get dissolved in fat globules inside the gut.

Over 60% of the ligands followed the Jorgensen's rule. The values for permeability of the Caco-2 cells and the number of likely metabolic reactions were inside the threshold recommended by Jorgensen for all compounds. The predicted water solubility values (QPlogS), in contrast, were below -5.7 for 37% of the compounds (See Figure 27c) [121, 123].

Molecular flexibility is another factor that may affect oral absorption and reduce the selectivity of the ligand. The presence of no more than 7 rotatable bonds is recommended for good oral absorption [128]. Among the 54 ligands studied here, just four molecules had more than 7 rotatable bonds (see Figure 27d). A parameter defined as "human oral absorption" by QikProp (see Table 6) showed that 72% of the ligands may have good oral absorption.

The predicted serum albumin binding ability (logKhsa) for all ligands was in the recommended range of values, indicating that the compounds are likely to circulate freely within the blood stream and access to the target site in sufficient amounts.

The blood-brain barrier partition coefficient (QPlogBB) values for all ligands were inside QikProp's recommended range of values (see Table 6 and Figure 27e). However, other authors state that compounds with QPlogBB values greater than 0.3 will penetrate the blood-brain barrier; compounds with QPlogBB values between -1 and 0.3 may still pass the blood-brain barrier; and compounds with QPlogBB below -1 will not penetrate the blood-brain barrier [129].

Considering the abovementioned ranges, five ligands would penetrate the brain-blood barrier, while 49 ligands would have less permeability, but maybe, still pass through the blood brain barrier. A "central nervous system" descriptor (CNS) was also predicted, according to the recommended values (see Table 6) most ligands (80%) were not active neither inactive (CNS = 0), 9 compounds were likely to be active (CNS > 0) and 2 compounds were likely to be inactive (CNS < 0).

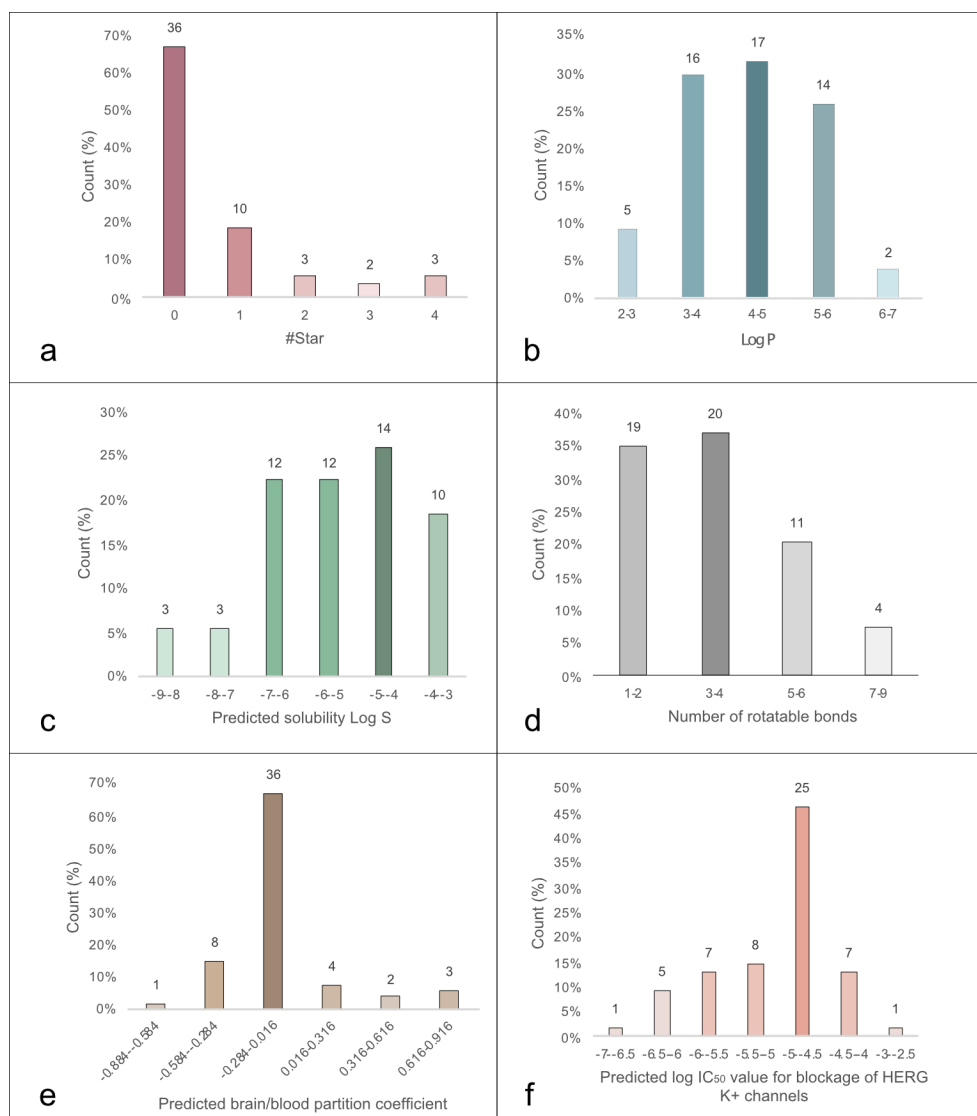


Figure 27

Distribution of predicted descriptors. *a.* #star, *b.* log *P*, *c.* log *S*, *d.* Number of rotational bonds, *e.* Predicted blood brain partition coefficient, *f.* Predicted log IC₅₀ values for blockage of HERG⁺ channels

The blockage of human ether-a-go-go-related gene potassium (HERG K⁺) channel was also predicted to determine possible cardiotoxicity of the ligands. As shown in Figure 27f, 70% of the compounds fall on the recommended range of values for HERG K⁺ binding.

5.3 Conclusions

We have developed a pharmacophore hypothesis for *T. cruzi*, *L. braziliensis* and *L. amazonensis*, and used several pharmacologically relevant descriptors to qualitatively evaluate the drug-likeness of the 54 pulchrol analogues presented in this study.

Pharmacophore models were generated to visualize the surroundings of the ligands and features involved in binding with the active site. The most important pharmacophoric sites were determined to be two hydrogen bond acceptors (one at the benzylic position in the A-ring and the other on heterocycle oxygen in the B-ring), and three hydrophobic features (one in the C-ring and the other two on the B-ring).

The only pharmacophore model capable of explaining the biological activity was developed for *T. cruzi*, while the models developed for the *Leishmania* species were unable to distinguish between active and inactive ligands. To improve the development of pharmacophore hypotheses for the *Leishmania* species modifying the activity threshold is recommended. The manual addition of excluded volumes to consider possible steric clashes is suggested as well. Validation of the pharmacophore hypothesis developed for *T. cruzi* using an appropriate set of test ligands is strongly advised before going ahead with quantitative structure-activity relationship studies (QSAR).

The pharmacokinetic evaluation showed that most of the molecules in this investigation comply with Lipinski's "Rule of five" and Jorgensen's "Rule of three". The predicted octanol/water partition coefficient and the predicted solubility in water, however, have not optimal values for some of the most hydrophobic compounds.

The rigidity of the pulchrol scaffold may benefit the pharmacokinetics and reduce the probability of interactions with undesired molecular targets.

Most of the compounds may not penetrate the blood brain barrier according to the recommended ranges, however care should be taken in the design of new compounds. Similarly, most of the compounds showed low binding affinity to the HERGK⁺ channels, but those compounds found outside the recommended range of values should be assayed to ascertain that cardiotoxicity is not a risk.

Overall, more than 80% of the compounds have good pharmacokinetic profile for oral administration. However, future studies should focus on the least hydrophobic active ligands may prevent issues concerning blood-brain barrier penetration, undesired central nervous system activity and poor absorption.

6 General Conclusions

Neglected diseases such as leishmaniasis and the Chagas disease are caused by protozoan parasites from the family Trypanosomatidae. The natural product pulchrol, isolated from the roots of the vegetal specie *Bourreria pulchra* showed potential toxicity toward *T. cruzi*, and moderate activity toward *L. braziliensis* and *L. amazonensis*, responsible for the Chagas disease, mucocutaneous leishmaniasis and cutaneous leishmaniasis, respectively.

In this investigation, an improved synthetic protocol to prepare pulchrol and its analogues was developed. Fifty-four compounds bearing the pulchrol scaffold were prepared and assayed toward *T. cruzi* epimastigotes, as well as *L. braziliensis* and *L. amazonensis* promastigotes. Selectivity indexes for each molecule were calculated as the ratio between the cytotoxicity measured in macrophage cells (RAW) and the antiparasitic activity.

The biological results indicate that the benzylic oxygen in the A-ring is important for the activity, probably acting as a hydrogen bond acceptor. A lipophilic pocket of unknown shape and size may exist in the target protein, localized where the hydrophobic substituents are attached to the benzylic oxygen or its ester. However, differences seem to exist between the parasites' hypothetical binding sites. The lipophilic pocket in *L. braziliensis* appears to fit alkyl chains with no more than 4 carbon atoms in the region in which the ester substituent is placed. While for *T. cruzi* and *L. amazonensis*, the same region seems to feature a planar surface in which aromatic and planar substituents may interact with the target. The analogue substituted with a vinyl ester at the benzylic position showed good activity and selectivity for all parasites, if it would act as Michael acceptor in the binding site then it could be used for fishing molecular targets.

Transformations at C-6 in the B-ring showed how important is the presence of two alkyl substituents in this position. Furthermore, the methyl substituents in pulchrol's B-ring not only seemed important for hydrophobic interactions, but they may also improve the orientation of the molecule in the active site. The activity toward the *Leishmania* species seems to improve with the length of the alkyl substituents at C-6, while the same region may have a limited size in *T. cruzi*'s binding site.

The presence of substituents in the C-ring was found to be important for the activity of all parasites. Hydrophobic interactions between bulky or long alkyl

groups at positions 2 and 3 seem to be the most beneficial substituents in the C-ring for the antiparasitic activity.

The combination of an aldehyde in the A-ring and isopropyl groups at C-2 and C-3 in the C-ring was beneficial for the antiparasitic activity. However, *Leishmania* species showed preference for the isopropyl substituent at C-3, whereas for *T. cruzi*, C-2 was the preferred position. The ligand with a ketone substituent in the A-ring and an isopropyl substituent at C-2 was the most potent compound for all parasites, showing that space for hydrophobic interactions with the ketone's methyl group may exist.

Butanoic acid esters in the A-ring combined with isopropyl groups at C-2 and C-3 reduced the activity. Particularly, the compound substituted with an isopropyl group at C-2 was inactive toward *L. braziliensis*, possibly due to steric clashes with the binding site.

The presence of at least one hydrogen bond acceptor (HBA) either in the A-ring or in the C-ring is essential for the antiparasitic activity. The region where the benzylic oxygen is located seems to be where the hydrogen bond interaction occurs. Compounds with the HBA in the C-ring and the hydrophobic group in the A-ring appear to rotate so that the C-ring's HBA is in the right position to interact with the target.

Nevertheless, two alkyl groups, one in the A-ring and the other in the C-ring, may increase the activity if they have a hydroxyl functionality at C-1 in the C-ring. The hydroxyl group at C-1 may participate in hydrogen bond interactions, but further studies are necessary to determine whether it acts as either HBA or HBD. Figure 28 shows a summary of the SARs.

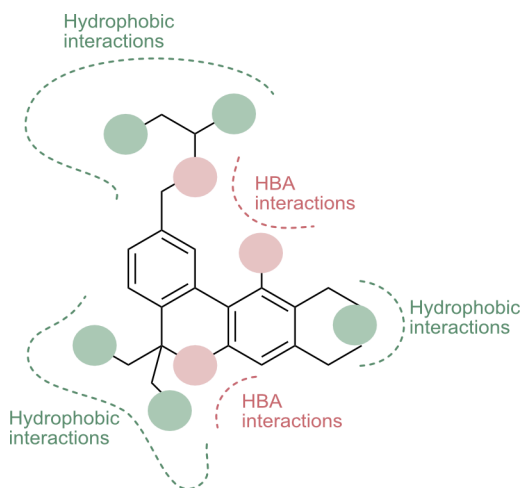


Figure 28
Summary of the structure activity relationship studies

A pharmacophore hypothesis developed for *T. cruzi* seems to agree with the structure activity relationships discussed before. The presence of two HBAs and 3 hydrophobic features shows the importance of the benzylic alcohol in the A-ring, the heterocyclic oxygen in the B-ring, the alkyl groups at C-6 in the B-ring and the alkyl group in the C-ring. However, the development of pharmacophore hypotheses was not successful for all parasites, thus for the *Leishmania* species, we suggest modifying the threshold in the activity values and we also recommend the manual addition of excluded volume. It is advised to validate the pharmacophore hypothesis developed for *T. cruzi*, in order to develop future QSAR studies that will be capable of predicting the antitrypanosomal activity of new molecules.

Most of the molecules showed potential for oral administration. However, the lipophilicity, possible CNS activity and cardiotoxicity, should be considered for the design of new derivatives. It is also recommended to assay the binding affinity of the compounds to the CB1 and CB2 receptors, to evaluate possible unwanted psychotropic activity, or in the contrary, detect possible selectivity to CB2 which may have a modulatory effect in the immune system.

7 Acknowledgments

I would like to sincerely thank...

The *Swedish International Development Cooperation Agency* (SIDA), for funding my doctoral studies.

Universidad Mayor de San Simón, for hosting me when I was in Bolivia.

My supervisor *Olov Sterner*, for your support, guide and consideration in the good times, but most importantly during the difficult times in the course of this investigation.

My supervisor *Marcelo Davila*, for your sympathy and positivity during the development of this work.

My co-supervisor *Sophie Manner*, for always being available when I needed advice.

José Luis Balderrama, agradecerle sinceramente por su apoyo y empatía.

Alberto Gimenez and *Efrain Salamanca*, for the biological assays.

Maria Levin and *Katarina Fredriksson*, for your help with all the administrative work, but also for your good attitude and nice disposition.

Sofia Essén, for the HRMS data presented in this work.

Bodil Eliasson, for your support this last years and for always asking how was I feeling, it was very nice to share the office with you.

Present and past members of the *Olov Sterner group*: Antonio, Leticia, Narda, Rodrigo, Juliao, Zilma, Mariela, Maribel, Eira and Ivan, for the good company.

Annika Beskow, *Lars Kjellberg*, *Mikael Beskow* and *Sofia Beskow*; for allowing me to be part of your family here in Sweden. Thanks for your caring support and all the time we spent together. I love you all.

Katja Beskow, *Maria Bengtsson*, *Kathinka Waldenström*, and *Martin Hjortsjö*, for sharing with me some thoughts and good advice about stress, mental health and life in general.

Eira Ruud Furusest, for helping me to adjust to the lab work when I arrived for the first time and generously sharing all your experience with me. Also, for the friendship that began in our lab and that I have the luck to still enjoy nowadays.

María Alicia Terrazas, Laura Terrazas, Tania Zubieta, Vania Zubieta y Doris Poka, por su apoyo en mi momento mas difícil; por su empatía, comprensión y sabios consejos, siempre las tengo en mi mente.

Ingrid Vargas, Gabriela Peña y Vanesa Castro, por compartir conmigo la experiencia del doctorado, los momentos de oscuridad y los momentos de luz.

Mi abuela *Hilda Zubieta* y mi padrino *Magín Zubieta,* por su sabiduría, buenos consejos y cariño.

Dr. Walter de Groot (QEPD), por haber sido un modelo de humildad, capacidad y generosidad que me inspira para ser mejor constantemente.

Mi abuela *Alta Gracia Terrazas (QEPD),* por que tu recuerdo me llena de fe en Dios.

A mi papá *Danilo Terrazas,* mi mamá *Gina Villarroel* y mi hermana *Lina Terrazas,* por su increíble apoyo durante este doctorado, por estar siempre en contacto conmigo y cuidando de mi, por decirme constantemente que lo único que esperan de mi es ser feliz. No se como agradecerles por tanto amor y disculparme por haberlos preocupado durante algunos los momentos. Los amo mucho.

To my dear *David,* because you have arrived suddenly to my life and like an angel you have rescued me from the darkness. You have brought an amazingly shining light into my life which is now filled with joy, laughter, love, friendship and a tad of dorkiness. I love you sweetheart, thank you for everything.

8 References

- [1] Dewick, P.M. Secondary Metabolism: The Building Blocks and Construction Mechanisms. *Medicinal Natural Products*, 2nd ed.; Wiley: Chichester, U.K., 2009; pp 7-38.
- [2] Leicach, S. R.; Chludil, H. D. Plant Secondary Metabolites: Structure–Activity Relationships in Human Health Prevention and Treatment of Common Diseases. In *Studies in Natural Products Chemistry*, Atta ur, R., Ed. Elsevier: 2014; Vol. 42, Chapter 9, pp 267-304.
- [3] Hong, J. Natural product synthesis at the interface of chemistry and biology. *Chemistry*. **2014**, 20 (33), 10204-10212.
- [4] David, B.; Wolfender, J.L.; Dias, D. A. The pharmaceutical industry and natural products: historical status and new trends. *Phytochem. Rev.* **2015**, 14 (2), 299-315.
- [5] Li, G.; Lou, H.-X. Strategies to diversify natural products for drug discovery. *Med. Res. Rev.* **2018**, 38 (4), 1255-1294.
- [6] Atanasov, A. G.; Waltenberger, B.; Pferschy-Wenzig, E. M.; Linder, T.; Wawrosch, C.; Uhrin, P.; Temml, V.; Wang, L.; Schwaiger, S.; Heiss, E. H.; Rollinger, J. M.; Schuster, D.; Breuss, J. M.; Bochkov, V.; Mihovilovic, M. D.; Kopp, B.; Bauer, R.; Dirsch, V. M.; Stuppner, H. Discovery and resupply of pharmacologically active plant-derived natural products: A review. *Biotechnol. Adv.* **2015**, 33 (8), 1582-1614.
- [7] Drašar, P.; Moravcova, J. Recent advances in analysis of Chinese medical plants and traditional medicines. *J. Chromatogr. B.* **2004**, 812 (1), 3-21.
- [8] Benyhe, S. Morphine: New aspects in the study of an ancient compound. *Life Sci.* **1994**, 55 (13), 969-979.
- [9] Sertürner, F.W. Säure im opium. *J. Pharmacie.* **1805**, 13, 234.
- [10] Wani, M. C.; Taylor, H. L.; Wall, M. E.; Coggon, P.; McPhail, A. T. Plant antitumor agents. VI. Isolation and structure of taxol, a novel antileukemic and antitumor agent from *Taxus brevifolia*. *J. Am. Chem. Soc.* **1971**, 93 (9), 2325-2327.
- [11] Wall, M. E.; Wani, M. C.; Cook, C. E.; Palmer, K. H.; McPhail, A. T.; Sim, G. A. Plant Antitumor Agents. I. The Isolation and Structure of Camptothecin, a Novel Alkaloidal Leukemia and Tumor Inhibitor from *Camptotheca acuminata* 1,2. *J. Am. Chem. Soc.* 1966, 88 (16), 3888-3890.
- [12] Neuss, N.; Gorman, M.; Hargrove, W.; Cone, N. J.; Biemann, K.; Buchi, G.; Manning, R. E. Vinca Alkaloids. XXI.1 The Structures of the Oncolytic Alkaloids Vinblastine (VLB) and Vincristine (VCR) 2. *J. Am. Chem. Soc.* **1964**, 86 (7), 1440-1442.

- [13] Nobili, S.; Lippi, D.; Witort, E.; Donnini, M.; Bausi, L.; Mini, E.; Capaccioli, S. Natural compounds for cancer treatment and prevention. *Pharmacol. Res.* **2009**, *59* (6), 365-378.
- [14] Oberlies, N. H.; Kroll, D. J. Camptothecin and Taxol: Historic Achievements in Natural Products Research. *J. Nat. Prod.* **2004**, *67* (2), 129-135.
- [15] Achan, J.; Talisuna, A. O.; Erhart, A.; Yeka, A.; Tibenderana, J. K.; Baliraine, F. N.; Rosenthal, P. J.; D'Alessandro, U. Quinine, an old anti-malarial drug in a modern world: role in the treatment of malaria. *Malar. J.* **2011**, *10* (1), 144.
- [16] White, N. J. Qinghaosu (Artemisinin): The Price of Success. *Science.* **2008**, *320* (5874), 330.
- [17] Qinghaosu Antimalarial Coordinating Research Group. *Chin. Med. J. (Engl).* **1979**, *92* (12), 811-816.
- [18] Choudhury, P.R.; Talukdar, A.D.; Saha, P.; Nath, D.; Nath, R. S. R. Traditional Folk Medicine and Drug Discovery: Prospects and Outcome. In *Advances in Pharmaceutical Biotechnology*, Patra, J.K., Shukla, A.C., Das, G., Eds.; Springer: Singapore, 2020; Chapter 1, pp 3-13.
- [19] Rodrigues, T.; Reker, D.; Schneider, P.; Schneider, G. Counting on natural products for drug design. *Nat. Chem.* **2016**, *8* (6), 531-541.
- [20] Chen, Y.; Garcia de Lomana, M.; Friedrich, N.O.; Kirchmair, J. Characterization of the Chemical Space of Known and Readily Obtainable Natural Products. *J.Chem. Inf. Model.* **2018**, *58* (8), 1518-1532.
- [21] Patridge, E.; Gareiss, P.; Kinch, M. S.; Hoyer, D. An analysis of FDA-approved drugs: natural products and their derivatives. *Drug Discovery Today* **2016**, *21* (2), 204-207.
- [22] Newman, D. J.; Cragg, G. M. Natural Products as Sources of New Drugs over the Nearly Four Decades from 01/1981 to 09/2019. *J. Nat. Prod.* **2020**, *83* (3), 770-803.
- [23] Moffat, J. G.; Vincent, F.; Lee, J. A.; Eder, J.; Prunotto, M. Opportunities and challenges in phenotypic drug discovery: an industry perspective. *Nat. Rev. Drug Discovery.* **2017**, *16* (8), 531-543.
- [24] Swinney, D. C.; Anthony, J., How were new medicines discovered? *Nature Reviews Drug Discovery* **2011**, *10* (7), 507-519.
- [25] Zheng, W.; Thorne, N.; McKew, J. C. Phenotypic screens as a renewed approach for drug discovery. *Drug Discovery Today.* **2013**, *18* (21), 1067-1073.
- [26] Al-Ali, H. The evolution of drug discovery: from phenotypes to targets, and back. *Med. Chem. Commun.* **2016**, *7* (5), 788-798.
- [27] Gilbert, I. H. Drug discovery for neglected diseases: molecular target-based and phenotypic approaches. *J. Med. Chem.* **2013**, *56* (20), 7719-7726.
- [28] Weng, H.-B.; Chen, H.-X.; Wang, M.W. Innovation in neglected tropical disease drug discovery and development. *Infect. Dis. Poverty.* **2018**, *7* (1), 67.
- [29] Reguera, R. M.; Calvo-Álvarez, E.; Álvarez-Velilla, R.; Balaña-Fouce, R. Target-based vs. phenotypic screenings in Leishmania drug discovery: A marriage of convenience or a dialogue of the deaf? *Int. J. Parasitol. Drugs Drug Resist.* **2014**, *4* (3), 355-357.

- [30] Haasen, D.; Schopfer, U.; Antczak, C.; Guy, C.; Fuchs, F.; Selzer, P. How Phenotypic Screening Influenced Drug Discovery: Lessons from Five Years of Practice. *Assay Drug Dev. Technol.* **2017**, *15* (6), 239-246.
- [31] Eder, J.; Sedrani, R.; Wiesmann, C. The discovery of first-in-class drugs: origins and evolution. *Nat. Rev.s Drug Discovery.* **2014**, *13* (8), 577-587.
- [32] World Health Organization Homepage. Available online: https://www.who.int/neglected_diseases/diseases/en/ (accessed on October 2020).
- [33] World Health Organization Homepage. A human rights-based approach to neglected tropical diseases. Available online: <https://www.who.int/gender-equity-rights/knowledge/ntd-information-sheet-eng.pdf?ua=1> (accessed on 22 October 2020).
- [34] Molyneux, D. H.; Savioli, L.; Engels, D. Neglected tropical diseases: progress towards addressing the chronic pandemic. *Lancet.* **2017**, 389 (10066), 312-325.
- [35] Jacobson, J.; Bush, S. Neglected Tropical Diseases, Neglected Communities, and Conflict: How Do We Leave No One Behind? *Trends Parasitol.* **2018**, *34* (3), 175-177.
- [36] Martins-Melo, F. R.; Ramos, A. N., Jr.; Alencar, C. H.; Heukelbach, J. Mortality from neglected tropical diseases in Brazil, 2000-2011. *Bull World. Health. Organ.* **2016**, *94* (2), 103-110.
- [37] World Health Organization Homepage. Second WHO report on neglected tropical diseases. Available online: https://www.who.int/neglected_diseases/9789241564540/en/ (accessed on 22 October 2020).
- [38] World Health Organization Homepage. Third WHO report on neglected tropical diseases. Available online: https://www.who.int/neglected_diseases/9789241564861/en/ (accessed on 22 October 2020).
- [39] Field, M. C.; Horn, D.; Fairlamb, A. H.; Ferguson, M. A. J.; Gray, D. W.; Read, K. D.; De Rycker, M.; Torrie, L. S.; Wyatt, P. G.; Wyllie, S.; Gilbert, I. H. Anti-trypanosomatid drug discovery: an ongoing challenge and a continuing need. *Nat. Rev. Microbiol.* **2017**, *15* (4), 217-231.
- [40] Kaufer, A.; Ellis, J.; Stark, D.; Barratt, J. The evolution of trypanosomatid taxonomy. *Parasites Vectors.* **2017**, *10* (1), 287.
- [41] World Health Organization Homepage. Chagas disease (also known as American trypanosomiasis). Available online: [https://www.who.int/news-room/fact-sheets/detail/chagas-disease-\(american-trypanosomiasis\)](https://www.who.int/news-room/fact-sheets/detail/chagas-disease-(american-trypanosomiasis)) (Accessed on 23 October 2020).
- [42] World Health Organization Homepage. World Chagas Disease Day: raising awareness of neglected tropical diseases. Available online: https://www.who.int/neglected_diseases/news/world-Chagas-day-approved/en/ (Accessed on 23 October 2020).
- [43] Tarleton, R. L. Chagas Disease: A Solvable Problem, Ignored. *Trends. Mol. Med.* **2016**, *22* (10), 835-838.

- [44] World Health Organization Homepage. Chagas disease (also known as American trypanosomiasis), data. Available online: https://www.who.int/docs/default-source/ntds/chagas-disease/chagas-2018-cases.pdf?sfvrsn=f4e94b3b_2 (Accessed on 23 October 2020).
- [45] Lewis, M. D.; Kelly, J. M. Putting Infection Dynamics at the Heart of Chagas Disease. *Trends parasitol.* **2016**, *32* (11), 899-911.
- [46] Pérez-Molina, J. A.; Molina, I. Chagas disease. *Lancet.* 2018, 391 (10115), 82-94.
- [47] Tanowitz, H. B.; Scherer, P. E.; Mota, M. M.; Figueiredo, L. M. Adipose Tissue: A Safe Haven for Parasites? *Trends parasitol.* **2017**, *33* (4), 276-284.
- [48] Chatelain, E., Chagas disease research and development: Is there light at the end of the tunnel? *Comput. Struct. Biotechnol. J.* **2016**, *15*, 98-103.
- [49] Bermudez, J.; Davies, C.; Simonazzi, A.; Pablo Real, J.; Palma, S. Current drug therapy and pharmaceutical challenges for Chagas disease. *Acta Trop.* **2016**, *156*, 1-16.
- [50] World Health Organization Homepage. Leishmaniasis. Available online: <https://www.who.int/news-room/fact-sheets/detail/leishmaniasis> (Accessed on 23 October 2020).
- [51] Shahnawaz, K.; Irfan, K.; Prem, M.S.C. Antileishmanial chemotherapy: present status and future perspectives. *Chem. Biol. Interface.* **2015**, *5*(1), 1-28.
- [52] Zavitsanou, A.; Koutis, C.; Babatsikou, F. Leishmaniasis: an overlooked public health concern. *Health. Sci. J.* **2008**, *2*(4), 196-205.
- [53] Veras, P. S. T.; Bezerra de Menezes, J. P. Using Proteomics to Understand How Leishmania Parasites Survive inside the Host and Establish Infection. *Int. J. Mol. Sci.* **2016**, *17* (8), 1270.
- [54] Bailey, F.; Eaton, J.; Jidda, M.; van Brakel, W. H.; Addiss, D. G.; Molyneux, D. H. Neglected Tropical Diseases and Mental Health: Progress, Partnerships, and Integration. *Trends Parasitol.* **2019**, *35* (1), 23-31.
- [55] World Health Organization Homepage. Leishmaniasis. Available online: <https://apps.who.int/gho/data/node.main.NTDLEISH?lang=en> (Accessed on 23 October 2020).
- [56] Kaye, P.; Scott, P. Leishmaniasis: complexity at the host–pathogen interface. *Nat. Rev. Microbiol.* **2011**, *9* (8), 604-615.
- [57] Séguin, O.; Descoteaux, A. Leishmania, the phagosome, and host responses: The journey of a parasite. *Cellular Immunology.* **2016**, *309*, 1-6.
- [58] Fernandes, F. R.; Ferreira, W. A.; Campos, M. A.; Ramos, G. S.; Kato, K. C.; Almeida, G. G.; Corrêa, J. D. J.; Melo, M. N.; Demicheli, C.; Frézard, F. Amphiphilic Antimony(V) Complexes for Oral Treatment of Visceral Leishmaniasis. *Antimicrob. Agents. Chemother.* **2013**, *57* (9), 4229-4236.
- [59] Croft, S. L.; Sundar, S.; Fairlamb, A. H. Drug Resistance in Leishmaniasis. *Clin. Microbiol. Rev.* **2006**, *19* (1), 111.
- [60] Singh, N.; Mishra, B. B.; Bajpai, S.; Singh, R. K.; Tiwari, V. K. Natural product based leads to fight against leishmaniasis. *Bioorg. Med. Chem.* **2014**, *22* (1), 18-45.

- [61] Erosa-Rejón, G. J.; Yam-Puc, A.; Chan-Bacab, M. J.; Giménez-Turbax, A.; Salamanca, E.; Peña-Rodríguez, L. M.; Sterner, O. Benzochromenes from the roots of *Bourreria pulchra*. *Phytochem. Lett.* **2010**, *3* (1), 9-12.
- [62] Campos-Ríos, M.G. Revisión del género *Bourreria* P.Browne (Boraginaceae) en México. *Polibotanica* **2005**, *19*, 39-103.
- [63] Argueta, A.; Cano, L.; Roderte, M.E. *Atlas de las Plantas de la Medicina Tradicional Mexicana*; Instituto Nacional Indigenista: Ciudad de Mexico, Mexico, 1994; pp. 483-485.
- [64] Polanco-Hernández, G.; Escalante-Erosa, F.; García-Sosa, K.; Acosta-Viana, K.; Chan-Bacab, M. J.; Sagua-Franco, H.; González, J.; Osorio-Rodríguez, L.; Moo-Puc, R. E.; Peña-Rodríguez, L. M. In vitro and in vivo trypanocidal activity of native plants from the Yucatan Peninsula. *Parasitol. Res.* **2012**, *110* (1), 31-35.
- [65] Hayden, W.J. Flora of Kaxil Kiuic. *Bourreria pulchra*. Available online: http://chalk.richmond.edu/flora-kaxil-kiuic/b/bourreria_pulchra.html (Accessed on 23 October 2020)
- [66] Killander, D.; Sterner, O. Synthesis of the Bioactive Benzochromenes Pulchrol and Pulchral, Metabolites of *Bourreria pulchra*. *Eur. J. Org. Chem.* **2014**, *2014* (8), 1594-1596.
- [67] Killander, D.; Sterner, O. Reagent-Controlled Cyclization-Deprotection Reaction to Yield either Fluorenes or Benzochromenes. *Eur. J. Org. Chem.* **2014**, 6507-6512.
- [68] Emilio, H.; Luis, A.; Guillermo, S.-H.; Jaime, R.; Cristina, T. Metabolites from *Microsphaeropsis olivacea*, an Endophytic Fungus of *Pilgerodendron uviferum*. *Z. Naturforsch.* **2005**, *60* (1-2), 11-21.
- [69] Kock, I.; Krohn, K.; Egold, H.; Draeger, S.; Schulz, B.; Rheinheimer, J. New Massarilactones, Massarigenin E, and Coniothyrenol, Isolated from the Endophytic Fungus *Coniothyrium sp.* from *Carpobrotus edulis*. *Eur. J. Org. Chem.* **2007**, *2007* (13), 2186-2190.
- [70] Song, Y. C.; Huang, W. Y.; Sun, C.; Wang, F. W.; Tan, R. X. Characterization of graphislactone A as the antioxidant and free radical-scavenging substance from the culture of *Cephalosporium sp.* IFB-E001, an endophytic fungus in *Trachelospermum jasminoides*. *Biol. Pharm. Bull.* **2005**, *28* (3), 506-509.
- [71] Zhang, H.-W.; Huang, W.-Y.; Song, Y.-C.; Chen, J.-R.; Tan, R.-X. Four 6H-Dibenzo[b,d]pyran-6-one Derivatives Produced by the Endophyte *Cephalosporium acremonium* IFB-E007. *Helv. Chim. Acta.* **2005**, *88* (11), 2861-2864.
- [72] Tanahashi, T.; Takenaka, Y.; Nagakura, N.; Hamada, N. 6H-Dibenzo[b,d]pyran-6-one derivatives from the cultured lichen mycobionts of *Graphis spp.* and their biosynthetic origin. *Phytochemistry.* **2003**, *62* (1), 71-75.
- [73] Bukuru, J. F.; Van, T. N.; Van Puyvelde, L.; Mathenge, S. G.; Mudida, F. P.; De Kimpe, N. A Benzochromene from the Roots of *Pentas bussei*. *J. Nat. Prod.* **2002**, *65* (5), 783-785.
- [74] Simon-Levert, A.; Arrault, A.; Bontemps-Subielos, N.; Canal, C.; Banaigs, B. Meroterpenes from the Ascidian *Aplidium aff. densum*. *J. Nat. Prod.* **2005**, *68* (9), 1412-1415.

- [75] Altemöller, M.; Gehring, T.; Cudaj, J.; Podlech, J.; Goesmann, H.; Feldmann, C.; Rothenberger, A. Total Synthesis of Graphis lactones A, C, D, and H, of Ulocladol, and of the Originally Proposed and Revised Structures of Graphis lactones E and F. *Eur. J. Org. Chem.* **2009**, 2009 (13), 2130-2140.
- [76] Kidwai, M.; Saxena, S.; Rahman Khan, M. K.; Thukral, S. S. Aqua mediated synthesis of substituted 2-amino-4H-chromenes and in vitro study as antibacterial agents. *Bioorg. Med. Chem. Lett.* **2005**, 15 (19), 4295-4298.
- [77] Soni, R.; Umar, S.; Shah, N. N.; Balkrishnan, S.; Soman, S. S. Design, Synthesis, and Anticancer Activity of 3H-benzo[f]chromen-3-one Derivatives. *J. Heterocycl. Chem.* **2017**, 54 (4), 2501-2510.
- [78] Mirjalili, B. F.; Zamani, L.; Zomorodian, K.; Khabnadideh, S.; Haghighijoo, Z.; Malakotikhah, Z.; Ayatollahi Mousavi, S. A.; Khojasteh, S. Synthesis, antifungal activity and docking study of 2-amino-4H-benzochromene-3-carbonitrile derivatives. *J. Mol. Struct.* **2016**, 1116, 102-108.
- [79] Halawa, A. H.; Fouda, A. M.; Al-Dies, A. M.; El-Agrody, A. M. Synthesis, Biological Evaluation and Molecular Docking Studies of 4H-benzo[h]chromenes, 7H-benzo[h]chromeno[2,3-d]pyrimidines as Antitumor Agents. *Lett. Drug. Des. Discovery.* **2016**, 13, 77-88.
- [80] Gulcan, H. O.; Unlu, S.; Esiringu, İ.; Ercetin, T.; Sahin, Y.; Oz, D.; Sahin, M. F. Design, synthesis and biological evaluation of novel 6H-benzo[c]chromen-6-one, and 7,8,9,10-tetrahydro-benzo[c]chromen-6-one derivatives as potential cholinesterase inhibitors. *Bioorg. Med. Chem.* **2014**, 22 (19), 5141-5154.
- [81] Sun, W.; Cama, L. D.; Birzin, E. T.; Warriar, S.; Locco, L.; Mosley, R.; Hammond, M. L.; Rohrer, S. P. 6H-Benzo[c]chromen-6-one derivatives as selective ER β agonists. *Bioorg. Med. Chem. Lett.* **2006**, 16 (6), 1468-1472.
- [82] Pratap, R.; Ram, V. J. Natural and Synthetic Chromenes, Fused Chromenes, and Versatility of Dihydrobenzo[h]chromenes in Organic Synthesis. *Chem. Rev.* **2014**, 114 (20), 10476-10526.
- [83] ElSohly, M. A.; Slade, D. Chemical constituents of marijuana: The complex mixture of natural cannabinoids. *Life Sci.* **2005**, 78 (5), 539-548.
- [84] Husni, A. S.; McCurdy, C. R.; Radwan, M. M.; Ahmed, S. A.; Slade, D.; Ross, S. A.; ElSohly, M. A.; Cutler, S. J. Evaluation of phytocannabinoids from high-potency Cannabis sativa using in vitro bioassays to determine structure-activity relationships for cannabinoid receptor 1 and cannabinoid receptor 2. *Med. Chem. Res.* **2014**, 23 (9), 4295-4300.
- [85] Mahadevan, A.; Siegel, C.; Martin, B. R.; Abood, M. E.; Beletskaya, I.; Razdan, R. K. Novel Cannabinol Probes for CB1 and CB2 Cannabinoid Receptors. *J. Med. Chem.* **2000**, 43 (20), 3778-3785.
- [86] Kaplan, B. L. F.; Rockwell, C. E.; Kaminski, N. E. Evidence for Cannabinoid Receptor-Dependent and -Independent Mechanisms of Action in Leukocytes. *J. Pharmacol. Exp. Ther.* **2003**, 306 (3), 1077.
- [87] Jan, T.-R.; Rao, G. K.; Kaminski, N. E. Cannabinol Enhancement of Interleukin-2 (IL-2) Expression by T Cells Is Associated with an Increase in IL-2 Distal Nuclear Factor of Activated T Cell Activity. *Mol. Pharmacol.* **2002**, 61 (2), 446.

- [88] Zhou, J.; Huang, L.-Z.; Li, Y.-Q.; Du, Z.-T. Synthesis of substituted 6*H*-benzo[*c*]chromenes: a palladium promoted ring closure of diazonium tetrafluoroborates. *Tetrahedron Lett.* **2012**, *53* (52), 7036-7039.
- [89] Campeau, L.-C.; Parisien, M.; Leblanc, M.; Fagnou, K. Biaryl Synthesis via Direct Arylation: Establishment of an Efficient Catalyst for Intramolecular Processes. *J. Am. Chem. Soc.* **2004**, *126* (30), 9186-9187.
- [90] Singha, R.; Ahmed, A.; Nuree, Y.; Ghosh, M.; Ray, J. K. KO^tBu mediated efficient approach for the synthesis of fused heterocycles via intramolecular O-/N-arylations. *RSC Adv.* **2015**, *5* (62), 50174-50177.
- [91] Roman, D. S.; Takahashi, Y.; Charette, A. B. Potassium tert-Butoxide Promoted Intramolecular Arylation via a Radical Pathway. *Org. Lett.* **2011**, *13* (12), 3242-3245.
- [92] Bajracharya, G. B.; Daugulis, O. Direct Transition-Metal-Free Intramolecular Arylation of Phenols. *Org. Lett.* **2008**, *10* (20), 4625-4628.
- [93] Singha, R.; Roy, S.; Nandi, S.; Ray, P.; Ray, J. K. Palladium-catalyzed one-pot Suzuki–Miyaura cross coupling followed by oxidative lactonization: a novel and efficient route for the one-pot synthesis of benzo[*c*]chromene-6-ones. *Tetrahedron Lett.* **2013**, *54* (7), 657-660.
- [94] Mahendar, L.; Krishna, J.; Gopi Krishna Reddy, A.; Venkat Ramulu, B.; Satyanarayana, G. A Domino Palladium-Catalyzed C–C and C–O Bonds Formation via Dual O–H Bond Activation: Synthesis of 6,6-Dialkyl-6*H*-benzo[*c*]chromenes. *Org. Lett.* **2012**, *14* (2), 628-631.
- [95] Mazimba, O. Synthetic protocols on 6*H*-benzo[*c*]chromen-6-ones: a review. *Turk. J. Chem.* **2016**, *40*, 1-27.
- [96] Minuti, L.; Temperini, A.; Ballerini, E. High-Pressure-Promoted Diels–Alder Approach to Biaryls: Application to the Synthesis of the Cannabinols Family. *The Journal of Organic Chemistry* **2012**, *77* (18), 7923-7931.
- [97] Ballerini, E.; Minuti, L.; Piermatti, O.; Pizzo, F. High Pressure Diels–Alder Approach to Hydroxy-Substituted 6a-Cyano-tetrahydro-6*H*-benzo[*c*]chromen-6-ones: A Route to Δ6-Cis-Cannabidiol. *J. Org. Chem.* **2009**, *74* (11), 4311-4317.
- [98] Leadbeater, N.E.; Marco, M. Rapid and amenable Suzuki coupling reaction in water using microwave and conventional heating. *J. Org. Chem.* **2003**, *68*, 888–892.
- [99] Terrazas, P.; Salamanca, E.; Dávila, M.; Manner, S.; Giménez, A.; Sterner, O. SAR:s for the antiparasitic plant metabolite pulchrol. 1. The benzyl alcohol functionality. *Molecules.* **2020**, *25*, 3058.
- [100] Norseeda, K.; Tummatorn, J.; Krajangsri, S.; Thongsornkleeb, C.; Ruchirawat, S. Synthesis of 6-Alkyl-6*H*-benzo[*c*]chromene Derivatives by cyclization/selective ether cleavage in one pot: Total synthesis of cannabinol. *Asian J. Org. Chem.* **2016**, *5* (6), 792-800.
- [101] Terrazas, P.; Salamanca, E.; Dávila, M.; Manner, S.; Giménez, A.; Sterner, O. SAR:s for the Antiparasitic Plant Metabolite Pulchrol. 2. B- and C-ring substituents. *Molecules.* **2020**, *25*, 4510.
- [102] Appendino, G.; Gibbons, S.; Giana, A.; Pagani, A.; Grassi, G.; Stavri, M.; Smith, E.; Rahman, M. M. Antibacterial Cannabinoids from *Cannabis sativa*: A Structure–Activity Study. *J. Nat. Prod.* **2008**, *71* (8), 1427-1430.

- [103] Munson, A. E.; Harris, L. S.; Friedman, M. A.; Dewey, W. L.; Carchman, R. A. Antineoplastic Activity of Cannabinoids. *J. Natl. Cancer Inst.* **1975**, *55* (3), 597-602.
- [104] Khanolkar, A. D.; Lu, D.; Ibrahim, M.; Duclos, J. R. I.; Thakur, G. A.; Malan, J. T. P.; Porreca, F.; Veerappan, V.; Tian, X.; George, C.; Parrish, D. A.; Papahatjis, D. P.; Makriyannis, A. Cannabilactones: A Novel Class of CB2 Selective Agonists with Peripheral Analgesic Activity. *J. Med. Chem.* **2007**, *50* (26), 6493-6500.
- [105] Munro, S.; Thomas, K. L.; Abu-Shaar, M. Molecular characterization of a peripheral receptor for cannabinoids. *Nature* 1993, 365 (6441), 61-65.
- [106] Yamamoto, I.; Watanabe, K.; Kuzuoka, K.; Narimatsu, S.; Yoshimura, H. The pharmacological activity of cannabinal and its major metabolite, 11-Hydroxycannabinol. *Chem. Pharm. Bull.* **1987**, *35* (5), 2144-2147.
- [107] Thakur, G. A.; Bajaj, S.; Paronis, C.; Peng, Y.; Bowman, A. L.; Barak, L. S.; Caron, M. G.; Parrish, D.; Deschamps, J. R.; Makriyannis, A. Novel Adamantyl Cannabinoids as CB1 Receptor Probes. *J. Med. Chem.* **2013**, *56* (10), 3904-3921.
- [108] Zygmunt, P. M.; Andersson, D. A.; Hogestatt, E. D. Delta 9-tetrahydrocannabinol and cannabinal activate capsaicin-sensitive sensory nerves via a CB1 and CB2 cannabinoid receptor-independent mechanism. *J. Neurosci.* **2002**, *22* (11), 4720-4727.
- [109] Rao, G. K.; Kaminski, N. E., Cannabinoid-Mediated Elevation of Intracellular Calcium: A Structure-Activity Relationship. *J. Pharmacol. Exp. Ther.* **2006**, *317* (2), 820.
- [110] Wilkinson, J. D.; Williamson, E. M. Cannabinoids inhibit human keratinocyte proliferation through a non-CB1/CB2 mechanism and have a potential therapeutic value in the treatment of psoriasis. *J. Dermatol. Sci.* **2007**, *45* (2), 87-92.
- [111] Caprioglio, D.; Mattoteia, D.; Minassi, A.; Pollastro, F.; Lopatriello, A.; Muñoz, E.; Tagliatela-Scafati, O.; Appendino, G. One-Pot Total Synthesis of Cannabinal via Iodine-Mediated Deconstructive Annulation. *Org. Lett.* **2019**, *21* (15), 6122-6125.
- [112] Chandrasekaran, B.; Agrawal, N.; Kaushik, S. Pharmacophore Development. In *Encyclopedia of Bioinformatics and Computational Biology*. **2019**; pp 677-687.
- [113] Roy, K.; Kar, S.; Das, R. N. Chapter 10 - Other Related Techniques. In *Understanding the Basics of QSAR for Applications in Pharmaceutical Sciences and Risk Assessment*. Roy, K.; Kar, S.; Das, R. N. Eds. Academic Press: Boston, **2015**; pp 357-425.
- [114] Wolber, G.; Seidel, T.; Bendix, F.; Langer, T. Molecule-pharmacophore superpositioning and pattern matching in computational drug design. *Drug Discovery Today*. **2008**, *13* (1), 23-29.
- [115] Yang, S.-Y. Pharmacophore modelling and applications in drug discovery: challenges and recent advances. *Drug Discovery Today*. **2010**, *15* (11), 444-450.
- [116] Leach, A. R.; Gillet, V. J.; Lewis, R. A.; Taylor, R. Three-Dimensional Pharmacophore Methods in Drug Discovery. *J. Med. Chem.* **2010**, *53* (2), 539-558.
- [117] Dixon, S. L.; Smondyrev, A. M.; Knoll, E. H.; Rao, S. N.; Shaw, D. E.; Friesner, R. A. PHASE: a new engine for pharmacophore perception, 3D QSAR model development, and 3D database screening: 1. Methodology and preliminary results. *J. Comput.-Aided Mol. Des.* **2006**, *20* (10), 647-671.

- [118] Dixon, S. L.; Smondryev, A. M.; Rao, S. N. PHASE: A Novel Approach to Pharmacophore Modeling and 3D Database Searching. *Chem. Biol. Drug Des.* **2006**, *67* (5), 370-372.
- [119] Sanders, M. P. A.; Barbosa, A. J. M.; Zarzycka, B.; Nicolaes, G. A. F.; Klomp, J. P. G.; de Vlieg, J.; Del Rio, A. Comparative Analysis of Pharmacophore Screening Tools. *J. Chem. Inf. Model.* **2012**, *52* (6), 1607-1620.
- [120] Lipinski, C. A. Lead- and drug-like compounds: the rule-of-five revolution. *Drug Discov. Today: Technologies.* **2004**, *1* (4), 337-341.
- [121] Jorgensen, W. L.; Duffy, E. M. Prediction of Drug Solubility from Monte Carlo Simulations. *Bioorg. Med. Chem. Lett.* **2000**, *10*, 1155-1158.
- [122] Duffy, E. M.; Jorgensen, W. L. Prediction of Properties from Simulations: Free Energies of Solvation in Hexadecane, Octanol, and Water. *J. Am. Chem. Soc.* **2000**, *122*, 2878-2888.
- [123] Jorgensen, W. L.; Duffy, E. M. Prediction of Drug Solubility from Structure. *Adv. Drug Delivery Rev.* **2002**, *54*, 355-366.
- [124] Colmenarejo, G.; Alvarez-Pedraglio, A.; Lavandera, J.-L. Cheminformatic Models To Predict Binding Affinities to Human Serum Albumin. *J. Med. Chem.* **2001**, *44*, 4370-4378.
- [125] Luco, J. M. Prediction of the Brain-Blood Distribution of a Large Set of Drugs from Structurally Derived Descriptors Using Partial Least-Squares (PLS) Modeling. *J. Chem. Inf. Comput. Sci.* **1999**, *39*, 396-404.
- [126] Potts, R. O.; Guy, R. H. Predicting skin permeability. *Pharm. Res.* **1992**, *9*, 663-669. Kelder J.; Grootenhuis, P. D.; Bayada, D.M.; Delbressine, L.P., Ploemen, J.P. Polar molecular surface as a dominating determinant for oral absorption and brain penetration of drugs. *Pharm. Res.* **1999**, *16*, 1514-1519.
- [127] Terrazas, P.; Salamanca, E.; Dávila, M.; Manner, S.; Giménez, A.; Sterner, O. SAR:s for the Antiparasitic Plant Metabolite Pulchrol. 3. New substituents in A/B-rings and A/C-rings. *In manuscript*.
- [128] Patrick, G. L. An Introduction to Medicinal Chemistry, 5th ed.; Oxford University Press: Oxford, U.K., **2013**; pp 227-265.
- [129] Kunwittaya, S.; Nantasenamat, C.; Treeratanapiboon, L.; Srisarin, A.; Isarankura-Na-Ayudhya, C.; Prachayasittikul, V. Influence of logBB cut-off on the prediction of blood-brain barrier permeability. *Biomedical and Applied Technology Journal.* **2013**, 16-34.